DISS. ETH NO 24499

Deciphering the mechanosensitivity of mesenchymal stem cells to their environment

A thesis submitted to attain the degree of
DOCTOR OF SCIENCES of ETH ZURICH
(Dr. sc. ETH Zurich)

presented by
Tojo Razafiarison
MSc, EPF Lausanne, Switzerland
born on 9TH March, 1984
citizen of Geneva GE, Switzerland

accepted on the recommendation of
Prof. Dr. Jess Snedeker, examiner
Prof. Dr. Viola Vogel, co-examiner
Prof. Dr. Marcy Zenobi-Wong, co-examiner

2017

“Strength lies in differences,
not in similarities”

Stephen Richards Covey

Table of Contents

Acknowledgements 8

Summary 11

Résumé........ 14

1 Introduction 18

1.1 Thesis motivation 18
1.2 Specific aims........ 19
1.3 Outline of the thesis 20
1.4 References 22

2 Background 25

2.1 Role of the microenvironment in controlling stem cell behavior........ 25
2.1.1 The extracellular matrix 25
2.1.2 Mesenchymal stem cell niche and tissue healing 29
2.1.3 Environmental factors directing stem cell behavior 30
2.2 Environmental sensing by stem cells........ 34
2.2.1 Mechanical cues as key regulators 34
2.2.1.1 The integrin signaling to the cytoskeleton 34
2.2.1.2 Discoidin domain receptors in collagen-mediated signaling 36
2.2.2 Mechanotransduction and lineage specification........ 37
2.3 Experimental platforms for investigating stem cell environmental sensing 41
2.3.1. A myriad of diverse platforms 41
2.3.1.1. Two-dimensional (2D) platform 41
2.3.1.2. Three-dimensional (3D) platform........ 44
2.3.2. Discrepancy and limitations from confounding factors 46
2.3.2.1. Mesenchymal stem cell culture 46
2.3.2.2. Cell sensitivity to material stiffness 47
2.3.2.3. Surface energy: an underappreciated element........ 48
2.4 References 52

3 Development and characterization of a surface energy tunable PDMS-based platform for 2D stem culture 59

3.1 Abstract 60
3.2 Introduction 61
3.3 Materials and methods 62
  3.3.1 Surface energy and stiffness tunable PDMS substrate preparation 62
  3.3.2 Contact angle measurement 63
  3.3.3 Macroscopic mechanical characterization 63
  3.3.4 Microscopic mechanical characterization 64
  3.3.5 Nanoscopic mechanical characterization 64
  3.3.6 Ligand loading and adsorbed protein quantification 64
  3.3.7 Statistical analysis 65
3.4 Results 66
  3.4.1 Contact angle characterization 66
  3.4.2 Multi-scale mechanical characterization 67
  3.4.3 Bioactivity characterization of the different surfaces: 71
3.5 Discussion 72
3.6 Supplementary Material 74
3.7 References 76

4 Surface-driven collagen assembly affects early osteogenic stem cell signaling 79

4.1 Abstract 80
4.2 Introduction 81
4.3 Materials and Methods 84
  4.3.1. Tunable hydrophobic/hydrophilic PDMS substrate preparation 84
  4.3.2. Fluorescent immunostaining of collagen-I for ligand surface coverage 85
  4.3.3. Scanning electron microscopy imaging of ligand assembly/conformation 85
  4.3.4. Atomic force microscopy imaging of ligand topography/roughness 85
  4.3.5. Cell culture 86
  4.3.6. Cell attachment and morphology 86
  4.3.7. Cell differentiation quantification 87
  4.3.8. Phosphorylated ERK1/2 quantification 88
  4.3.9. Alizarin red staining for osteogenic differentiation 88
  4.3.10. Real time and quantitative PCR 89
  4.3.11. Fluorescence-activated cell sorting 89
  4.3.12. Statistical analysis 90
4.4 Results 90
  4.4.1 Bioactivity characterization of the different surfaces 90

4.4.2 Cell attachment and morphology 92
4.4.3 Osteogenic cell differentiation 93
4.4.4 Molecular investigation of focal adhesion related components, integrin and discoidin domain receptors 96
4.5 Discussion 97
4.6 Supplementary material 102
4.7 References 105
5 Biomaterials surface energy driven ligand assembly strongly regulates stem cell mechanosensitivity and fate on very soft substrates 111
5.1 Abstract 112
5.2 Introduction 113
5.3 Materials and Methods 115
5.3.1. Tunable surface energy PDMS substrate preparation 115
5.3.2. Ligand loading and adsorbed protein quantification 116
5.3.3. Atomic force microscopy imaging of ligand topography/roughness 117
5.3.4. Cell culture 117
5.3.5. Cell attachment and morphology 118
5.3.6. Cell differentiation quantification 119
5.3.7. Microscopy and image analysis 120
5.3.8. Real time and quantitative PCR 120
5.3.9. Phosphorylated ROCK quantification 121
5.3.10. Traction force microscopy 121
5.3.11. Time-of-Flight Secondary Ion Mass Spectrometry 122
5.3.12. Stastistical analysis 123
5.4 Results 123
5.4.1. Surface energy driven collagen assembly is consistent across different PDMS stiffness 123
5.4.2. Surface energy regulates cell adhesion and dominates substrate stiffness 125
5.4.3. Surface energy directs stem cell differentiation 127
5.4.4. Surface energy affects cell contractility 128
5.4.5. Surface energy alters gene expression of collagen receptors and focal adhesion elements 130
5.4.6. Coating with a minimal collagen synthetic peptide rescues mesenchymal stem cell sensitivity to PDMS stiffness 132
5.5 Discussion 134
5.6 Supplementary material 138
5.7 References 143
6 Synthesis 148

6.1 Summary of achievement and main findings 148
6.2 Limitations and future research 151
6.3 Conclusion 155
6.4 References 158
Curriculum vitae 161

Acknowledgements

Obviously, the first person that I would like to thank is Prof. Jess Snedeker that gave me this unique chance to conduct my PhD research in his laboratory. Against all odds, he gave me total freedom and a constant support that allowed me to achieve this work. I am highly grateful for everything he has done for me. I would like to thank my two co-supervisors: Prof. Viola Vogel and Prof. Marcy Zenobi-Wong for giving insightful comments and taking time to read carefully this thesis.

I am also eternally grateful to the staff members of the laboratory for orthopaedic biomechanics at the Balgrist Campus, in particular:

- Barbara Niederöst, who has been enormously generous and kind with helping me in the last phases of my work, I promise I will pay you back for all of this.
- Maja Bollhalder, our wonder woman in the laboratory that did not only push us to join the Kondi and run a triathlon but contributed a lot to this study with her support.
- Hansruedi Sommer that left the laboratory too early who helped me with designing various platforms and the last person with whom I could speak French.
- Dr. Unai Silvan and Dr Niels Goedecke that brought their skills and expertise to this study.
- Claude Holenstein, who was not only my TFM collaborator but also my best buddy in the laboratory. We had fun, depression and joy together during the last four years.
- My motivated students that participated a lot to the success of this project: Milan Jovic, Edward Vertudes, Stephan Reichmuth and Tscherina Janisch.
- The last but not least all the remaining people that already left or are still present in the laboratory with whom I had some helpful discussion and shared some amazing time: Amro Hussein, Stefania Wunderli, Dr. Yufei Li, Dr. Jennifer Cadby, Dr. Gion Fessel, Dr. Xiang Li, Angelina

Schonenberger, Fabian Passini, Elias Bachmann, Beda Rutishauser, Jonas Widmer, Aron Horvath and Dr. Jasper Foolen.

I also would like to thank the institute for biomechanics that brought up some interesting questions during the colloquia and also the members of the osteosarcoma group that gave some very helpful biological support and also simply because I had some really good time with them: Dr. Ana Gvozdenovic, Dr. Carmen Campanile, Dr. Bernhard Robl, Alek Majumbar, Joaquin Urdinez and Dr. Alexander Boro.

Furthermore, I would like to thank the great people at the center for microscopy at University of Zürich and the FACS facility in Hönggerberg.

Outside of the laboratory, I am extremely lucky to be surrounded by some amazing friends that always supported me in Zürich, in Romandie and in the rest of the world, in particular: Dr. Evelyne Nguyen, Dr. Reda Hasballa, Dr. Lucas Sinclair, Dr. Giorgio Corbellini, Dr. Julien Bryois, Dr. Aline Roch, Dr. Olivier Mégel, Dr. Marc Jordi, Loïc Saulnier, Xavier Adam, Xavier Fouinat, Xavier Fontana, Adriana De Pesters, Yannick Bohren, Layal Bohren, Guillaume Saurais, Céline Gandar, Maelis Nibourel, Mirjam Lutz, Lukas Nibourel, Lukas Pinzger, the Baden crew (Angie, Annina, Alex, Nix, Eliane, Marco, René, Florian, Marc and Beni), the whole Feldmeilen football team (Paolo, Quincy, Niels, Max, Alan, …) and my very understanding working colleagues at Nobel Biocare (Dr. Jessica Gilgenbach Blume, Dr. Angelines Gasser, Dr. Michael Sandholzer, Dr. Philipp Lienemann, Dr. Agnieszka Kubanska, Mauro Caggio and many more).

All this work would have never been possible without the education, love and the generous financial support from my family and particularly my parents Jean and Nirisoa but also my brothers Haja and Herizo and the rest of my big family in Europe, Canada and Madagascar. I cannot of course forget my second family, the Meiers (Dorli, Werner, Roger, Tanja, Remo and Daniela) that have been so great and nice to me during the last years. I would like to especially thank Dorli and Werner that were so supportive, generous, patient, kind and simply marvelous. I promise I will now attend more regularly the raclette’s Tuesday and be more often in Saas-Fee.

I would like to conclude the acknowledgement part with the most important person in my life who is Dr. Daniela Meier. I was probably unbearable several times during the last years but she always infinitely supported me. I will never be able to say enough thank you to her for being her and for being always present when I needed her. I hope my PhD gift will be great ;).

Summary

Stem cell-extracellular matrix interactions are driven by topological, mechanical and biochemical properties of a biomaterial substrate. Studies until now have failed to elucidate the unexpected inability of stem cells to sense and react to soft elastomer substrates like polydimethylsiloxane (PDMS) in comparison to hydrogels like polyacrylamide (PAA). While such comparative experiments widely attributed this insensitivity to factors such as substrate noncompliance or amorphous topology, they neglected inherent differences in surface energy between highly hydrophobic PDMS and hydrophilic PAA. This body of work examines the implication of surface energy in stem cell mechanosensitivity.

The first goal of the present doctoral thesis was to develop a PDMS-based platform whose stiffness and surface energy could be independently modulated without altering other potential confounding factors such as mechanical properties and surface topology. Secondly, it was investigated whether altering the surface energy of the platform could affect the assembly of protein ligands, which in turn could influence stem cell adhesion and osteogenic differentiation. Thirdly, it was investigated whether the surface energy-driven ligand assembly could affect stem cell mechanosensitivity to a broad range of PDMS stiffness.

To develop a PDMS-based platform whose particularly surface energy could be modulated, we employed a PDMS-b-PEO surfactant that could be directly added in a very small amount to the standard PDMS slurry. By simply adjusting the weight percentage of surfactant to the PDMS base polymer from 0% to 1.0%, the measured contact angle that determines the surface energy could be tuned from 110° to 40°. Considering the reported contact angle range for optimal cell adhesion, we have selected the adequate surfactant percentage (0.2%) that led to a moderately hydrophilic surface (80°) and named the resulting substrate PEO-PDMS. Mechanical

characterization by bulk compression revealed very similar viscoelastic properties and rigidity for both pristine PDMS and PEO-PDMS of different base to catalyst ratios. Multi-scale mechanical testing exhibited a broad range of PDMS stiffness. Furthermore, indentation at microscale within the focal adhesion dimensions indicated homogeneity and integrity of the surface prior and after surface treatment with a commonly used heterobifunctional linker to allow covalent protein ligand coating, which is activated under UV.

Next, we evaluated whether controlling for surface energy on our previously developed platform could influence our collagen model ligand assembly and affect in turn osteogenic stem cell signalling early events. While we first ensured to have the same ligand density on the different substrates by adapting empirically the collagen loading molarity, we observed by scanning electron microscopy (SEM) and atomic force microscopy (AFM) a difference in ligand assembly on the hydrophobic PDMS and hydrophilic PEO-PDMS surfaces. While collagen molecules appeared clumpy and formed a relatively rough layer with numerous aggregates on PDMS, they formed a smooth layer on PEO-PDMS. Cellular and molecular investigations with human bone marrow stromal cells indicated higher osteogenic differentiation and upregulation of focal adhesion-related molecules on the resulting smooth collagen layer coated surfaces.

Finally, we fabricated various PDMS and PEO-PDMS substrates of different stiffness to assess whether the surface energy-driven ligand assembly may alter stem cell mechanosensitivity. When seeded on hydrophobic PDMS of different stiffness, stem cells could spread and osteogenically differentiate on all the substrates. In contrast, cells cultured on hydrophilic PEO-PDMS of different stiffness presented on softer substrates (<1kPa) a reduced cell spreading and lower osteogenic differentiation. Furthermore, we developed a novel traction force microscopy (TFM) platform to assess cellular contractility. Although cells could spread on soft PDMS (<1kPa), the measured cell contractility by TFM and activity of Rho Kinase (ROCK) were diminished in comparison with stiffer substrates (> 5kPa).

In conclusion, a novel silicone-based system whose stiffness and surface energy can be independently modulated to investigate quantitatively stem cell mechanobiology has been developed. Furthermore, the use of the platform has proven to be relevant in open biological questions: (i) the key role of surface energy in driving stem cell differentiation by modulating ligand assembly and the resulting topography; (ii) the relationship between cell morphology, contractility and fate.

Résumé

Les interactions entre la matrice extracellulaire et les cellules souches sont contrôlées par les propriétés mécaniques et biochimiques du substrat composé de biomatériaux. Les études jusqu'à ce jour n'ont pas pu expliquer l'incapacité inattendue des cellules souches à sentir et réagir aux substrats mous d'élastomère tels que le polydimethysiloxane (PDMS) en comparaison des hydrogels tels que le polyacrylamide (PAA). Alors que les précédentes expériences comparatives attribuent essentiellement cette insensibilité aux facteurs tels que la non-souplesse des substrats ou encore la topologie amorphe du polymère, ils ont négligé les différences inhérentes d'énergie de surface entre le PDMS hautement hydrophobe et le PAA hydrophile. Cette thèse doctorale examine l'implication de l'énergie de surface dans la mechanosensibilité des cellules souches.

Le premier but de cette thèse doctorale était de développer une plateforme composée de PDMS dont la dureté et l'énergie de surface pouvaient être indépendamment modulés sans affecter les autres facteurs pouvant influer tels que les propriétés mécaniques et la topologie de surface. Deuxièmement, nous avons investigué si la modification de l'énergie de surface de la plateforme pouvait affecter l'assemblage des ligands protéiques qui en retour pourrait influencer l'adhésion des cellules souches et la différentiation ostéogénique. Troisièmement, nous avons investigué si l'assemblage des ligands contrôlé par l'énergie de surface pouvait affecter la méchanosensibilité des cellules souches à une large gamme de rigidité de PDMS.

Pour développer une plateforme composée de PDMS dont l'énergie de surface pouvait être modulée, nous avons utilisé un surfactant de PDMS-b-PEO qui peut être ajouté directement en petite quantité à la mixture de PDMS. En ajustant simplement le pourcentage du poids du surfactant en fonction du poids du polymère de PDMS de base de 0% à 1%, l'angle de

contact mesuré qui détermine l'énergie de surface, pouvait être réduit de 110° à 40°. Prenant en considération la gamme reportée pour l'angle de contact étant optimale pour l'adhésion cellulaire, nous avons choisi le pourcentage adéquat de surfactant (0.2%) qui menait à une surface hydrophile modérée que nous avons appelé le substrat PEO-PDMS. La caractérisation mécanique par compression à des ratios différents de base par rapport au catalyseur indiquait des propriétés viscoélastiques et une rigidité très similaires pour le PDMS et le PEO-PDMS. Les tests mécaniques du PDMS à plusieurs niveaux montraient une large gamme de souplesse et de dureté. De plus, l'indentation à l'échelle du micron dans les dimensions de l'adhésion focale indiquait une homogénéité et une intégrité de la surface avant et après le traitement de surface avec un connecteur covalent pour des ligands protéiques qui est hétéro-bifonctionnel et activé sous UV.

Ensuite, nous avons évalué si le contrôle de l'énergie de surface de notre plateforme précédemment développée pouvait influencer l'assemblage du ligand modèle que nous avons choisi qui est le collagène et ainsi affecter en retour les évènements précurseurs de la signalisation ostéogénique des cellules souches. Après avoir vérifié que la densité de ligand était la même sur les différents substrats en adaptant de manière empirique la molarité du collagène qui est utilisée, nous avons observé sous SEM et AFM une différence dans l'assemblage des ligands sur les surfaces du PDMS hydrophobe et du PEO-PDMS hydrophile. Alors que les molécules de collagène apparaissaient agglutinées et formaient une couche rugueuse avec des nombreux agrégats sur le PDMS, elles formaient une couche lisse sur le PEO-PDMS. Les analyses moléculaires et cellulaires avec des cellules stromales humaines originaires de la moelle osseuse indiquaient que sur les surfaces couvertes d'une couche lisse de collagène présentaient une plus haute différentiation ostéogénique et une régulation positive des molécules impliquées dans l'adhésion focale.

Dernièrement, nous avons fabriqué différents substrats de PDMS et PEO-PDMS avec différentes rigidités pour évaluer si l'assemblage des ligands contrôlé par l'énergie de surface pouvait affecter la mechanosensibilité des cellules souches. Quand les cellules souches sont cultivées sur le PDMS hydrophobe de différentes rigidités, elles pouvaient se répandre et se différencier de manière ostéogénique sur tous les substrats. A l'inverse, les cellules cultivées sur les substrats hydrophiles de PEO-PDMS ayant différentes rigidités présentaient sur les substrats mous (<1kPa) un épandage réduit et une diminution de la différentiation ostéogénique. De plus, nous avons développé une nouvelle plateforme de « traction force microscopy » (TFM) pour évaluer la contractilité cellulaire. Alors que les cellules pouvaient se répandre sur le PDMS mou (<1kPa), la contractilité cellulaire mesurée par le TFM ansi que l'activité du Rho Kinase (ROCK) étaient diminuées en comparaison avec les substrats plus rigides (>5 kPa).

En conclusion, un nouveau système à base de silicone dont la dureté et l'énergie de surface peuvent être indépendamment modulées a été développé pour investiguer de manière quantitative la biologie mécanique des cellules souches. De plus, l'utilisation de la plateforme a montré son utilité dans diverses questions biologiques telles que : (i) le rôle clef de l'énergie de surface dans le contrôle de la différentiation des cellules souches en modulant l'assemblage des ligands et la topographie résultante ; (ii) la relation entre la morphologie cellulaire, la contractilité et le destin des cellules souches.

Chapter 1

1 Introduction

1.1 Thesis motivation

Interest in Mesenchymal Stem Cells (MSCs) has drastically increased over the last years in different biomedical disciplines because of their key role in orchestrating tissue healing and homeostasis. MSCs present remarkable attributes by having high self-renewal capacity and differentiation ability towards various cell phenotypes. Cues from the extracellular matrix (ECM) to which MSCs adhere are known to regulate their fate. Mechanical factors including rigidity and topography have appeared to be key determinants among the cues that govern cell fate [1]. While environmental sensing is mainly attributed to the integrin receptors that connect to the force generating cytoskeleton and activate downstream signalling [2], recently described receptors such as discoidin domain receptors were found to recognize different ECM structures but a little is known about their activity [3]. To elucidate the mechanism of stem cell-ECM interaction, researchers have engineered a myriad of synthetic polymer-based platforms that can be tuned for their stiffness and topography. Although previous studies observed MSC sensitivity to material stiffness [4-8], a recent study has challenged the current view of how cells sense and respond to matrix rigidity [6]. Trappmann et al. compared cellular reactions on amorphous polydimethylsiloxane (PDMS) elastomers and porous polyacrylamide (PAAm) hydrogels of different stiffness. They reported an inability for cells to sense PDMS stiffness and suggested that stem cell fate is not governed by the stiffness but the topography of the substrate, which varies in a pore-size dependent manner with hydrogel elasticity [6]. Although PDMS and PAA are regularly compared for investigating stem cell mechanobiology [6, 9], they present very distinct features in terms of mechanical properties, topology and surface energy that may confound the interpretation of cellular reactions. In this dissertation, we decided to focus on the potential critical role of surface energy at the stem cell-material interface.

PDMS is often used as a substrate for 2D cell culture but also for microfluidic systems due to its combination of inertness and excellent physical properties. Its chemicophysical properties and structure can be easily tailored that makes it a convenient platform to investigate the mechanosensitivity of stem cells to their environment. In contrast to PAA hydrogels, PDMS presents a low surface energy from the abundance of methyl groups which renders the elastomer highly hydrophobic (water contact angle is around 120°[10]) ,which is known to affect protein adsorption, assembly and cell adhesion [11-13]. To increase the surface energy, several surface modification methods exist which can be classified intro three main categories: surface activation, physical modification and chemical modification [14]. However, effects of these approaches are often just temporary or very complicated and modify the mechanical properties of the upper layer surface [15, 16].

The goal of this doctoral work was to develop a novel PDMS-based platform that met the criteria for studying the relationship between surface energy, ligand assembly and mesenchymal stem cell mechanosensitivity i.e. isotropic, amorphous, tunable for stiffness and surface energy, biocompatible and functionalizable with ECM protein ligands.

1.2 Specific aims

Specifically, the three following aims have been defined:

Aim 1. Development and characterization of a surface energy-tunable PDMS-based platform for 2D stem cell culture.

Aim 2. Study of the effects of surface energy on ligand topography and stem cell differentiation using the platform developed in Aim 1.

Aim 3. Study of the effects of surface energy-driven ligand topography on stem cell mechanosensitivity using the platform developed in Aim1

1.3 Outline of the thesis

This dissertation is presented into the following six chapters: an introduction to the doctoral work defining the specific aims, a chapter of general background information, three chapters containing each a scientific study that addressed the specific aims and a concluding synthesis of the accomplished work, including possible future directions for further investigation.

Chapter 1 presents the motivation for this doctoral thesis and its specific aims.

Chapter 2 contains the necessary background for the study of stem cell mechanobiology and the state of the art regarding platforms for investigating stem cell material interactions.

Chapter 3 describes the development of a novel PDMS-based platform whose stiffness and surface energy can be independently modulated while preserving the pristine mechanical properties of the elastomer. It highlights the feasibility of controlling PDMS hydrophobicity with an easy and straightforward method.

Chapter 4 refers to the characterization of surface energy driven collagen assembly on the previously developed platform. It describes an important difference in resulting collagen coated surface topography on hydrophobic and hydrophilic PDMS surfaces. Furthermore, the effects on stem cell adhesion and differentiation were investigated.

Chapter 5 extends the previous investigation to a broad range of matrix stiffness to evaluate the interplay between surface energy and ligand assembly on mechanosensitivity of stem cells to their substrate. The development of a novel Traction Force Microscopy, which has the main advantage of limiting confounding factors and improving traction measurement accuracy, is also described.

Chapter 6 summarizes the main achievements and findings of the work, along with a discussion regarding the different limitations and potential directions for future investigation.

1.4 References

[1] D.A. Lee, M.M. Knight, J.J. Campbell, D.L. Bader, Stem cell mechanobiology, Journal of Cellular Biochemistry 112(1) (2011) 1-9.

[2] B. Geiger, J.P. Spatz, A.D. Bershadsky, Environmental sensing through focal adhesions, Nat Rev Mol Cell Biol 10(1) (2009) 21-33.

[3] H.L. Fu, R.R. Valiathan, R. Arkwright, A. Sohail, C. Mihai, M. Kumarasiri, K.V. Mahasenan, S. Mobashery, P. Huang, G. Agarwal, R. Fridman, Discoidin domain receptors: unique receptor tyrosine kinases in collagen-mediated signaling, The Journal of biological chemistry 288(11) (2013) 7430-7.

[4] A.J. Engler, S. Sen, H.L. Sweeney, D.E. Discher, Matrix Elasticity Directs Stem Cell Lineage Specification, Cell 126(4) (2006) 677-689.

[5] N.D. Evans, C. Minelli, E. Gentleman, V. LaPointe, S.N. Patankar, M. Kallivretaki, X.Y. Chen, C.J. Roberts, M.M. Stevens, Substrate Stiffness Affects Early Differentiation Events in Embryonic Stem Cells, European cells & materials 18 (2009) 1-14.

[6] B. Trappmann, J.E. Gautrot, J.T. Connelly, D.G.T. Strange, Y. Li, M.L. Oyen, M.A. Cohen Stuart, H. Boehm, B. Li, V. Vogel, J.P. Spatz, F.M. Watt, W.T.S. Huck, Extracellular-matrix tethering regulates stem-cell fate, Nature materials 11(7) (2012) 642-649.

[7] R.I. Sharma, J.G. Snedeker, Biochemical and biomechanical gradients for directed bone marrow stromal cell differentiation toward tendon and bone, Biomaterials 31(30) (2010) 7695-7704.

[8] J. Fu, Y.-K. Wang, M.T. Yang, R.A. Desai, X. Yu, Z. Liu, C.S. Chen, Mechanical regulation of cell function with geometrically modulated elastomeric substrates, Nat Meth 7(9) (2010) 733-736.

[9] J.H. Wen, L.G. Vincent, A. Fuhrmann, Y.S. Choi, K.C. Hribar, H. Taylor-Weiner, S. Chen, A.J. Engler, Interplay of matrix stiffness and protein tethering in stem cell differentiation, Nature materials 13(10) (2014) 979-87.

[10] S.H. Tan, N.-T. Nguyen, Y.C. Chua, T.G. Kang, Oxygen plasma treatment for reducing hydrophobicity of a sealed polydimethylsiloxane microchannel, Biomicrofluidics 4(3) (2010) -.

[11] D.P. Dowling, I.S. Miller, M. Ardhaoui, W.M. Gallagher, Effect of surface wettability and topography on the adhesion of osteosarcoma cells on plasma-modified polystyrene, J Biomater Appl 26(3) (2011) 327-347.

[12] N.M. Coelho, C. Gonzalez-Garcia, J.A. Planell, M. Salmeron-Sanchez, G. Altankov, Different assembly of type IV collagen on hydrophilic and hydrophobic substrata alters endothelial cells interaction, European cells & materials 19 (2010) 262-72.

[13] F.G.a.M.K. Feld, Fibronectin adsorption on hydrophilic and hydrophobic surfaces detected by antibody binding and analyzed during cell adhesion in serum-containing medium, J Biol Chem. 10;257(9):4888-93 (1982).

[14] I. Wong, C.-M. Ho, Surface molecular property modifications for poly(dimethylsiloxane) (PDMS) based microfluidic devices, Microfluid Nanofluid 7(3) (2009) 291-306.

[15] D.T. Eddington, J.P. Puccinelli, D.J. Beebe, Thermal aging and reduced hydrophobic recovery of polydimethylsiloxane, Sensors and Actuators B: Chemical 114(1) (2006) 170-172.

[16] Y.L. G. Bartalena, T. Zambellid and J. G. Snedeker, Biomaterial surface modifications can dominate cell–substrate mechanics: the impact of PDMS plasma treatment on a quantitative assay of cell stiffness, Soft Matter 8(3) (2012) 673-681.

CHAPTER 2

2 Background

2.1 Role of the microenvironment in controlling stem cell behavior

2.1.1 The extracellular matrix

Every cell is surrounded by the extracellular matrix, which is a complex and dynamic macromolecular network. While each tissue has a unique composition, the ECM is essentially composed of water, proteins and polysaccharides [1]. ECM macromolecules usually form supramolecular structures with various molecular classes that differ both in their type and their relative amount [2]. Fibrillar collagens are the most dominant proteins in the ECM. While formed by three polypeptide α-chains, all collagen molecules present a triple helical structure, which is determinant for cell receptor binding [3]. Each α-chain exhibits one or more regions containing the repeating amino acid motif Gly-X-Y, where X and Y can be any amino acid, but commonly they are proline and hydroxyproline (Fig. 2.1). Four different integrin receptors have been shown to bind collagen: α1β1, α2β1, α10β1 and α11β1. The interaction between integrin and collagen involves the von Willbrand factor A-like domain (A-domain), also named an inserted domain (I-domain). By employing synthetic peptides that could form a triple helix, Knight and coworkers found the sequence GFOGER as a major binding site in collagen for α1β1 and α2β1 integrin receptors [4]. While both α1β1 and α2β1 bind to collagen types I and IV, α1β1 binds to collagen IV with higher affinity than to type I and conversely for α2β1 [5].

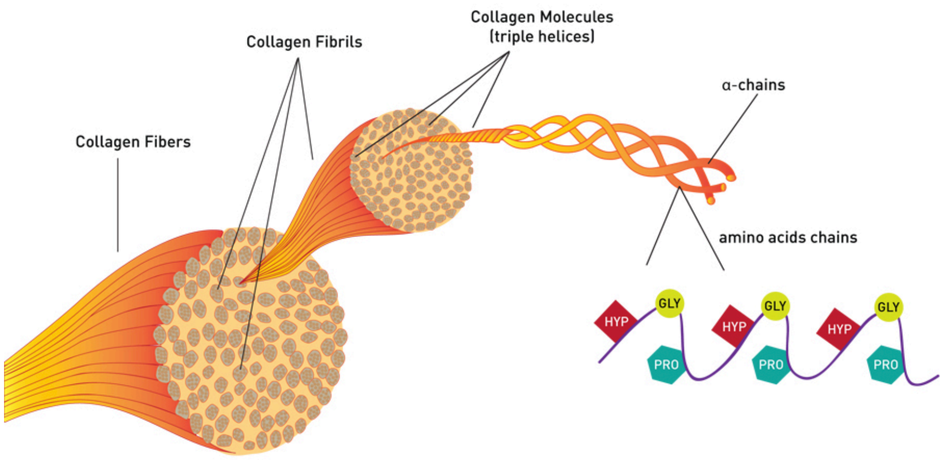

Figure 2.1 | Triple-stranded helical structure of the collagen fibrils (adapted from www.protocol.com)

Other major structural components such as proteoglycans and hyaluronic acid also contribute to the supportive scaffold within which other ECM components and cells interact. Additional ECM components, such as laminin or fibronectin (FN), make the bridge between different structural ECM components and connect the ECM to cells and to soluble molecules. Fibronectin has been shown to not only be important in cell adhesion and differentiation during wound healing by being accumulated during the first 24 hours after injury but also has a critical role in vertebrate development [6, 7]. While FN consists of a dimer, each monomer is composed of three types of repeating units: type I, type II and type III. These repeating units contain specific binding sites for cell surface receptors such as the Arg-Gly-Asp (RGD) amino acid sequence. Among the various cell surface receptors, integrin family play not only an important role as anchoring molecules but are also important in processes like cell differentiation, wound healing and immune response. About half of the integrin family were found to bind to ECM molecules in a RGD dependent manner [8].

Collagen fibrils represent the major biomechanical scaffold for cell attachment and anchorage of macromolecules. The arrangement of collagen fibrils influences their mechanical and physical properties with for example narrow fibrils (around 20 nm) in the cornea and large fibrils (around 500 nm) in mature tendons [9]. The assembly of collagen molecules into fibrils, named fibrillogenesis, is an entropy-driven protein self-assembly/polymerization through the loss of solvent molecules from the surface of protein molecules, which results in assemblies with a circular cross-section reducing the surface area-to-volume ratio of the final assembly (Fig. 2.1) [10]. The stability of the collagen fold is ensured by the high proline content, which represents for about 20% of the collagen residues. While half of these prolines are hydroxylated, hydroxyproline content was shown to influence the denaturation temperature by increasing thermal stability [11]. While the formation of fibrils occurs in the extracellular space, the collagen molecules are regulated in the cellular environment by many collagen binding proteins such as the Fibril Associated Collagens with Interrupted Triple Helices (FACIT) family collagens and Small Leucine-Rich Proteoglycans (SLRPs). Fibrillogenesis requires the initial conversion of the procollagen molecules secreted by cells into fibril forming-competent molecules by the procollagen metalloproteinases. After removal of the N- and C-propeptides, the fibril-forming collagen molecules are flanked by short telopeptides that do not exhibit a triple-helical conformation and were described as critical for fibril synthesis (Fig. 2.2). The spontaneously formed cross-striated fibrils are stabilized by covalent lysil oxidase cross-linking and inter-helix hydrogen bonds [9]. Furthermore, active FN fibrillogenesis and cellular mechanical forces were shown to play a key role in collagen fibril formation. Previous studies have shown by blocking collagen-binding site on FN that the collagen fibrillogenesis was inhibited [10]. Kubow et al. have recently demonstrated that the interactions between FN and collagen I are mechano-regulated [12].

Surprisingly, collagen fibril formation occurs in vitro in absence of cells. While fibrillar collagen presents in vivo more than 50 binding protein partners to create the diversity in fibril patterns of different tissues such as tendon, ligament, bone and blood vessel, collagen free molecules can bind to each other in vitro and spontaneously assemble into fibrils. Collagen is commonly extracted from various tissues and diluted into acidic solutions, which yields to a collagen monomeric form comprising some variable amounts of cross-linked components. This so-called gelatin is formed by heating the collagen extract in an acidic environment with the breaking of hydrogen bonds between triple helices. Upon neutralization and exposure to temperature between 20 and 34°C, such denatured collagen solutions produce a gel of D-periodic fibrils. While the method to initiate fibrillogenesis was shown to influence the features of the formed fibrils, the diameter of the formed fibrils was shown to be temperature-dependent with larger fibrils at 20°C. In contrast to fibrils formed in vivo that can be polar with N-terminal ends, fibrils formed from acidic solution are only unipolar, presenting a C-terminal and an N-terminal end, therefore influencing fibril fusion. Furthermore, the reconstituted fibrils from collagen extracts do not exhibit the same diameters as the fibrils from which the collagen was isolated [9].

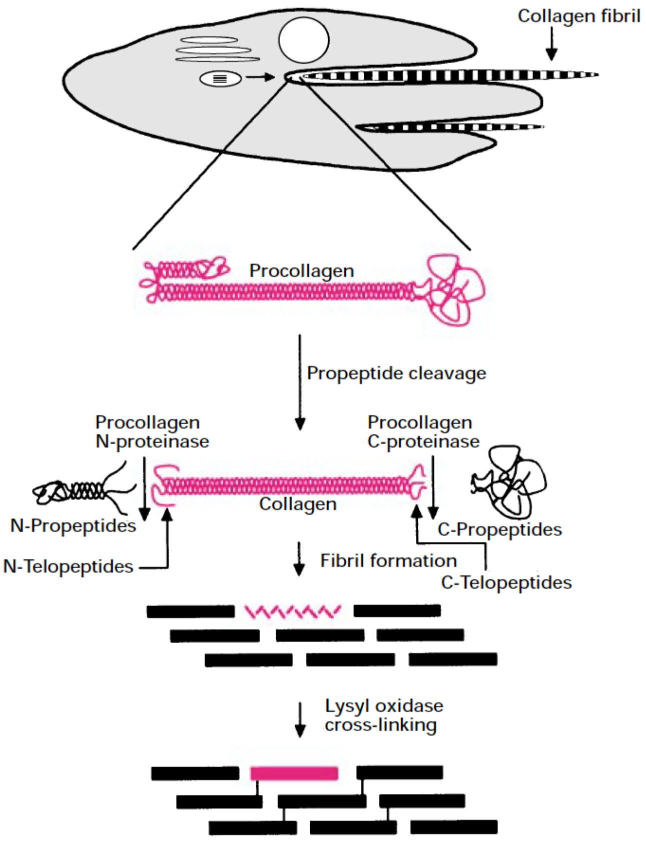
Collagen fibril
Procollagen
Propeptide cleavage
Procollagen
N-proteinase
Procollagen
C-proteinase
Collagen
N-Propeptides
C-Propeptides
N-Telopeptides
Fibril formation
C-Telopeptides
Lysyl oxidase
cross-linking

Figure 2.2 | Extracellular activities in the formation of fibrillar collagens [9]

The role of the ECM is more than just providing a physical support for tissue integrity since it is a dynamic structure that is continuously remodeled to control tissue homeostasis, particularly in response to injury [13]. Cells constantly rebuild the ECM via synthesis, degradation, reassembly and chemical modification. The ECM can be cleaved by various families of proteases such as the matrix metalloproteinases (MMPs), adamalysins and meprins. Several other enzymes such as MMP inhibitors are required to orchestrate and regulate ECM proteolysis to avoid excessive and deleterious tissue degradation. Since the ECM plays an essential role during development and for the maintenance of tissue homeostasis, a failure in ECM component regulation can lead to disease.

2.1.2 Mesenchymal stem cell niche and tissue healing

Tissue healing is a dynamic process involving complex coordinated events in three overlapping phases: inflammatory, proliferative and remodeling. It requires a coordinated interplay between cells, growth factors, and extracellular matrix components. Mesenchymal stem cells (MSC) play a central role in orchestrating the repair response by recruiting other host cells, secreting growth factors, having antimicrobial activities and synthesizing ECM components [14]. MSCs, also referred to as multipotent mesenchymal stromal cells to denote their origin from the stromal component of bone marrow, have attracted interest of investigators from various biological and medical fields due to their particular biological properties to retain their stemness by self-renewal and their potential for differentiation into several cell types such as bone, cartilage, tendon and fat (Fig. 2.3).

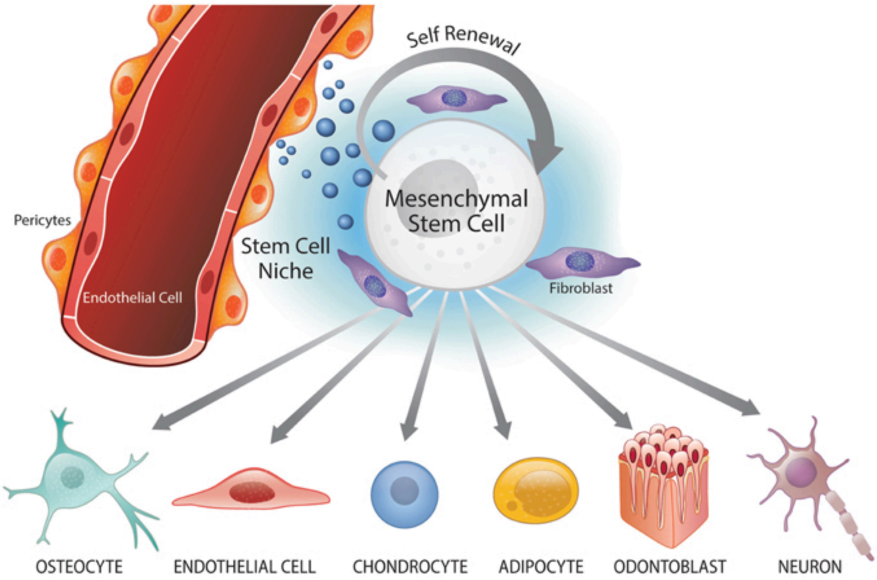
Self Renewal
Pericytes
Endothelial Cell
Stem Cell Niche
Mesenchymal Stem Cell
Fibroblast
OSTEOCYTE
ENDOTHELIAL CELL
CHONDROCYTE
ADIPOCYTE
ODONTOBLAST
NEURON

Figure 2.3 | Perivascular niche and multipotency of mesenchymal stem cells [15]

In culture, MSCs are a heterogeneous population composed of early progenitors and mature cells [16]. A subpopulation of cells named rapidly self-renewing (RS) cells is small, proliferates rapidly and undergoes cyclical renewal. While the more mature cells are bigger, proliferate more slowly, and have a more limited potential to differentiate, they play an important role as a feeder layer and secrete growth factors. MSCs usually remain in a quiescent state until they undergo a cell division to generate either one stem and one differentiated cell via asymmetric self-renewal or two daughter stem cells to maintain the stem cell population through a symmetric self-renewal. Stem cells reside in a dynamic and specific microenvironment, named as '*niche*', which regulates stem cell fate, ensuring a balance between quiescence, self-renewal and differentiation. The niche creates a sort of crosstalk between the need of the surrounding tissue and the maintenance of the stem cell population [17].

2.1.3 Environmental factors directing stem cell behavior

Cells that are not longer preserved in the niche might undergo differentiation, which is controlled by the cues associated with their new microenvironment. The microenvironmental factors are very diverse including soluble and insoluble macromolecular cues, but also mechanical loading [18]. Soluble factors include growth factors, cytokines, hormones and other chemicals. Many previous in-vitro studies have shown that stem cell fate can be easily controlled with a defined medium containing specific supplements such as growth factors of the transforming growth factor (TGF)-β superfamily, β-glycerol phosphate and dexamethasone that are known to induce osteogenic differentiation or 3-isobutyl-1-methyxanthine, insulin and indomethacin to promote adipogenic differentiation [19].

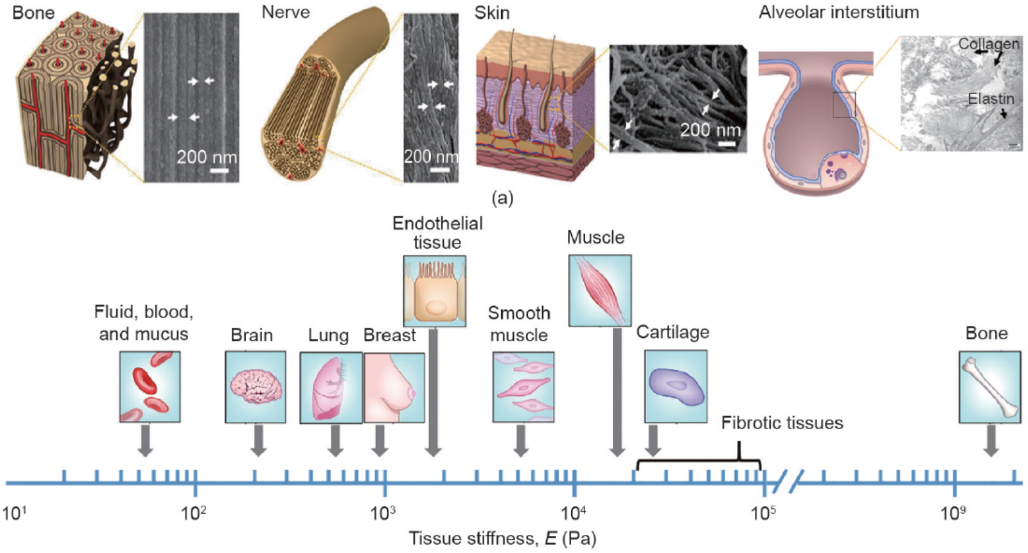
Bone
200 nm
Nerve
200 nm
Skin
200 nm
Alveolar interstitium
Collagen
Elastin
(a)
Endothelial tissue
Muscle
Fluid, blood, and mucus
Brain
Lung
Breast
Smooth muscle
Cartilage
Bone
Fibrotic tissues
10¹
10²
10³
10⁴
10⁵
10⁹
Tissue stiffness, E (Pa)

Figure 2.4 | Biophysical characteristics of human tissues with (a) different nanostructures and (b) different stiffness [20]

While each tissue presents an environment with a specific composition and structure, chemical and physical cues from the extracellular matrix were also found to direct stem cell fate. As mentioned earlier, cells interact with the ECM by employing adhesive interactions with specific protein molecules. Previous studies have shown that the nature of the present ligand can determine the fate. They demonstrated that the various ligand proteins such as collagen, fibronectin and laminin modulate the expression of neurogenic, myogenic and osteogenic markers [21, 22].

Over the last decade, the role of physical cues in guiding stem cell fate became a major field of interest. Considering the range of stiffness of solid tissues (Fig. 2.4), Engler and coworkers have proven that the elasticity of a porous gel coated with collagen direct the stem cell lineage differentiation: (i) in the range of 0.1-1kPa, cells differentiate towards neurogenic lineage; (ii) in the range of 8-17kPa, cells differentiate towards myogenic lineage and; (iii) in the range of 25-40kPa, cells differentiate towards osteogenic lineage [23]. Topography of the microenvironment is another physical cue that influences stem cell differentiation. The ECM of various tissues such as bone, cartilage or blood vessels present different micro- and nanoscale topographic features. For example, blood vessels present an anisotropic alignment of nanofibers in the basement membrane. In contrast to blood vessels, bone tissues present a complex and hierarchical structure in their ECM [24]. While microtopography with a feature size bigger than 10 μm mainly affects the whole cell morphology, evidences indicated that micro/nanotography influences subcellular mechanisms [25] . In vitro studies demonstrated that average roughness (R_a) close to 1 μm is optimal to induce osteogenic differentiation of mesenchymal stem cells [26]. While adhesion of various cells is influenced by a surface roughness value R_a between 10 and 100 nm, Takeuchi et al. reported that a R_a of 110 nm on acid-etched titanium surface promoted more strongly osteogenic differentiation when compared to a R_a of 49 nm [24, 27]. Besides the dimension of topographical cues, Dalby et al have shown that the distribution of topographical features affects also stem cell fate. A controlled disorder of nanopits on a surface induced MSCs to differentiate towards bone cells in the absence of osteogenic supplements [28].

Dynamic mechanical strains were proven to play an important role in the development and preservation of functional connective tissues, which suggests their implication in controlling stem cell differentiation. For instance, Kearney et al. have demonstrated that MSCs cultured on elastomer substrates that underwent cyclic tensile mechanical strain for 14 days showed a significant increase in BMP2 which, is an autocrine osteogenic growth factor [29]. Furthermore, another study has shown that cyclic mechanical stretching could promote osteogenic differentiation of MSCs cultured on flexible-bottomed culture plates without any osteogenic supplements [30].

2.2 Environmental sensing by stem cells

2.2.1 Mechanical cues as key regulators

2.2.1.1 The integrin signaling to the cytoskeleton

Among the microenvironmental cues that direct stem cell fate, mechanical factors including elasticity and topology of the ECM have emerged as key regulators. Cells sense the mechanical properties of their environment by exerting contractile forces via focal adhesion complexes that link the ECM to the force-generating cytoskeleton through transmembrane receptors such as integrins (Fig. 2.5). The associated molecular transduction cascades are then activated based on binding specificity and stresses that are generated during contraction [31]. Integrins are a family of around 25 heterodimeric receptors, which are composed of different combinations of α and β subunits. The combination of αβ subunits defines binding affinity and signaling properties. Most integrins recognize multiple ECM proteins, and some matrix proteins such as collagen and fibronectin bind to several different integrins: 4 collagen receptor integrins (α1β1, α2β1, α10β1 and α11β1) and around 10 different fibronectin receptor integrins [32]. After their activation from conformational change, integrins bind to their ligand and often cluster into focal adhesion complexes that ensure cell-substrate adhesion and play an important role in mechanical signaling. Focal adhesions assemble in response to substrate properties such as rigidity and topography. The cell cytoskeleton is composed of several different interacting molecular networks that involve intermediate filaments, microtubules and actin-based microfilaments. The spatiotemporal regulation of the filamentous actin (F-actin) cytoskeleton networks controls cell morphology change and force generation in cellular migration and division [33]. Several actin-binding proteins regulate the kinetics of F-actin assembly and the organization of the network. Mechanical properties of the contractile F-actin networks linked to focal adhesions determine the magnitude of forces transmitted to outside the cell as well as the mechanical response of the cell to applied stresses and strains. Stress fibers are a specific type of contractile F-actin bundle composed of repeating units of myosin-II motor proteins and actinin. Each actin bundle is made of 10-30 filaments and can develop contractile forces in the range of 100pN. A Ca^{2+}-dependent calmodulin/myosin light chain kinase (MLCK) system and a Ca^{2+}-independent Ras homology (Rho)-kinase system through MLC phosphorylation control stress fiber contraction [31].

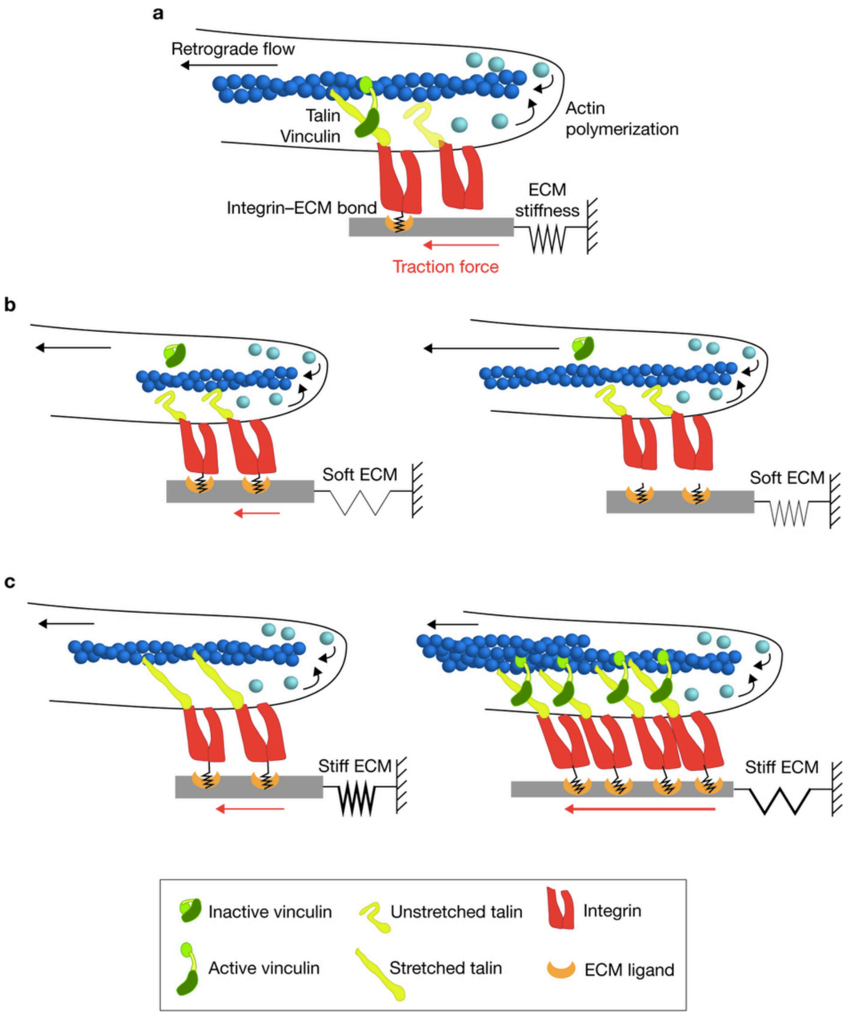
a
Retrograde flow
Talin
Vinculin
Actin
polymerization
Integrin–ECM bond
ECM
stiffness
Traction force
b
Soft ECM
Soft ECM
c
Stiff ECM
Stiff ECM
Inactive vinculin
Unstretched talin
Integrin
Active vinculin
Stretched talin
ECM ligand

Figure 2.5 | The molecular clutch model for mechanotransduction [34]

2.2.1.2 Discoidin domain receptors in collagen-mediated signaling

Another less described ECM signaling is the interaction of collagen with the discoidin domain receptors (DDR) (Fig. 2.6). DDRs were found to regulate cell adhesion, proliferation, differentiation and extracellular matrix remodeling [35]. The DDR family is composed of two distinct receptor tyrosine kinase (RTK) members, DDR1 and DDR2, which undergo tyrosine autophosphorylation upon collagen binding. All DDRs are single-pass type I transmembrane glycoproteins that contain six different protein domains including the discoidin domain. The discoidin domain is believed to be responsible for modulating DDR specificity for fibrillar and non-fibrillar collagens. For example, culturing cells on monomeric collagen showed a reduced DDR2 activity when compared to cells on polymerized collagen. Therefore, structural ECM modifications that support collagen remodeling may affect DDR signaling [36]. While both DDRs are activated by fibrillar collagens I-III and V, collagen IV was shown to trigger only DDR1 and non-fibrillar collagen X to stimulate DDR2 [36].

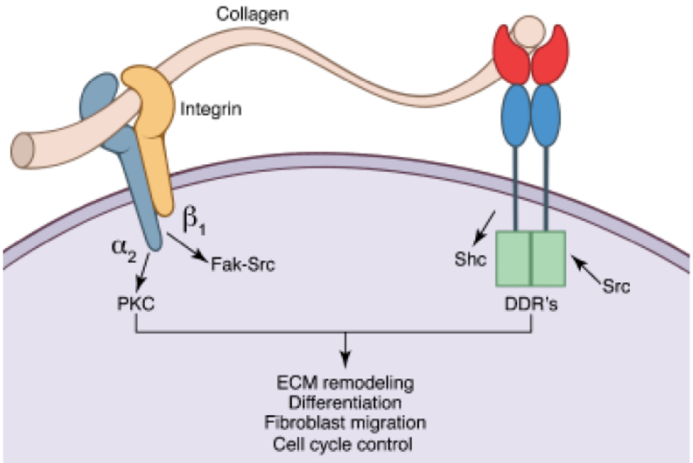

Figure 2.6 | Fibrillar collagen binding to integrin and discoidin domain receptors [37]

2.2.2 Mechanotransduction and lineage specification

To enable a rapid reaction to environmental change, cells employ focal adhesion-associated adaptor proteins to recruit key factors of mechanotransduction pathways. Talin and vinculin are important FA proteins mediating the molecular mechanical "*clutch*" linkage between ECM-bound integrins and actin (Fig. 2.5). Activation of vinculin through a conformational change leads to a strong affinity binding to talin that stabilizes and induces the growth of the FA [38]. Vinculin is composed of a globular head linked to a tail domain, which presents numerous binding sites mainly for actin, α-actinin, talin and paxillin. Talin has also a globular head that binds β-integrins to couple the cytoskeleton to the ECM and can activate signaling through vinculin binding, for assembly and reorganization of the actin skeleton [39]. Paxillin is another signal transduction adaptor protein that contributes to the recruitment of several regulatory and structural proteins including vinculin to FA [40].

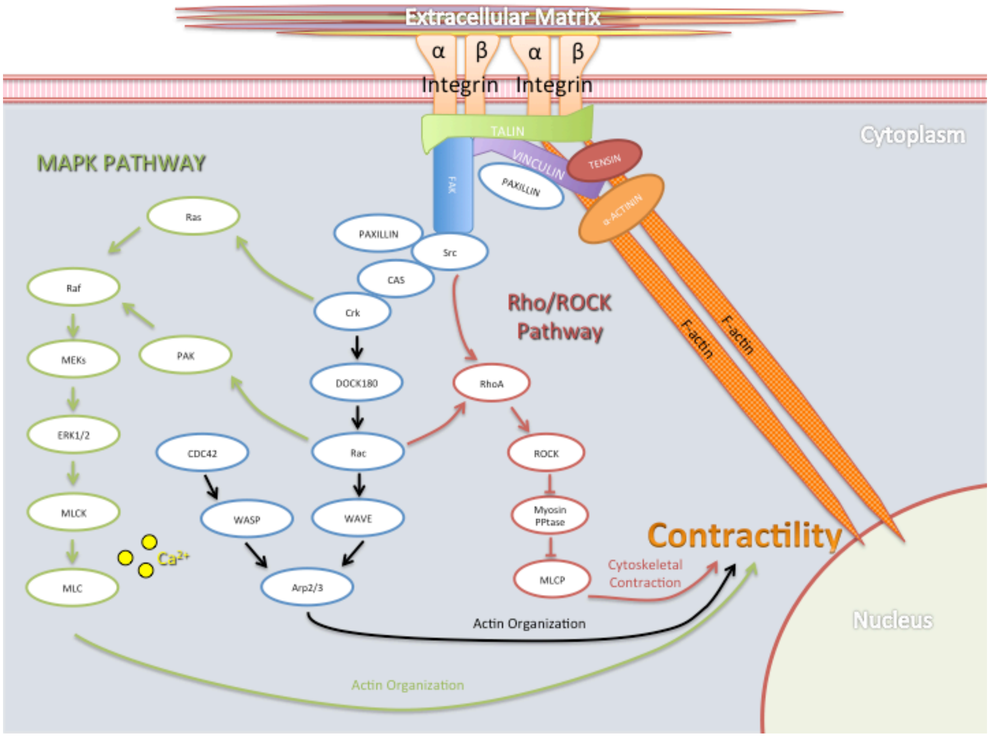
Extracellular Matrix
α
β
α
β
Integrin
Integrin
TALIN
Cytoplasm
MAPK PATHWAY
VINCULIN
TENSIN
FAK
PAXILLIN
α-ACTININ
Ras
PAXILLIN
Src
Raf
CAS
Crk
Rho/ROCK
Pathway
F-actin
F-actin
MEKs
PAK
DOCK180
RhoA
ERK1/2
CDC42
Rac
ROCK
MLCK
WASP
WAVE
Myosin
PPtase
Contractility
Ca2+
MLC
Arp2/3
MLCP
Cytoskeletal
Contraction
Actin Organization
Nucleus
Actin Organization

Figure 2.7 | The mitogen-activated protein kinase (MAPK) and Rho Kinase (ROCK) pathways regulating cellular contractility

Recent studies have demonstrated that stretching of cytoskeletal attached molecules expose binding sites for other proteins to amplify biochemical signals upon activation by force. For example, del Rio and coworkers showed that physiologically relevant forces (0-12pN) induced stretching of single talin rods that exposed cryptic binding sites for vinculin [39].

The RhoA/ROCK pathway (Fig. 2.7) has been extensively investigated for its central role in cytoskeleton organization and contractility [41]. Through the activation by RhoA, ROCK phosphorylates in a Ca^{2+}-independent manner the myosin light chain, which directly modulates stress fibers and focal adhesion [42]. Focal adhesion kinase (FAK) and Src kinase are tyrosine kinases that play a role of early mediator of integrin-mediated signaling. Autophosphorylation on Tyr397 of FAK leads to the recruitment of Src through the SH3 domain which activates RhoA GTPase [43]. Additionally, FAK/Src signaling complex also involves the recruitment of Cas and paxillin, which creates additional binding sites for Crk. Crk and FAK recruit FA and activate the downstream mitogen-activated protein kinases (MAPK) pathway [44]. MAPK pathway activates calmodulin and MLC kinase, which stimulates contractility by phosphorylation of MLC. Evidences demonstrated that calcium ion concentration alters particularly MLC phosphorylation [42]. Stretch-activated ion channels may act as important mechanosensors by allowing calcium influx under mechanical stimulation of the plasma membrane [45].

While a little is known about these signalling molecules, several adaptor proteins were also identified to be recruited to phosphorylated sites on the DDRs including the ShcA, the Nck1/2 and Shp-2 (Fig. 2.8). The activated downstream signalling pathways are not fully understood and seem to be cell-type dependent. For example, DDR1 was reported to modulate the MAPK pathway via activation of ERK 1/2 in smooth muscles and repression in mesangial cells [46]. While DDR activation occurs independently of integrins, evidence shows that DDRs and integrins can regulate each other function. It has been previously shown that DDR1 may affect the integrin α2β1 by inhibiting the activity of signal transducers and activators of transcription (STAT) 1/3 and the small Rho GTPase CDC42 in Madin-Darby canine kidney (MDCK) cells [36].

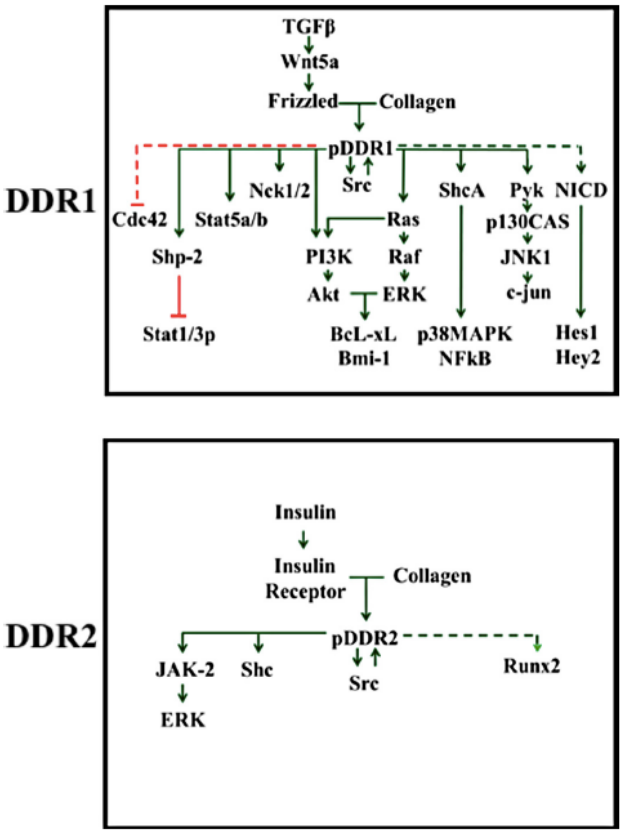
DDR1
TGFβ
Wnt5a
Frizzled
Collagen
pDDR1
Src
Cdc42
Stat5a/b
Nck1/2
Shp-2
Stat1/3p
PI3K
Akt
Ras
Raf
ERK
BcL-xL
Bmi-1
ShcA
p38MAPK
NFkB
Pyk
p130CAS
JNK1
c-jun
NICD
Hes1
Hey2
DDR2
Insulin
Insulin Receptor
Collagen
pDDR2
Src
JAK-2
ERK
Shc
Runx2

Figure 2.8 | Discoidin domain receptor (DDR) signaling. Solid and dashed green lines designate respectively direct and indirect positive signaling effectors. Solid and dashed red lines designate direct and indirect negative signalling effectors [36].

In contrast to the inhibition of MDCK cell adhesion, overexpression of DDR1 or DDR2 was shown to enhance activation of integrin-mediated cell adhesion to collagen-I in human embryonic kidney cells. Therefore, the DDRs can positively or negatively modulate the integrin pathway in several manners [46]. Cell contractility-associated pathways were demonstrated to be crucial for MSC fate regulation. When MSCs were cultured on various substrates having different elasticities, upregulation of ROCK, FAK but also osteogenic markers such as the Runt-related transcription factor (RUNX2) were observed on the stiffer ones. In contrast, MSCs cultured on soft matrices presented a low cell spreading with small Rho-induced stress fibers. While differentiation supplements are usually necessary, adipogenic and chondrogenic differentiations were strongly increased on soft substrates in the range of 1kPa with upregulation of respective transcription factors such as Sox9 and the peroxisome proliferator-activated receptor (PPARY) [31]. Activation of specific lineage transcription factors requires the nuclear translocation of associated key molecules such as smads, yes-associated protein/ transcriptional coactivator with PDZ binding motif (YAP/TAZ) and β-catenin of the Wnt signalling pathway (Fig. 2.9). YAP and TAZ were shown to interact with TGF-β/smad pathway and regulate cell differentiation via BMP2, Runx2 and PPARY [31]. Furthermore, the cytoskeletal tension is transduced across the nuclear envelope via the linker of nucleoskeleton and cytoskeleton (LINC) complex that connects the cytoskeleton with the nuclear lamina. The interaction between the nuclear and cytoplasmic mechanotransduction has been recently described and highlights the role for the nucleus as a rheostat in translating the cell-mechanical response [47, 48]. The phosphorylation level of lamin A/C has been shown to correlate with tissue stiffness, with variation promoting substrate stiffness directed differentiation [47].

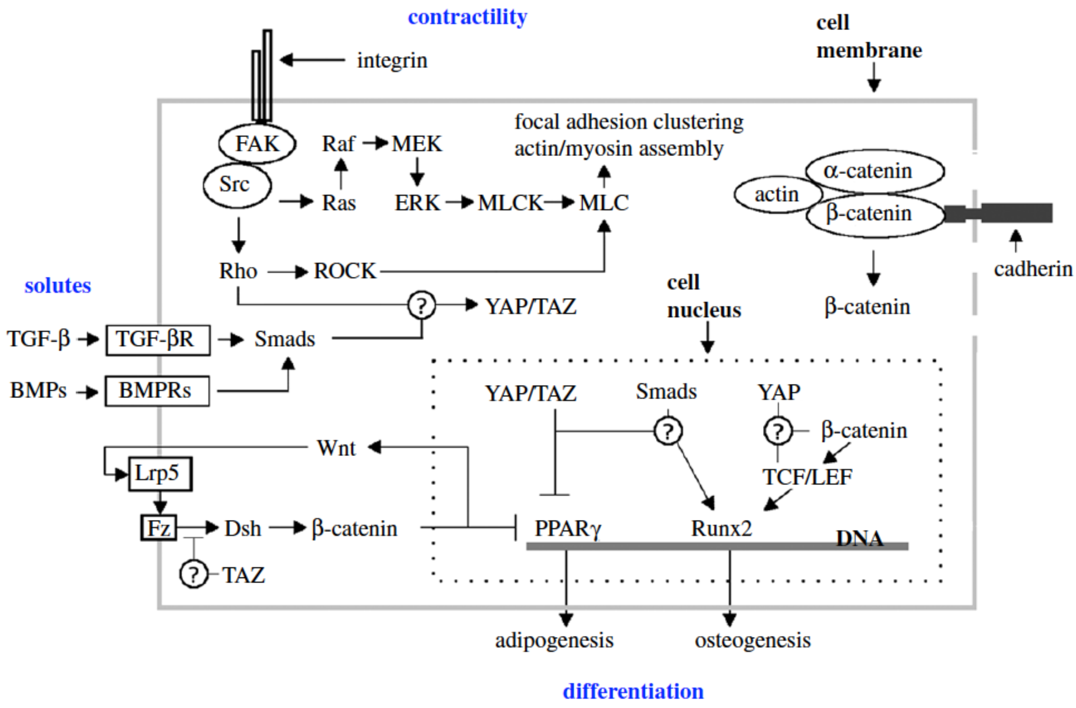
contractility
integrin
cell
membrane
FAK
Src
Raf
MEK
Ras
ERK
MLCK
MLC
focal adhesion clustering
actin/myosin assembly
actin
α-catenin
β-catenin
cadherin
solutes
Rho
ROCK
?
YAP/TAZ
cell
nucleus
β-catenin
TGF-β
TGF-βR
Smads
BMPs
BMPRs
YAP/TAZ
Smads
YAP
?
?
β-catenin
TCF/LEF
Wnt
Lrp5
Fz
Dsh
β-catenin
?
TAZ
PPARγ
Runx2
DNA
adipogenesis
osteogenesis
differentiation

Figure 2.9 | Schematic of the integrin and contractile signalling implicated in MSC differentiation [31].

2.3 Experimental platforms for investigating stem cell environmental sensing

2.3.1. A myriad of diverse platforms

To evaluate how MSCs sense their environment and regulate their fate, a myriad of in-vitro platforms emerged to mimic in-vivo-like micromechanical settings . While cells are usually cultured on glass or plastic, softer and stiffness tunable materials could be more suitable to mimic the broad stiffness range of the natural environment. As listed in the Figure 2.10, two major types of polymer are employed as substrate for culturing stem cells: (i) synthetic polymers including polydimethylsiloxane (PDMS), polyacrylamide (PAA) and polyethylenglycol (PEG); (ii) biopolymers including hyaluronic acid (HA) and alginate [25]. The elasticity of these various substrates is usually tailored through the number of cross-linking groups. While natural biopolymers possess biological activities of native ECM molecules, they generally present limitations for biochemical and biophysical modifications compared to the synthetic polymers [49]. Although several methods exist to employ these different polymers, we only describe here the 2D and 3D platforms that have been recently used to evaluate the effects of stiffness and topographical cues on driving stem cell differentiation.

2.3.1.1. Two-dimensional (2D) platform

Two-dimensional platforms (Fig. 2.11) have been mainly used over the last decade because of their great convenience, potential for high throughput analysis and reduced technical challenges compared to three-dimensional ones [50]. To improve cell adhesion on 2D substrates, proteins or synthetic peptides are commonly covalently bound or passively adsorbed on the surface. When seeded on a soft substrate having an elastic modulus below 1 kPa, MSCs present a rounded morphology associated with adipogenic fate. In contrast, MSCs on a stiff polymer exhibit a flat morphology with a dense formation of stress fibers and osteogenic fate. Moreover, substrates with a pathological stiffness gradient were also engineered with a microfluidic system to investigate stem cell durotaxis in the context of a more dynamic environment, where MSCs migrate and accumulate in stiff regions [51].

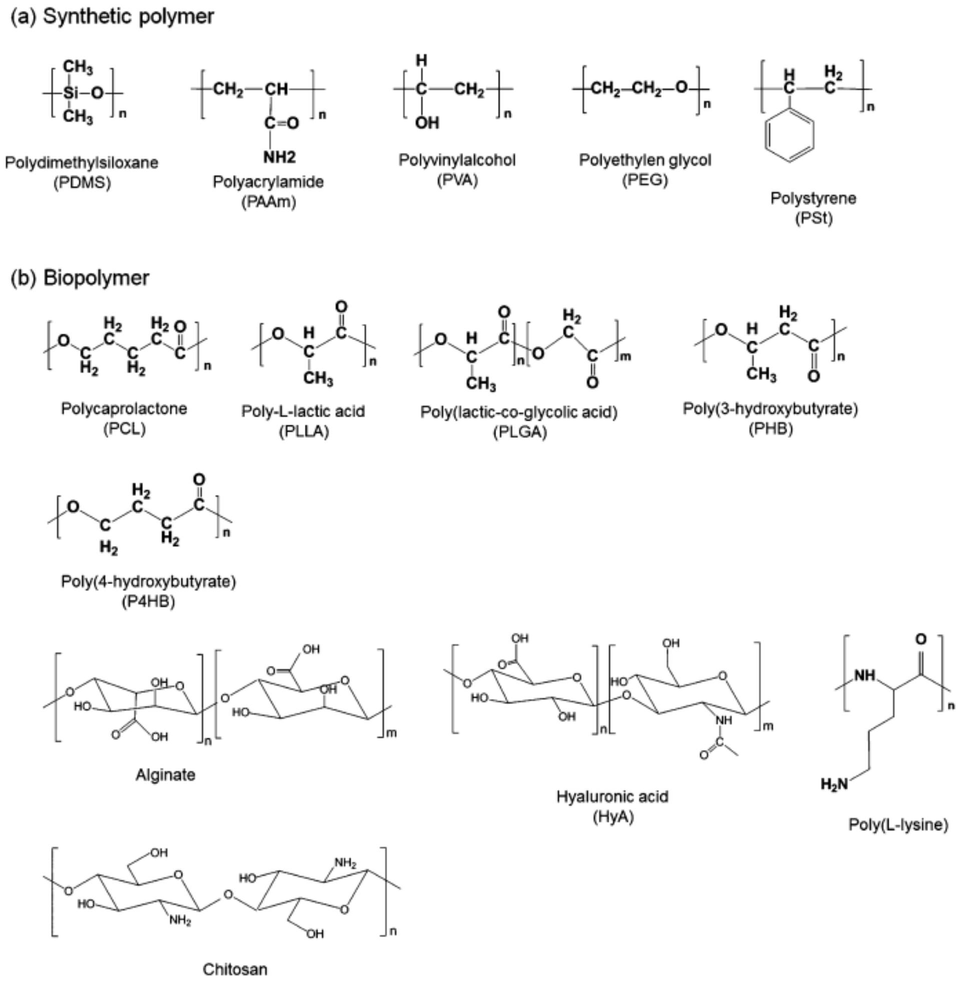
(a) Synthetic polymer
Polydimethylsiloxane (PDMS)
Polyacrylamide (PAAm)
Polyvinylalcohol (PVA)
Polyethylen glycol (PEG)
Polystyrene (PSt)
(b) Biopolymer
Polycaprolactone (PCL)
Poly-L-lactic acid (PLLA)
Poly(lactic-co-glycolic acid) (PLGA)
Poly(3-hydroxybutyrate) (PHB)
Poly(4-hydroxybutyrate) (P4HB)
Alginate
Hyaluronic acid (HyA)
Poly(L-lysine)
Chitosan

Figure 2.10 | Chemical schematics of synthetic polymers and biopolymers [25]

Recent progress in material surface engineering enabled to create accurately specific small features down to the nanoscale. Lithographic techniques are the most common used nanofabrication procedures for micro- and nanotopographic patterning. While limited to diffraction with a 200 nm maximal resolution, photolithography is the most popular approach by employing light to transfer a geometric pattern from a mask to a light-sensitive photoresist. To obtain features below 10 nm, lithography techniques with different sources having smaller wavelengths such as electron beams and X-rays were developed. Electron beam lithography enabled to create nanogrooves, nanopit arrays and nanopillars on PDMS elastomers. While the previous techniques necessitate costly equipment and time, soft lithography is a convenient alternative to generate structures as small as 30 nm on PDMS substrates with the use of stamps or molds [52]. Furthermore, the stamping of ECM components on substrates permitted to control the cell geometry, which is an early signal in governing the fate. MSCs that were cultured on small micropatterned islands had a very limited cell adhesion and became rounded and adipogenic, whereas they became flat and osteogenic on larger islands [53]. Chemical and physical etching are also common techniques to create random nanofeatures especially for tissue engineering scaffolds and biomedical implants. Chemical etching involves chemical reactions between the substrate and etchant that are tightly controlled in time and temperature to modulate the topographic size. Reactive ion etching is the most popular physical etching method, which uses chemically reactive plasma to remove material deposited on wafers [52]. A combination of photolithography and reactive ion etching enabled Fu et al. to develop micromolded elastomeric micropost arrays having different heights to modulate substrate rigidity and observed an adipogenic fate of MSCs seeded on microposts having a height of 12.9 µm and an osteogenic fate with a height of 0.97 µm [54].

These 2D platforms can further incorporate additional micro- or nanofabrication technology to evaluate the stem cell response to extracellular mechanical cues. For example, fluorescent microbead trackers are coated on the surface, on which cells adhere, so the effects of substrate stiffness and topography on cellular forces can be evaluated using traction force microscopy [55]. Displacement of the microbeads due to cell contraction that deforms the substrate is examined to quantify traction forces. Guvendiren et al. investigated the effects of dynamic matrix stiffening by employing light-mediated crosslinking hydrogels with embedded fluorescent microspheres that stiffen in the presence of cells. When the substrates get stiffer, hMSCs spread more and exert more traction. Osteogenic differentiation was promoted with earlier stiffening [56]. Several research groups have implemented fluorescence resonance energy transfer (FRET)-based molecular tension microscopy to track the stretching magnitude of various molecules. The technology involves a molecular sensor, which is genetically encoded within a protein of interest [57]. For example, Grashoff et al. developed a vinculin tension sensor with piconewton sensitivity and showed that vinculin undergoes a tension around 2.5pN in stable FAs and that vinculin recruitment to FAs and force transmission across vinculin are regulated independently [58].

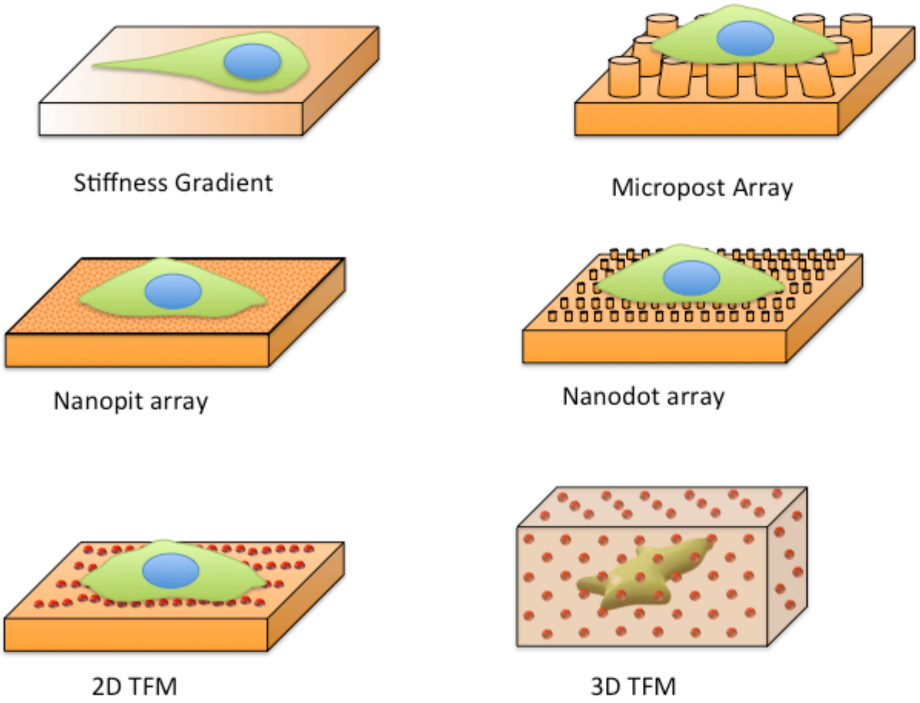

Figure 2.11 | A myriad of two-dimensional and three-dimensional platforms for investigating stem cell mechanobiology

2.3.1.2. Three-dimensional (3D) platform

While cells have a limited contact area on two-dimensional substrates, cells are surrounded in tissues by a three-dimensional environment that makes their morphology appear highly different from the two-dimensional cultures. In three dimensions, cells exert contractile forces on each area that is in contact with the plasma membrane. Diverse 3D platforms were developed to evaluate the scaffold stiffness in driving specific lineage differentiation [25]. For example, Murphy et al. made scaffolds composed of natural ECM components incorporating collagen and glycosaminoglycan. Two different glycosaminoglycans comprising chondroitin sulfate and hyaluronic acid were employed and compared. By modulating the level of crosslinking with dehydrothermal (DHT) physical treatment and 1-ethyl-3-3-dimethyl aminopropyl carbodiimide (EDAC) chemical crosslinking agent, three scaffolds were produced with the same composition but different stiffness: 0.5, 1 and 1.5 kPa. They observed that MSCs cultured in the scaffolds containing hyaluronic acid and having a stiffness of 0.5kPa showed the highest upregulation of Sox9 expression. When cultured in scaffolds with chondroitin sulfate and a stiffness of 1.5kPa, cells presented the highest upregulation of Runx2 expression. These results demonstrate that, even in the absence of differentiation supplements, scaffold stiffness in combination with a specific glycosaminoglycan-type can drive MSC fate in 3D culture [59].

Emergence of rapid prototyping technology such as 3D printing and stereolithography allowed the development of scaffolds with controlled architecture and mechanical properties [60]. One of the most common techniques for controlling architecture is electrospinning. The technology utilizes electrical forces to produce polymer fibers with diameters ranging from 2 nm to several micrometers from polymer solutions of both synthetic and biopolymers. While the pore size of nanofibrous scaffolds can be controllable and consistently reproduced from batch to batch, modulating the pore size was found to improve the cell infiltration [61, 62]. Wang et al. produced poly(propylene carbonate/poly(epsilon-caprolactone) nanofibers having a nanoscale topography with inter-surface-connected pores from 50 nm to a few hundreds nanometers in diameter. MSCs cultured on these nanoporous scaffolds compared to regular smooth PCL ones presented a higher calcium deposit, which is a common bone differentiation marker [63].

Although physical accessibility for imaging is very limited and computation is more complex, 3D traction force microscopy platforms emerged recently to determine fully the three-dimensional traction field [31]. Legant et al. were among the pioneers to develop a technique to track bead displacement exerted by embedded fibroblasts in relatively soft hydrogels (0.6-1.0kPa) and reported strong tractions few microns behind the leading edge of a lamellipodia [64]. Khetan et al. demonstrated that hMSCs within HA hydrogels that allows cell-mediated degradation could highly spread, exerted strong tractions and favored osteogenesis when compared to cells within hydrogels that prevent cell-mediated degradation, independently of substrate mechanical properties [65].

2.3.2. Discrepancy and limitations from confounding factors

2.3.2.1. Mesenchymal stem cell culture

Although diversity in platform creates flexibility, this suffers from major drawbacks. One of many disadvantages is the difficulty to compare study outcomes. Due to a lack of consensus, researchers may arbitrarily select their cell model and culture medium. While cells can be isolated, expanded and characterized differently, the international society for cellular therapy has described the minimal criteria for defining multipotent stromal cells to achieve a more consistent characterization of MSC and help the exchange of data among researchers [66]. Furthermore, composition of the cell-culture media plays a major role in driving cellular reactions. Most of investigators employ media supplemented with fetal bovine serum (FBS), which contains a multitude of bioactive compounds such as growth hormones, insulin and alkaline phosphatase. Unfortunately, FBS is highly variable from lot to lot and may drastically impair reproducibility [67]. To overcome such problems, serum-free media were developed and are chemically defined. While most serum-free formulations are specific to a cell type, firms have manufactured media for the growth of adult human mesenchymal stem cells [68].

2.3.2.2. Cell sensitivity to material stiffness

While the goal of stem cell mechanobiology is to understand how cells sense and respond to mechanical signals from their environment, researchers tend to draw comprehensive conclusions based on observations on synthetic materials that are coated with ECM proteins with similar as well as deviating properties [23, 69, 70]. As discussed earlier, Engler et al. were among the pioneers to show that synthetic material stiffness can direct stem cell fate [23]. While Engler and coworkers' study was performed on PAA gels, Trappmann et al. challenged the view of how stem cells sense synthetic material stiffness by reporting cell inability to react to PDMS rigidity [69]. While PDMS is relatively amorphous, they suggested that differential stem cell reaction on PAA gels is attributed to pore-size modulation, which varies in a dependent manner with the bulk stiffness (Fig. 2.12). More precisely, the distance between anchoring points for ECM protein ligands coated on substrate surfaces is the driving factor for mechanical feedback [69].

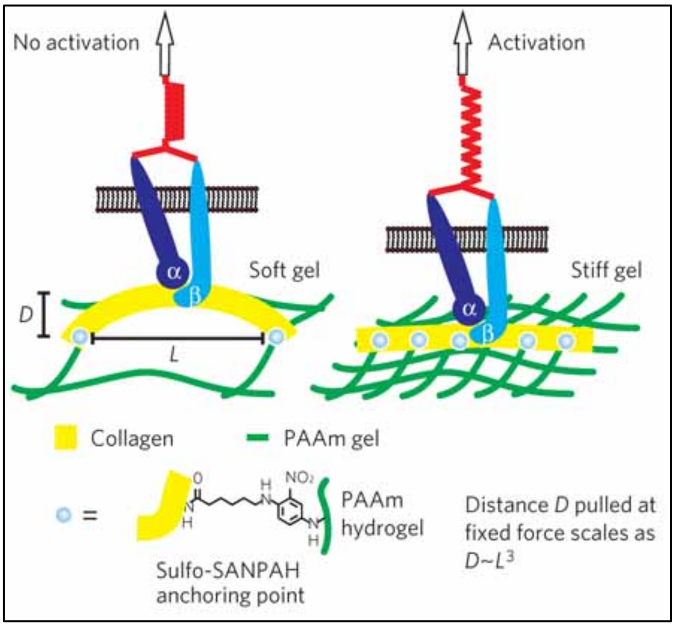
No activation
Activation
α
β
Soft gel
Stiff gel
D
L
Collagen
PAAm gel
=
Sulfo-SANPAH anchoring point
PAAm hydrogel
Distance D pulled at fixed force scales as D~L³

Figure 2.12| Model for collagen binding suggested by Trappmann et al. [69]

In contrast, Evans et al. demonstrated by culturing embryonic stem cells on PDMS that an increase in stiffness promoted proliferation and osteogenic differentiation [71]. Furthermore, Vertelov et al. recently observed a reduced cell spreading and adipogenic differentiation on soft silicone substrates [72]. These conflicting results suggest that some unexpected confounding factors may play a critical role at the cell-material interface, which leads to incorrect conclusions.

Numerous studies have tried to elucidate the inability of cells to sense stiffness on silicone substrates. While surface treatment is usually performed to render PDMS hydrophilic and allow covalent protein coating [73], Li et al. have demonstrated that strong UV radiation forms a silica-like layer on PDMS surface that can dominate the cell-material interaction [74]. In contrast to elastic PAA gels, Wen et al. suggested that viscoelastic PDMS is not cell compliant [70]. In contrast to previous studies that reported moduli below 1 kPa [69], they described moduli as high as 245kPa for PDMS high ratios (100:1) of base-to-catalyst (Fig. 2.13). Chaudhuri et al. concluded in the same direction by reporting that the stress relaxation of viscoelastic substrates supports cell spreading [75]. However, these conclusions are not consistent with the observations made by Evans et al. and Vertelov et al. [71, 72].

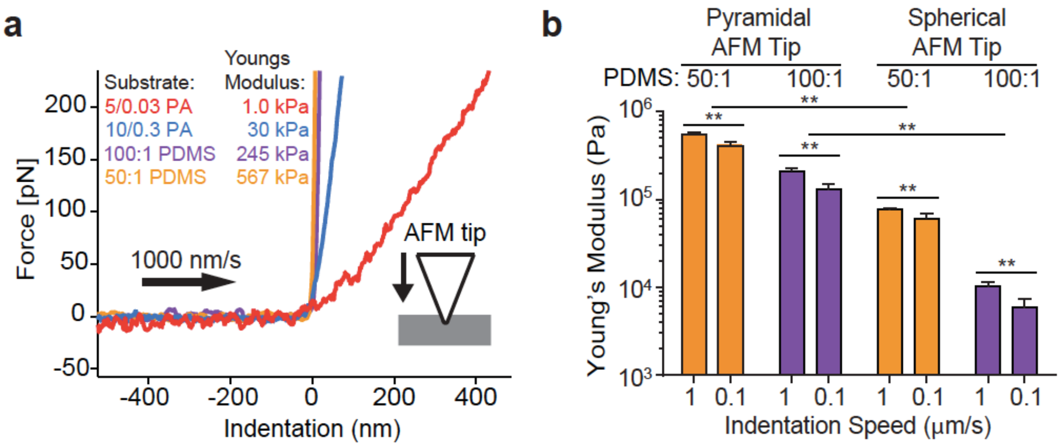

Figure 2.13 | Mechanical characterization by atomic force microscopy (AFM) of PDMS and PAA (here PA) reported by Wen et al. [70]

2.3.2.3. Surface energy: an underappreciated element

As mentioned earlier, synthetic materials employed for investigating stem cell mechanobiology present significant differences in chemical and physical properties. In this thesis, we decided to focus on one aspect that has been widely ignored by the field, which is the difference in surface energy between usually employed synthetic materials such as PAA and PDMS.

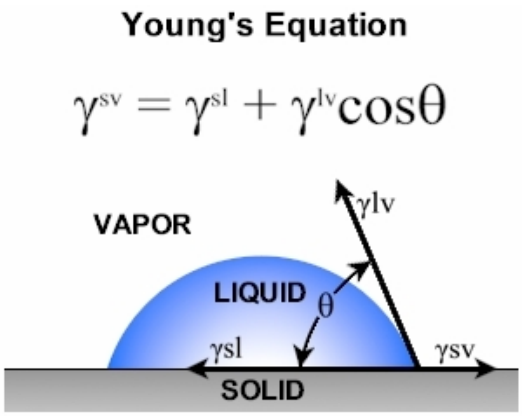

Fig. 2.14 | Representation of the contact angle (θ) in function of the surface energy (γ_{sv}), surface tension of the liquid (γ_{lv}) and the interfacial tension between the liquid and solid (γ_{sl}) (adapted from www.ramehart.com)

Surface energy (SF) can be seen as the work that has to be expended in order to increase the size of the surface of a phase. Based on Owens-Wendt-Rabel & Kaelble model, SF can also be described as the sum of components due to dispersion and polar forces. Covalent, ionic, and metallic bonds are strong contributors to high surface energy compared to forces such as van der Waals and hydrogen bonding that are mainly present in low surface energy substrates. Surface energy has a decisive effect on surface wettability, which can be measured with the water contact angle. High energy substrates are more hydrophilic than low energy substrates. Furthermore, more complete substrate wetting will happen if the material has a higher surface energy than water [76]. Young's equation describes a relationship between the surface energy γ_{sv}, the contact angle θ, the surface tension of the liquid γ_{lv} and the interfacial tension between liquid and solid γ_{sl} (Fig. 2.14).

Although surface wettability is also dependent of the roughness, we mainly considered the studies that evaluated the effects from the differences in polarity of the present surface functional groups that were described to influence cell behavior [77]. For example, Dowling et al. have observed an optimal adhesion of osteosarcoma cells at a moderately hydrophilic contact angle (θ=64°) by altering apolar (hydrophobic) siloxane coating on polystyrene surface with an atmospheric plasma technique. More precisely, they modified the nature of the deposited coating by modulating the level of exposure of the PDMS precursor to the helium/oxygen plasma and obtained a water contact angle range of 12-98° [78]. Several previous studies have also reported an optimal water contact angle for cell adhesion in the 60-80 range [79, 80].

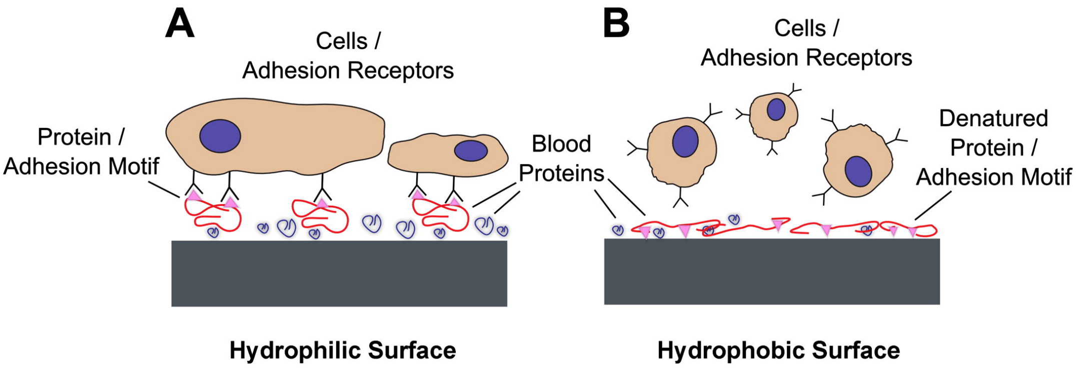

Figure 2.15 | schematic of differential deposition and conformation of proteins on hydrophobic and hydrophilic surfaces [81]

While observed cellular reactions on surfaces are mainly attributed to bulk material properties, surfaces are covered by adsorbed proteins from ligand coating and the medium serum as well (Fig. 2.15). As thoroughly discussed by Schaap-Oziemlak et al., the surface chemical properties such as surface energy alter the nature of adsorbed protein ligands, which in turn affects cell adhesion and differentiation [82]. For example, Ayala et al. developed a hydrogel system whose hydrophobicity can be modified without affecting surface roughness and mechanical properties by varying the number of apolar methylene side chain groups. They demonstrated that stem cell responses are dependent of a differential binding of fibronectin resulting from hydrophobicity-driven conformational changes. As previously, they observed the highest cell adhesion and osteogenic differentiation with a moderately hydrophilic water contact angle (θ=58°) [83]. Coelho et al. have described a difference in collagen assembly and resulting surface topography on polar and apolar substrates (Fig. 2.16). When coated on polar glass surfaces (θ=25°), the arrangement appeared like a single molecular size – network and turned into a noticeable and increasing polygonal network composed of molecular aggregates on hydrophobic glasses (θ=103°). Cell attachment and spreading were found to be higher on hydrophilic substrates [84].

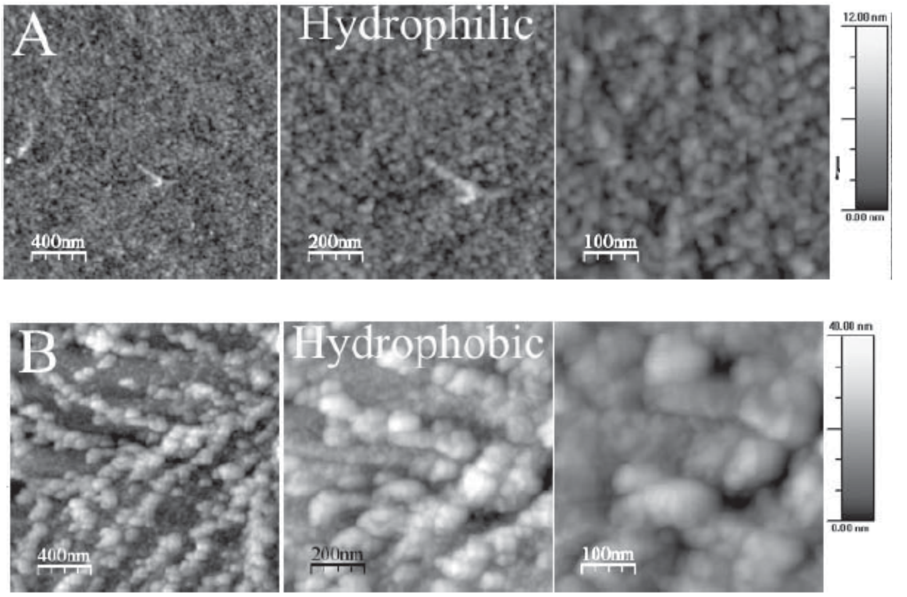
A
Hydrophilic
400nm
200nm
100nm
12.00 nm
0.00 nm
B
Hydrophobic
400nm
200nm
100nm
40.00 nm
0.00 nm

Figure 2.16 | AFM images of adsorbed collagen IV on hydrophilic and hydrophobic glass surfaces [84]

2.4 References

[1] C. Frantz, K.M. Stewart, V.M. Weaver, The extracellular matrix at a glance, J Cell Sci 123(Pt 24) (2010) 4195-200.
[2] J.K. Mouw, G. Ou, V.M. Weaver, Extracellular matrix assembly: a multiscale deconstruction, Nat Rev Mol Cell Biol 15(12) (2014) 771-85.
[3] H. Gardner, Integrin alpha1beta1, Advances in experimental medicine and biology 819 (2014) 21-39.
[4] L.F.M. C. Graham Knight, David J. Onley, Anthony R. Peachey, Anthea J. Messent, Peter A. Smethurst, Danny S. Tuckwell, Richard W. Farndale and Michael J. Barnes, Identification in Collagen Type I of an Integrin $\alpha 2 \beta 1$-binding Site Containing an Essential GER Sequence, Journal of Biological Chemistry (1998).
[5] Y. Xu, S. Gurusiddappa, R.L. Rich, R.T. Owens, D.R. Keene, R. Mayne, A. Hook, M. Hook, Multiple binding sites in collagen type I for the integrins alpha1beta1 and alpha2beta1, The Journal of biological chemistry 275(50) (2000) 38981-9.
[6] R. Pankov, Fibronectin at a glance, Journal of Cell Science 115(20) (2002) 3861-3863.
[7] P. Olczyk, L. Mencner, K. Komosinska-Vassev, The role of the extracellular matrix components in cutaneous wound healing, Biomed Res Int 2014 (2014) 747584.
[8] U. Hersel, C. Dahmen, H. Kessler, RGD modified polymers: biomaterials for stimulated cell adhesion and beyond, Biomaterials 24(24) (2003) 4385-4415.
[9] K.E. Kadler, D.F. Holmes, J.A. Trotter, J.A. Chapman, Collagen fibril formation, Biochemical Journal 316(Pt 1) (1996) 1-11.
[10] K.E. Kadler, A. Hill, E.G. Canty-Laird, Collagen fibrillogenesis: fibronectin, integrins, and minor collagens as organizers and nucleators, Current Opinion in Cell Biology 20(5-24) (2008) 495-501.
[11] J.H. Fessler, Self-assembly of collagen, Journal of Supramolecular Structure 2(2-4) (1974) 99-102.
[12] K.E. Kubow, R. Vukmirovic, L. Zhe, E. Klotzsch, M.L. Smith, D. Gourdon, S. Luna, V. Vogel, Mechanical forces regulate the interactions of fibronectin and collagen I in extracellular matrix, Nat Commun 6 (2015) 8026.
[13] C. Bonnans, J. Chou, Z. Werb, Remodelling the extracellular matrix in development and disease, Nat Rev Mol Cell Biol 15(12) (2014) 786-801.
[14] S. Maxson, E.A. Lopez, D. Yoo, A. Danilkovitch-Miagkova, M.A. Leroux, Concise review: role of mesenchymal stem cells in wound repair, Stem Cells Transl Med 1(2) (2012) 142-9.
[15] M. Oh, J.E. Nor, The Perivascular Niche and Self-Renewal of Stem Cells, Front Physiol 6 (2015) 367.
[16] S.R. Husain, Y. Ohya, J. Toguchida, R.K. Puri, Current status of multipotent mesenchymal stromal cells, Tissue Eng Part B Rev 20(3) (2014) 189.

[17] F. Gattazzo, A. Urciuolo, P. Bonaldo, Extracellular matrix: a dynamic microenvironment for stem cell niche, Biochim Biophys Acta 1840(8) (2014) 2506-19.
[18] E. Alsberg, H.A. von Recum, M.J. Mahoney, Environmental cues to guide stem cell fate decision for tissue engineering applications, Expert Opin Biol Ther 6(9) (2006) 847-66.
[19] T. Nakamoto, Control of Simultaneous Osteogenic and Adipogenic Differentiation of Mesenchymal Stem Cells, Journal of Stem Cell Research & Therapy 04(08) (2014).
[20] K.W. Yong Yang, Xiaosong Gu, Kam W. Leong, Biophysical Regulation of Cell Behavior&mdash;Cross Talk between Substrate Stiffness and Nanotopography, Engineering 3(1) (2017) 36-54.
[21] A.S. Rowlands, P.A. George, J.J. Cooper-White, Directing osteogenic and myogenic differentiation of MSCs: interplay of stiffness and adhesive ligand presentation, Am J Physiol Cell Physiol 295(4) (2008) C1037-44.
[22] J. Lee, A.A. Abdeen, D. Zhang, K.A. Kilian, Directing stem cell fate on hydrogel substrates by controlling cell geometry, matrix mechanics and adhesion ligand composition, Biomaterials 34(33) (2013) 8140-8.
[23] A.J. Engler, S. Sen, H.L. Sweeney, D.E. Discher, Matrix Elasticity Directs Stem Cell Lineage Specification, Cell 126(4) (2006) 677-689.
[24] A.T. Nguyen, S.R. Sathe, E.K. Yim, From nano to micro: topographical scale and its impact on cell adhesion, morphology and contact guidance, J Phys Condens Matter 28(18) (2016) 183001.
[25] A. Higuchi, Q.D. Ling, Y. Chang, S.T. Hsu, A. Umezawa, Physical cues of biomaterials guide stem cell differentiation fate, Chem Rev 113(5) (2013) 3297-328.
[26] K. Metavarayuth, P. Sitasuwan, X. Zhao, Y. Lin, Q. Wang, Influence of Surface Topographical Cues on the Differentiation of Mesenchymal Stem Cells in Vitro, ACS Biomaterials Science & Engineering 2(2) (2016) 142-151.
[27] K. Takeuchi, L. Saruwatari, H.K. Nakamura, J.M. Yang, T. Ogawa, Enhanced intrinsic biomechanical properties of osteoblastic mineralized tissue on roughened titanium surface, Journal of biomedical materials research. Part A 72(3) (2005) 296-305.
[28] M.J. Dalby, N. Gadegaard, R. Tare, A. Andar, M.O. Riehle, P. Herzyk, C.D. Wilkinson, R.O. Oreffo, The control of human mesenchymal cell differentiation using nanoscale symmetry and disorder, Nature materials 6(12) (2007) 997-1003.
[29] E. Kearney, E. Farrell, P. Prendergast, V. Campbell, Tensile strain as a regulator of mesenchymal stem cell osteogenesis, Ann Biomed Eng 38 (2010) 1767 - 1779.
[30] C. Huang, M. Chen, T. Young, J. Jeng, Y. Chen, Interactive effects of mechanical stretching and extracellular matrix proteins on initiating osteogenic differentiation of human mesenchymal stem cells, J Cell Biochem 108 (2009) 1263 - 1273.
[31] L. MacQueen, Y. Sun, C.A. Simmons, Mesenchymal stem cell mechanobiology and emerging experimental platforms, Journal of the Royal Society, Interface / the Royal Society 10(84) (2013) 20130179.

[32] L. Ramage, Integrins and extracellular matrix in mechanotransduction, Cell Health and Cytoskeleton (2011) 1.
[33] J. Stricker, T. Falzone, M.L. Gardel, Mechanics of the F-actin cytoskeleton, Journal of biomechanics 43(1) (2010) 9-14.
[34] V. Swaminathan, C.M. Waterman, The molecular clutch model for mechanotransduction evolves, Nat Cell Biol 18(5) (2016) 459-61.
[35] W.F. Vogel, R. Abdulhussein, C.E. Ford, Sensing extracellular matrix: an update on discoidin domain receptor function, Cell Signal 18(8) (2006) 1108-16.
[36] H.L. Fu, R.R. Valiathan, R. Arkwright, A. Sohail, C. Mihai, M. Kumarasiri, K.V. Mahasenan, S. Mobashery, P. Huang, G. Agarwal, R. Fridman, Discoidin domain receptors: unique receptor tyrosine kinases in collagen-mediated signaling, The Journal of biological chemistry 288(11) (2013) 7430-7.
[37] G.S. Schultz, A. Wysocki, Interactions between extracellular matrix and growth factors in wound healing, Wound Repair Regen 17(2) (2009) 153-62.
[38] J.D. Humphries, P. Wang, C. Streuli, B. Geiger, M.J. Humphries, C. Ballestrem, Vinculin controls focal adhesion formation by direct interactions with talin and actin, J Cell Biol 179(5) (2007) 1043-57.
[39] A. del Rio, R. Perez-Jimenez, R. Liu, P. Roca-Cusachs, J.M. Fernandez, M.P. Sheetz, Stretching Single Talin Rod Molecules Activates Vinculin Binding, Science 323(5914) (2009) 638-641.
[40] N.O. Deakin, C.E. Turner, Paxillin comes of age, J Cell Sci 121(Pt 15) (2008) 2435-44.
[41] C.S. Chen, J. Tan, J. Tien, Mechanotransduction at cell-matrix and cell-cell contacts, Annu Rev Biomed Eng 6 (2004) 275-302.
[42] K. Katoh, Y. Kano, Y. Noda, Rho-associated kinase-dependent contraction of stress fibres and the organization of focal adhesions, Journal of the Royal Society, Interface / the Royal Society 8(56) (2011) 305-11.
[43] W.H. Goldmann, Mechanotransduction and focal adhesions, Cell Biol Int 36(7) (2012) 649-52.
[44] W.Q. Wang, Y. Liu, K. Liao, Tyrosine phosphorylation of cortactin by the FAK-Src complex at focal adhesions regulates cell motility, Bmc Cell Biology 12 (2011).
[45] S. Huveneers, E.H. Danen, Adhesion signaling - crosstalk between integrins, Src and Rho, J Cell Sci 122(Pt 8) (2009) 1059-69.
[46] B. Leitinger, Discoidin domain receptor functions in physiological and pathological conditions, Int Rev Cell Mol Biol 310 (2014) 39-87.
[47] S.D. Thorpe, D.A. Lee, Dynamic regulation of nuclear architecture and mechanics-a rheostatic role for the nucleus in tailoring cellular mechanosensitivity, Nucleus 8(3) (2017) 287-300.
[48] T.O. Ihalainen, L. Aires, F.A. Herzog, R. Schwartlander, J. Moeller, V. Vogel, Differential basal-to-apical accessibility of lamin A/C epitopes in the nuclear lamina regulated by changes in cytoskeletal tension, Nature materials 14(12) (2015) 1252-61.
[49] Y. Shao, J. Sang, J. Fu, On human pluripotent stem cell control: The rise of 3D bioengineering and mechanobiology, Biomaterials 52 (2015) 26-43.

[50] K.M. Warren, M.M. Islam, P.R. LeDuc, R. Steward, Jr., 2D and 3D Mechanobiology in Human and Nonhuman Systems, ACS Appl Mater Interfaces 8(34) (2016) 21869-82.
[51] L.G. Vincent, Y.S. Choi, B. Alonso-Latorre, J.C. del Alamo, A.J. Engler, Mesenchymal stem cell durotaxis depends on substrate stiffness gradient strength, Biotechnol J 8(4) (2013) 472-84.
[52] Y. Zhang, A. Gordon, W. Qian, W. Chen, Engineering nanoscale stem cell niche: direct stem cell behavior at cell-matrix interface, Adv Healthc Mater 4(13) (2015) 1900-14.
[53] K.A. Kilian, B. Bugarija, B.T. Lahn, M. Mrksich, Geometric cues for directing the differentiation of mesenchymal stem cells, Proceedings of the National Academy of Sciences of the United States of America 107(11) (2010) 4872-7.
[54] J. Fu, Y.K. Wang, M.T. Yang, R.A. Desai, X. Yu, Z. Liu, C.S. Chen, Mechanical regulation of cell function with geometrically modulated elastomeric substrates, Nature methods 7(9) (2010) 733-6.
[55] C.N. Holenstein, U. Silvan, J.G. Snedeker, High-resolution traction force microscopy on small focal adhesions - improved accuracy through optimal marker distribution and optical flow tracking, Scientific reports 7 (2017) 41633.
[56] M. Guvendiren, J.A. Burdick, Stiffening hydrogels to probe short- and long-term cellular responses to dynamic mechanics, Nat Commun 3 (2012) 792.
[57] C. Gayrard, N. Borghi, FRET-based Molecular Tension Microscopy, Methods 94 (2016) 33-42.
[58] C. Grashoff, B.D. Hoffman, M.D. Brenner, R. Zhou, M. Parsons, M.T. Yang, M.A. McLean, S.G. Sligar, C.S. Chen, T. Ha, M.A. Schwartz, Measuring mechanical tension across vinculin reveals regulation of focal adhesion dynamics, Nature 466(7303) (2010) 263-6.
[59] C.M. Murphy, A. Matsiko, M.G. Haugh, J.P. Gleeson, F.J. O'Brien, Mesenchymal stem cell fate is regulated by the composition and mechanical properties of collagen-glycosaminoglycan scaffolds, Journal of the mechanical behavior of biomedical materials 11 (2012) 53-62.
[60] F. Guilak, D.L. Butler, S.A. Goldstein, F.P. Baaijens, Biomechanics and mechanobiology in functional tissue engineering, Journal of biomechanics 47(9) (2014) 1933-40.
[61] N. Bhardwaj, S.C. Kundu, Electrospinning: a fascinating fiber fabrication technique, Biotechnol Adv 28(3) (2010) 325-47.
[62] M.C. Phipps, W.C. Clem, J.M. Grunda, G.A. Clines, S.L. Bellis, Increasing the pore sizes of bone-mimetic electrospun scaffolds comprised of polycaprolactone, collagen I and hydroxyapatite to enhance cell infiltration, Biomaterials 33(2) (2012) 524-34.
[63] Y. Wang, J. Deng, R. Fan, A. Tong, X. Zhang, L. Zhou, Y. Zheng, J. Xu, G. Guo, Novel nanoscale topography on poly(propylene carbonate)/poly(ε-caprolactone) electrospun nanofibers modifies osteogenic capacity of ADCs, RSC Adv. 5(101) (2015) 82834-82844.

[64] W.R. Legant, J.S. Miller, B.L. Blakely, D.M. Cohen, G.M. Genin, C.S. Chen, Measurement of mechanical tractions exerted by cells in three-dimensional matrices, Nature methods 7(12) (2010) 969-71.
[65] S. Khetan, M. Guvendiren, W.R. Legant, D.M. Cohen, C.S. Chen, J.A. Burdick, Degradation-mediated cellular traction directs stem cell fate in covalently crosslinked three-dimensional hydrogels, Nature materials 12(5) (2013) 458-65.
[66] M. Dominici, K. Le Blanc, I. Mueller, I. Slaper-Cortenbach, F. Marini, D. Krause, R. Deans, A. Keating, D. Prockop, E. Horwitz, Minimal criteria for defining multipotent mesenchymal stromal cells. The International Society for Cellular Therapy position statement, Cytotherapy 8(4) (2006) 315-7.
[67] J.R. Vetsch, S.J. Paulsen, R. Muller, S. Hofmann, Effect of fetal bovine serum on mineralization in silk fibroin scaffolds, Acta Biomater 13 (2015) 277-85.
[68] F. Mannello, G.A. Tonti, Concise review: no breakthroughs for human mesenchymal and embryonic stem cell culture: conditioned medium, feeder layer, or feeder-free; medium with fetal calf serum, human serum, or enriched plasma; serum-free, serum replacement nonconditioned medium, or ad hoc formula? All that glitters is not gold!, Stem Cells 25(7) (2007) 1603-9.
[69] B. Trappmann, J.E. Gautrot, J.T. Connelly, D.G.T. Strange, Y. Li, M.L. Oyen, M.A. Cohen Stuart, H. Boehm, B. Li, V. Vogel, J.P. Spatz, F.M. Watt, W.T.S. Huck, Extracellular-matrix tethering regulates stem-cell fate, Nature materials 11(7) (2012) 642-649.
[70] J.H. Wen, L.G. Vincent, A. Fuhrmann, Y.S. Choi, K.C. Hribar, H. Taylor-Weiner, S. Chen, A.J. Engler, Interplay of matrix stiffness and protein tethering in stem cell differentiation, Nature materials 13(10) (2014) 979-87.
[71] N.D. Evans, C. Minelli, E. Gentleman, V. LaPointe, S.N. Patankar, M. Kallivretaki, X.Y. Chen, C.J. Roberts, M.M. Stevens, Substrate Stiffness Affects Early Differentiation Events in Embryonic Stem Cells, European cells & materials 18 (2009) 1-14.
[72] G. Vertelov, E. Gutierrez, S.A. Lee, E. Ronan, A. Groisman, E. Tkachenko, Rigidity of silicone substrates controls cell spreading and stem cell differentiation, Scientific reports 6 (2016) 33411.
[73] Y.L. G. Bartalena, T. Zambellid and J. G. Snedeker, Biomaterial surface modifications can dominate cell–substrate mechanics: the impact of PDMS plasma treatment on a quantitative assay of cell stiffness, Soft Matter 8(3) (2012) 673-681.
[74] J. Li, D. Han, Y.-P. Zhao, Kinetic behaviour of the cells touching substrate: the interfacial stiffness guides cell spreading, Sci. Rep. 4 (2014).
[75] O. Chaudhuri, L. Gu, M. Darnell, D. Klumpers, S.A. Bencherif, J.C. Weaver, N. Huebsch, D.J. Mooney, Substrate stress relaxation regulates cell spreading, Nat Commun 6 (2015) 6364.
[76] P.G. de Gennes, Wetting: statics and dynamics, Reviews of Modern Physics 57(3) (1985) 827-863.
[77] X. Liu, J.Y. Lim, H.J. Donahue, R. Dhurjati, A.M. Mastro, E.A. Vogler, Influence of substratum surface chemistry/energy and topography on the human fetal osteoblastic cell line hFOB 1.19: Phenotypic and genotypic responses observed in vitro, Biomaterials 28(31) (2007) 4535-4550.

[78] D.P. Dowling, I.S. Miller, M. Ardhaoui, W.M. Gallagher, Effect of surface wettability and topography on the adhesion of osteosarcoma cells on plasma-modified polystyrene, J Biomater Appl 26(3) (2011) 327-347.
[79] S.K. Moon, N.S. Yu, H.C. Mi, H.K. Soon, K.K. Sun, H.C. Young, K. Gilson, L. Il Woo, L. Hai Bang, Adhesion Behavior of Human Bone Marrow Stromal Cells
on Differentially Wettable Polymer Surfaces, Tissue Engineering 13 (2007).
[80] C.-C. Wu, C.-Y. Yuan, S.-J. Ding, Effect of polydimethylsiloxane surfaces silanized with different nitrogen-containing groups on the adhesion progress of epithelial cells, Surface and Coatings Technology 205(10) (2011) 3182-3189.
[81] R.A. Gittens, L. Scheideler, F. Rupp, S.L. Hyzy, J. Geis-Gerstorfer, Z. Schwartz, B.D. Boyan, A review on the wettability of dental implant surfaces II: Biological and clinical aspects, Acta Biomater 10(7) (2014) 2907-18.
[82] A.M. Schaap-Oziemlak, P.T. Kuhn, T.G. van Kooten, P. van Rijn, Biomaterial-stem cell interactions and their impact on stem cell response, RSC Advances 4(95) (2014) 53307-53320.
[83] R. Ayala, C. Zhang, D. Yang, Y. Hwang, A. Aung, S.S. Shroff, F.T. Arce, R. Lal, G. Arya, S. Varghese, Engineering the cell-material interface for controlling stem cell adhesion, migration, and differentiation, Biomaterials 32(15) (2011) 3700-11.
[84] N.M. Coelho, C. Gonzalez-Garcia, J.A. Planell, M. Salmeron-Sanchez, G. Altankov, Different assembly of type IV collagen on hydrophilic and hydrophobic substrata alters endothelial cells interaction, European cells & materials 19 (2010) 262-72.

CHAPTER 3

3 Development and characterization of a surface energy tunable PDMS-based platform for 2D stem culture

[1,2]Tojo Razafiarison, [1,2]Unai Silvan, [1,2]Jess G Snedeker

[1]Department of Orthopedics, Balgrist University Hospital, University of Zurich, Lengghalde 5, 8008 Zürich, Switzerland
[2]Laboratory for Orthopedic Biomechanics, ETH Zurich, 8008 Zürich, Switzerland

A part of the work was published in Advanced Healthcare Materials (2016) [1] **and the other part was submitted to** PNAS (2017)**.**

3.1 Abstract

Polydimethylsoxane (PDMS) is a widely used silicone-based polymer substrate for two-dimensional cell culture, which is relatively cheap and easy to fabricate. In addition to its non-cytoxicity and biological inertness, the elastomer presents some excellent physical properties and a convenient optical transparency. However, the use of PDMS can be constrained due to its high surface hydrophobicity, which may impact protein adsorption and cell attachment. To increase the surface energy, various surface treatments exist but are often very complicated and time-consuming or tend to modify the surface topology and mechanical properties. Here, we describe a simple method that creates hydrophilic PEO-PDMS by adding a small amount of the poly(dimethylsiloxane-ethylene oxide polymeric) PDMS-b-PEO surfactant directly to the PDMS slurry. The water contact angle measured with a goniometer could be modulated from 120° to 40° with increasing surfactant amounts. To evaluate the integrity of the viscoelastic properties of PEO-PDMS, we performed multi-scale mechanical characterization of substrates with different mixing ratios. Our results demonstrate that PDMS effectively exhibits a broad range of stiffness, the addition of PDMS-b-PEO surfactant has no significant effect on the viscoelastic properties and our platform can be functionalized with protein ligands to promote cell adhesion.

3.2 Introduction

Polydimethysiloxane (PDMS), a silicone rubber fabricated by mixing a base agent and a curing agent, is commonly employed for microfluidic applications but also for engineering diverse two-dimensional cell culture platforms [2]. For instance, the particular elastomeric properties of PDMS allow the easy and fast fabrication of micro- and nanostructures, and to modulate the substrate stiffness by simply adjusting the amount of crosslinker. Although PDMS has many qualities such as being biocompatible, transparent and inexpensive, the fabricated elastomer has a very hydrophobic surface from the abundance of apolar methyl groups.

While a hydrophobic surface presents a low surface energy (SF), the charge and polarity of the outermost functional groups of the material determine the surface energy. Previous studies have demonstrated that surface hydrophobicity may alter protein adsorption and cell attachment [3] but also affect stem cell differentiation [4]. In this context, controlling for PDMS surface hydrophobicity may be essential for improving its application not only for microfluidic devices but also for cell culture substrates.

Several methods to increase PDMS surface energy exist that can be divided into three main categories: surface activation, physical modification, and chemical modification [5]. However, most of these modifications are either very complicated or modify the physical and mechanical properties of the surface. For instance, it has only recently been appreciated that the common surface activation with oxygen plasma treatment substantially stiffens a soft substrate surface in a manner that can heavily affect cell–matrix interaction [6].

In the present study, we sought to develop a platform by which surface wettability could be controlled, without affecting the biomaterial surface mechanics or topology. To this end, we adopted a recently described method [7] by which an otherwise hydrophobic PDMS system is rendered hydrophilic by adding a small amount of poly(dimethylsiloxane-ethylene oxide polymeric) (PDMS-b-PEO) directly to a bulk slurry. The block copolymer presents a hydrophobic PDMS segment that can polymerize with the bulk elastomer and a hydrophilic PEO segment, which length can be varied to modulate the hydrophobic/hydrophilic balance [7]. We demonstrate that PDMS surface energy can be modulated while still preserving mechanical and topological properties of the bulk elastomer. Furthermore, we show that our platform can be functionalized with protein ligands to create a favorable environment for cell adhesion.

3.3 Materials and methods

3.3.1 Surface energy and stiffness tunable PDMS substrate preparation

12 mm glass coverslips (Thermo Scientific Menzel, 11708701) were cleaned with milli-Q H2O and ethanol. The surfactant polydimethylsiloxane-bethylene oxide (molecular weight = 600, Chemie Brunschwig, 09780) was mixed first in different amounts from 0% to 1.0% (v/w_{total}) with the base of PDMS kit for 5 min (Sylgard 184, Biesterfeld, Germany). The catalyst of PDMS kit was then added at different mixing ratios from 10:1 to 80:1 and the slurry was mixed again thoroughly for 10 min. The homogeneously mixed slurry was degased for 30 min and spin coated on the glass coverslips with a 200 µm thickness. The substrates were cured for ≈14 h at 80°C.

For cell substrate fabrication, collagen I monomers (Sigma, C3867) were covalently bound to the surface of the elastomers using the heterobifunctional linker N-sulfosuccinimidyl-6-(4'-azido-2'-nitrophenylamino) hexanoate (sulfo-SANPAH, ProteoChem, C1111). Collagen and sulfo-SANPAH were aliquoted in single-use vials and stored respectively at 4°C and -20°C. The substrates were placed in a 24-well plate and washed with milli-Q H2O. 500 µL of a 0.2 mg/mL solution of sulfo-SANPAH in 50mM HEPES (Life Technologies, 7001629) were added to each well. The substrates were then placed in a Stratalinker 2400 ultraviolet light crosslinker (Stratagene) for 10 minutes. The sulfo-SANPAH was removed and the substrates were overlaid with fresh sulfo-SANPAH and exposed again to ultraviolet light for 10 minutes. At this point the substrates were sterilized and washed three times with PBS. The substrates were coated with 10 or 50 µg/mL collagen I diluted in PBS for 3 hours at 37°C.

3.3.2 Contact angle measurement

A contact angle measurement system was set up with a camera Nikon D5000 mounted with a telecentric objective, a moving sample holder, and a light source [8]. The substrates were prepared in triplicate and a 5 µL droplet of milli-Q H2O was delivered on seven different locations on each replicate. Droplets were left for 10 min until complete stabilization of the contact angle. Images were taken and analyzed with the dropShape imageJ plug-in [9].

3.3.3 Macroscopic mechanical characterization

Elastomers were cast in triplicate in flat Petri dishes to obtain substrates with 50 mm diameter and 7 mm height. The samples were lubricated with water or silicon oil and brought to a compression test machine (Zwick GmbH, 1456). For elastomers with a mixing ratio of 10:1, the compression force was measured with a 1 kN load cell. For elastomers with a mixing ratio from 60:1 to 80:1, the test machine was equipped with a 4cm-diameter steel ball and a 50 N load cell and measured within a physiological strain rate range from 0.05 to 10% s-1 but also for their long-term modulus after an initial load at 10% s-1 and a relaxation for 1 hour. A Hertz model for spherical indentation was applied to determine the elastic modulus (Fig. 3.1).

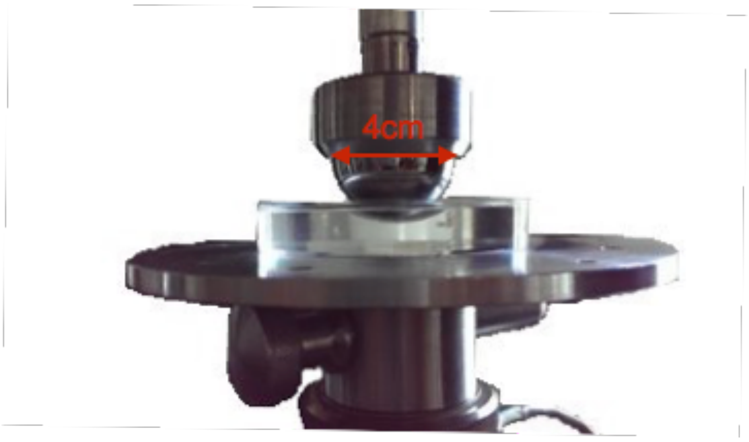

Figure 3.1 | Compression test machine for macroscopic mechanical characterization

3.3.4 Microscopic mechanical characterization

The substrates were prepared as explained above on 12 mm glass coverslips (Menzel, 11708701). Each substrate was measured at nine randomly selected locations by microindentation with a micromechanical-testing machine (Femtotool, FT-RS1002) equipped with a microforce sensing probe with either a 1 μm or 10 μm radius tungsten tip. A Hertz model for spherical indentation was applied to determine the elastic modulus.

3.3.5 Nanoscopic mechanical characterization

Substrates were prepared as explained above and measured with a Nanosurf FlexAFM system mounted with OTESPA probes having 7 nm tip radius and 42 N m-1 force constant. Measurements were performed at 3 to 5 locations with 256 force curves per location 16 μm s-1 indentation speed. Data were processed with the ARTIDIS tool.

3.3.6 Ligand loading and adsorbed protein quantification

A micro-BCA protein assay kit (Thermo Scientific, 10249133) was used to determine the protein that was adsorbed on the different substrate surfaces according to the stated protocol in the kit, where the absorbance was measured at 562nm with a microplate reader. A standard curve with the collagen used for coating was plotted to determine the effective amount of collagen bound to the surface.

3.3.7 Statistical analysis

All experiments were performed in triplicate with five independent experiments ($n=5$) unless indicated. Data are represented as means and standard error (bars in the figure). When only two groups were analyzed, the results were normalized by the mean values of the corresponding hydrophobic PDMS groups. For multiple comparisons, a two-way ANOVA with Bonferroni correction was applied to reveal main effect. The unpaired two-tailed student's t-test with a confidence level of 95% was applied to see if two sets of data differ significantly. Significance was indicated for $p \leq 0.05$ (*$p\leq0.05$, **$p\leq0.01$, ***$p\leq0.001$, **** $p\leq0.0001$). All the charts and analysis were processed with Prism 6 software.

3.4 Results

3.4.1 Contact angle characterization

As previously described by others [7, 10], we obtained hydrophilic PDMS by adding the surfactant PDMS-b-PEO directly to the PDMS slurry (Fig. 3.2). To characterize the surface energy, we fabricated a sessile-drop contact angle measurement system [8]. While water contact angle measurement varies with the surface energy but also with the surface roughness, experiments were performed on the smooth and standard PDMS recipe with a ratio 10:1.

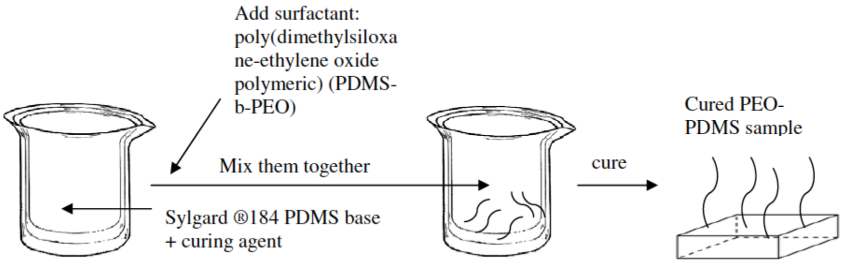
Add surfactant: poly(dimethylsiloxane-ethylene oxide polymeric) (PDMS-b-PEO)
Mix them together
Sylgard ®184 PDMS base + curing agent
cure
Cured PEO-PDMS sample

Figure 3.2 | Schematic of hydrophilic PEO-PDMS fabrication [7]

Hydrophilicity could be effectively controlled by varying the weight percentage of surfactant to the PDMS base polymer. By increasing the amount of surfactant from 0% to 1.0%, the water contact angle was reduced from 115° to 35° (Fig. 3.3A). A percentage of 0.2% was already sufficient to reduce from a hydrophobic contact angle of 115° to a moderately hydrophilic contact angle of 75° (Fig. 3.3B-C). We note that increasing surfactant correspondingly increased PDMS opacity, with adverse effect on optical transparency of the PDMS. However with a percentage of 0.2% and a thin substrate layer, bright-field microscopy was not affected.

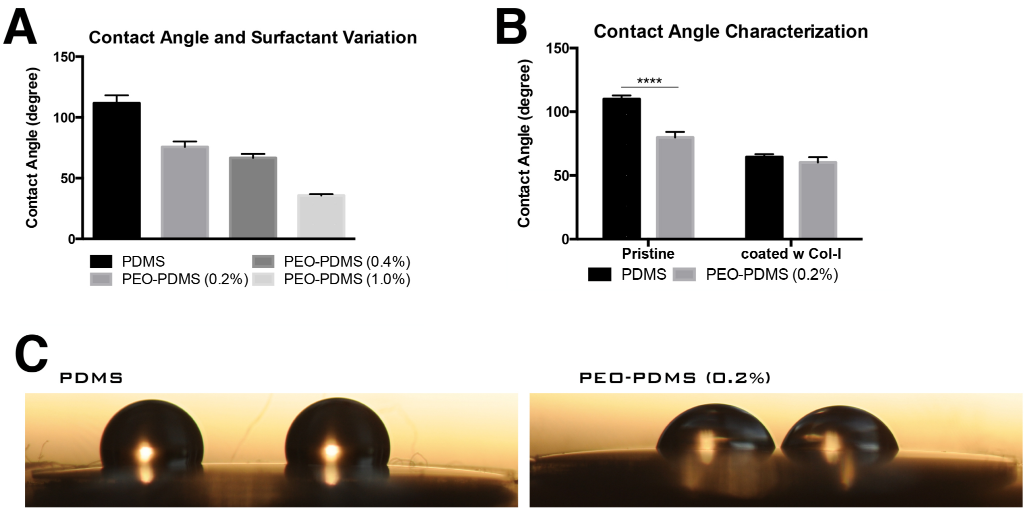

Figure 3.3 | Contact angle measurement results of PDMS substrates with different amounts of PEO-b-PDMS surfactant. (A) An increase in surfactant amount from 0% to 1.0% reduces the contact angle from 115° to 35°; mean± s.d (n=3-5); (B) when coated with similar collagen-I density, PDMS and PEO-PDMS (0.2% v/w) substrates both reduced significantly their contact angle to reach a similar value around 60°; mean±s.d; ****p=0.0001; (C) representative pictures of the contact angle on pristine PDMS and PEO-PDMS (0.2% v/w).

3.4.2 Multi-scale mechanical characterization

While effects of surfactant additive on PDMS mechanical properties has not been previously reported, we performed testing first with the standard PDMS 10:1 ratio and secondly with higher ratios from 60:1 to 80:1 that create intermediate stiff and soft substrates.

Our testing with the 10:1 ratio (Fig. 3.4) showed that the elastic modulus was slightly reduced (10% below a baseline modulus of 2.40 MPa; ***p=0.0009) and that stress relaxation was comparable to the standard PDMS formulation (Fig. 3.4C). Substrates left in culture for 21 days (Fig. 3.4A) both showed slight increases in elastic moduli (15-20% above) probably due to the fact that the samples were still curing as previously reported [11]. No difference in weight between day 0 and day 21 was observed confirming that the substrates did not swell (data not shown). Physical homogeneity of the surface was verified at the microscale in the focal adhesion range with a 1µm-radius tip (Fig. 3.4B). In contrast to other surface treatments [6, 12], the sulfo-sanpah coating only slightly increased the elastic modulus (15% above baseline) of both surfaces, thus with minimal effects on the mechanical properties (Fig. 3.4B).

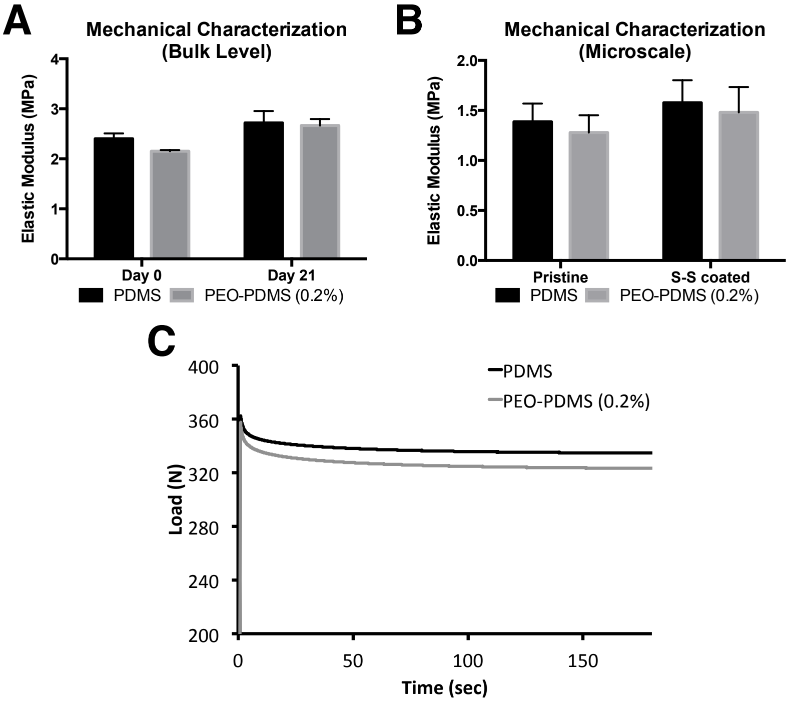

Figure 3.4 | Mechanical properties results of pristine PDMS substrates and treated PEO-PDMS (0.2% v/w) substrates at bulk level and microscale. (A) Mechanical properties at bulk level measured with a compression testing machine on day 0 and after 21 days in culture at 37°C indicated similar elastic moduli for both substrates; mean± s.d; ***p=0.0009. (B) Mechanical properties at microscale measured with a 1µm-radius tungsten tip micromechanical testing system showed homogeneity of both substrates and did not indicate any significant effect of sulfo-sanpah coating (S-S) on elastic modulus; mean± s.d (n=3). (C) As seen on the typical load-time compression curves at bulk level, stress-relaxation experiments revealed addition of 0.2% (v/w) PEO-b-PDMS surfactant to PDMS did not affect the viscoelastic properties of the elastomer.

To further verify that surfactant additive did not affect PDMS mechanical properties of softer substrates, we performed mechanical testing on the bulk material of PDMS and PEO-PDMS with mixing base to catalyst ratios of 60:1 to 80:1 within a physiological range of mechanical strains. As previously reported [13], the softer the elastomer, the more substantial was the viscous component of the material response (Fig. 3.5A). Our testing revealed equivalent elastic and viscoelastic response of the PDMS and PEO-PDMS, with long-term moduli found to range from 0.07 to 6kPa (Fig. 3.5B). Similarly to the measurements on PDMS 10:1, Microscale mechanical surface homogeneity was demonstrated using indenter tips with dimensions (10 µm radius) in the range of focal adhesion sizes (Fig. 3.6).

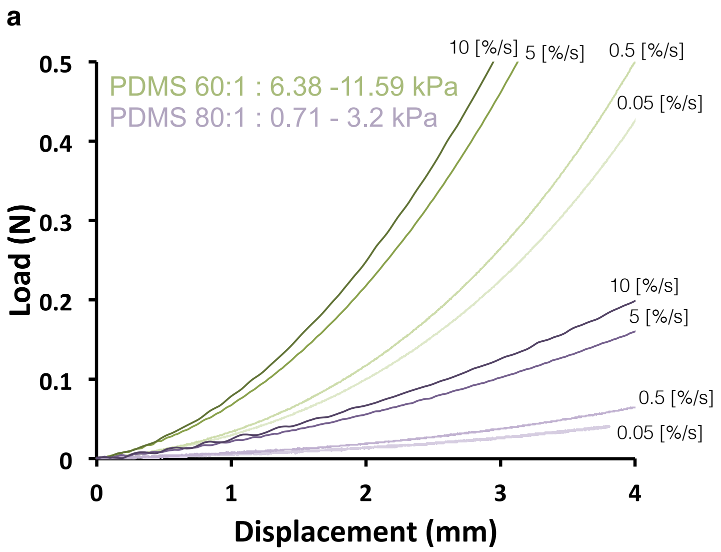

b

	Ratio (Base:Catalyst)	Long-term Modulus	Physiological strain rate range modulus (0.05-10%.s^{-1})
PDMS	60:1	6.00 ± 0.70 kPa	6.38 -11.59 kPa
	70:1	0.35 ± 0.14 kPa	1.20 - 2.86 kPa
	80:1	0.10 ± 0.06 kPa	0.71 - 3.2 kPa
PEO-PDMS	60:1	4.96 ± 1.44 kPa	5.20 - 10.18 kPa
	70:1	0.22 ± 0.05 kPa	1.14 - 2.73 kPa
	80:1	0.07 ± 0.04 kPa	0.67 - 3.6 kPa

Figure 3.5 | Mechanical characterization of PDMS and PEO-PDMS at bulk level shows a broad range of compliance. (a) Typical load-displacement curves of PDMS having a ratio of 60:1 and 80:1 measured with a compression testing machine at different strain rates. (b) Summary of long-term modulus measured during stress-relaxation experiments and modulus measured within the physiological strain rate range from 0.05 to 10% s^{-1} of PDMS and PEO-PDMS of different stiffness from 60:1 to 80:1. (n= 5-7). Data are represented as mean±s.d.

In contrast to a previous study which reports very high elastic moduli with a similar range of mixing ratio [14], our data indicated that soft PDMS (80:1) has an elastic modulus of 0.7kPa in response to a 10% s^{-1} strain rate (Fig. 3.5B). Our finding that the mechanical properties of soft PDMS are similar at the microscopic and macroscopic scales findings is consistent with our previous investigations of stiff elastomeric substrates. While collagen coating slightly increased the surface stiffness, surface treatment with a heterobifunctional protein crosslinker (sulfo-SANPAH) did not alter surface mechanics (Fig. 3.6).

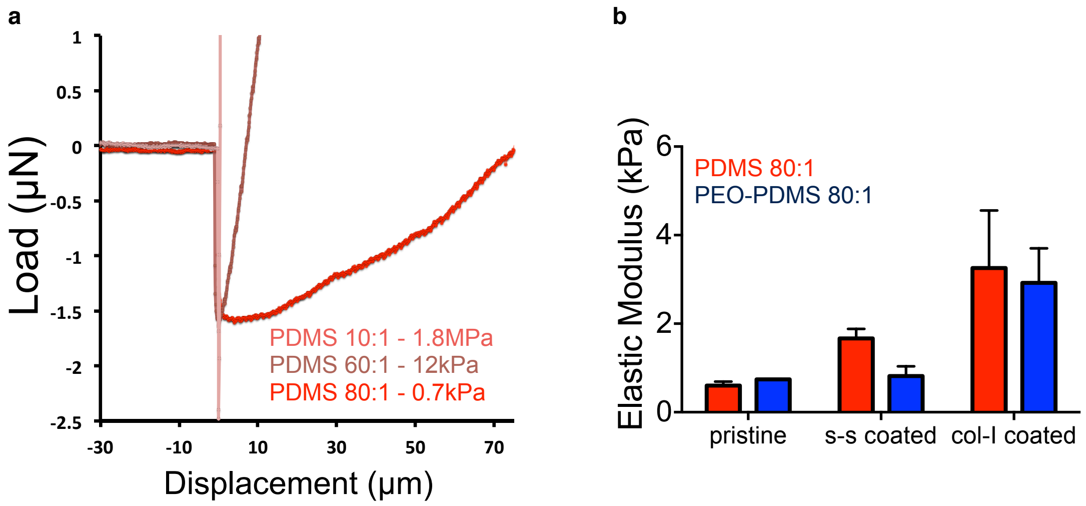

Figure 3.6 | Mechanical characterization of PDMS and PEO-PDMS substrates at microscale exhibits consistent results with bulk level and no significant effect from surface treatment and collagen coating. (a) Typical load-displacement curves of PDMS having a ratio of 10:1, 60:1 and 80:1 measured with a micromechanical testing system equipped with a sensor with a 10 µm radius tungsten tip at 1 µm s^{-1}. (b) Elastic Modulus of PDMS and PEO-PDMS substrates having a ratio of 80:1 measured when the substrates were pristine, coated with sulfo-SANPAH (s-s coated) and coated with collagen (col-I coated). (n= 3-4). Data are represented as mean±s.d.

Measurement at the nanoscale by atomic force microscopy (AFM) was performed to additionally verify mechanical equivalence, with measured values ranging from 3.6 kPa (soft) to 2.5 MPa (stiff) (Fig.3.7).

	10:1	20:1	40:1	60:1	80:1
Forward	1823 ± 167 kPa	536 ± 44 kPa	76 ± 7.9 kPa	17.1 ± 1.8 kPa	3.6 ± 0.6 kPa
Backward	2490 ± 267 kPa	976 ± 167 kPa	191.7 ± 27.5 kPa	51.2 ± 5.8 kPa	11.2 ± 2.6 kPa

Figure 3.7 | Mechanical characterization of PDMS substrates at nanoscale exhibits a broad range of compliance and consistent values with bulk level and microscale. Elastic modulus of PDMS substrates having a ratio of 10:1 to 80:1 measured at 16 µm s^{-1} with a Nanosurf FlexAFM system mounted with OTESPA probes having 7 nm tip radius and 42 N m^{-1} force constant. Data are represented as mean±s.d.

3.4.3 Bioactivity characterization of the different surfaces:

We observed that kinetics of protein adsorption were affected by substrate wettability, with hydrophobic surfaces being prone to adsorb collagen more readily than hydrophilic surfaces [3], We thus empirically adapted the molarity of the respective ligand solutions to result in equivalent protein loading on the hydrophobic and hydrophilic substrates of different stiffness (Fig. 3.8 and Supplementary Fig. S3.1). We could observe that collagen could be passively adsorbed on PDMS without using crosslinker, as reported by others [15]. However, crosslinker was able to promote protein adsorption more than 2-fold (supplementary Fig. S3.2). Contact angle measurements after coating showed that the contact angles for both substrates reached similar values of approximately 60° (Fig. 3.1B).

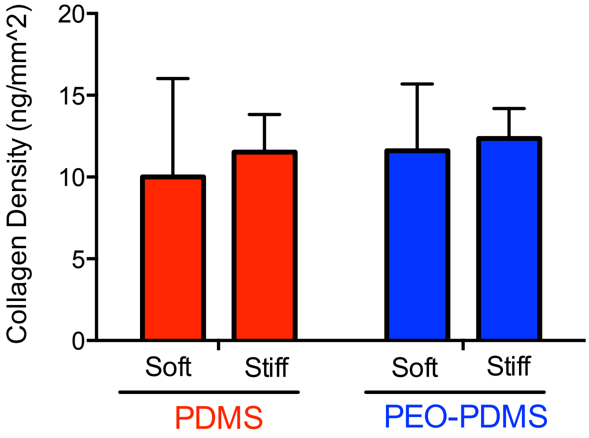

Figure 3.8 | Ligand loading is empirically adjusted to obtain a similar ligand density on PDMS and PEO-PDMS. Adsorbed collagen-I amount on PDMS and PEO-PDMS substrates of different stiffness. Collagen-I monomers were coated at a concentration of 10 µg mL^{-1} on PDMS and of 50 µg mL^{-1} on PEO-PDMS. (n = 5-7).

3.5 Discussion

We achieved the development of a PDMS-based platform that can be mechanically tuned within a wide range of potential stiffness (from 70 Pa to 2.3MPa) and surface energies that enables the creation of hydrophilic and hydrophobic variants of a given material stiffness, without otherwise affecting baseline physical properties of the substrate surface – most critically, topology. This system allows one to limit variation in topology that is a key confounding factor that often plagues parametric study of cell-biomaterial interaction.

Although widely used, PDMS presents several drawbacks that diminish its suitability as a platform for biological studies. One critical issue is that PDMS can adsorb small molecules such as soluble factors from media, a characteristic that has been shown to affect cell behavior [2, 16]. Another potential issue is that residual (non-crosslinked) PDMS polymer chains can freely diffuse out of the bulk material over time in culture. These oligomers can interact with the membrane of surrounding cells [16]. Less cross-linked formulations with lower PDMS stiffness leads to a higher rate of oligomers leaching, potentially another important confounding factor that one should consider when using PDMS to investigate cell sensitivity to substrate mechanics. Moreover, any two dimensional elastomeric substrate is likely to lack potentially critical spatial cues that exist in an *in-vivo-like* environment [17]. Still despite its limitations, PDMS remains a convenient and flexible platform for micro-engineering fabrication, and more broadly for investigation of cell-material interaction.

We have described a hydrophilic-tunable PDMS by a straightforward addition of a proportionally small (0.2%) amount of PDMS-b-PEO surfactant to the mixing slurry. As previously observed [7], the contact angle rapidly decreased within the first minutes when the surface is exposed to water, probably due to the reorientation of the hydrophilic segments from the block copolymer.

Our preliminary experiments revealed that the addition of more than 0.2% of surfactant noticeably reduced the amount of coated collagen on the surface and resulted in a very low human bone marrow stromal (hBMSC) cell attachment (supplementary Fig. S3.3). For the purpose of our study, 0.2% of surfactant was sufficient to create substrates within the reported 60-80° range for optimal cell adhesion [18-20]. Despite a slight decrease of the elastic modulus, PEO-PDMS remained in the same stiffness range with fully preserved viscoelastic properties of the standard PDMS. Furthermore, we demonstrated through multi-scale mechanical characterization that mechanical properties of these materials were consistent across size scales. This contrasts with a recent study reporting inconsistent mechanical properties of PDMS across metric scales [14], a discrepancy that we at least partly attribute to uncontrolled deformation rates in the earlier study. Because viscoelastic effects can be large in these materials [21, 22], we probed mechanical properties within a range of physiological strain rates (up to 10% s^{-1}). We also considered probe fouling due to adhesion of soft PDMS, a factor that can lead to dramatic overestimation of material stiffness in measurements at micro- and nanoscales [23].

Since hydrophobic surfaces tend to adsorb more collagen [3], we ensured that the amount of bound collagens was similar on the different substrates to minimize ligand-density dependent promotion of attachment and differentiation [24]. Contact angle measurements after collagen coating indicated that the both the standard and hydrophilic substrates presented a homogeneous and moderately hydrophilic surface to the cells. This is perhaps important, as it highlights that although the most commonly assessed bulk surface properties appear similar (mechanics, wettability, ligand loading, porosity) without controlling the wettability of the bulk substrate ligand conformation differences remains with potentially important and biologically relevant consequences.

3.6 Supplementary Material

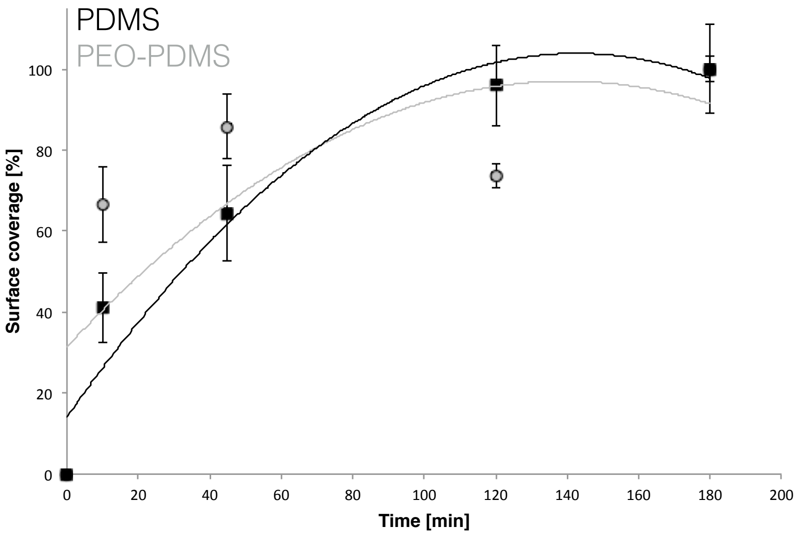

Supplementary Figure S3.1 | Kinetic study of collagen adsorption to the surface measured by BCA assay indicates a similar trend for both PDMS and PEO-PDMS to reach saturation after 3 hours. Adsorbed collagen-I amount on PDMS and PEO-PDMS substrates measured with a microBCA assay at different time points. Collagen-I monomers were coated at a concentration of 10 µg mL^{-1} on PDMS and of 50 µg mL^{-1} on PEO-PDMS. Data are represented as mean±s.d. (n=2).

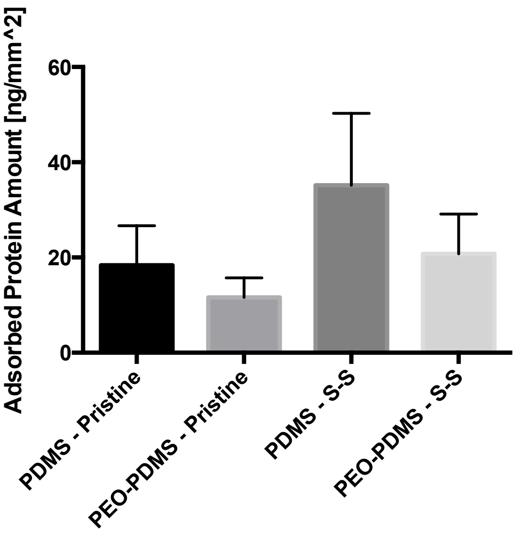

Supplementary Figure S3.2 | Adsorbed collagen-I amount on PDMS and PEO-PDMS (0.2%) substrates. Collagen-I monomers were coated at a concentration of 100µg/ml on pristine and sulfo-sanpah treated PDMS and PEO-PDMS substrates. mean± s.d.

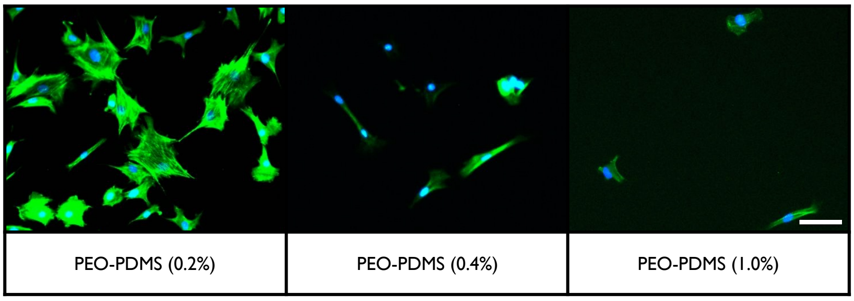

PEO-PDMS (0.2%)

PEO-PDMS (0.4%)

PEO-PDMS (1.0%)

Supplementary Figure S3.3 | hBMSCs attachment and morphology on PEO-PDMS substrates having various surfactant amounts (0.2%; 0..4% and 1.0%) when seeded at 25’000 cells/ cm^2 after 24 h culture. An increase in surfactant presented an important reduction in cell attachment and cell spreading. Cells were stained with FITC-phalloidin (green) and DAPI (blue). Scale bar = 50 µm.

3.7 References

[1] T. Razafiarison, U. Silvan, D. Meier, J.G. Snedeker, Surface-Driven Collagen Self-Assembly Affects Early Osteogenic Stem Cell Signaling, Adv Healthc Mater 5(12) (2016) 1481-92.
[2] E. Berthier, E.W. Young, D. Beebe, Engineers are from PDMS-land, Biologists are from Polystyrenia, Lab on a chip 12(7) (2012) 1224-37.
[3] N.M. Coelho, C. Gonzalez-Garcia, J.A. Planell, M. Salmeron-Sanchez, G. Altankov, Different assembly of type IV collagen on hydrophilic and hydrophobic substrata alters endothelial cells interaction, European cells & materials 19 (2010) 262-72.
[4] R. Ayala, C. Zhang, D. Yang, Y. Hwang, A. Aung, S.S. Shroff, F.T. Arce, R. Lal, G. Arya, S. Varghese, Engineering the cell-material interface for controlling stem cell adhesion, migration, and differentiation, Biomaterials 32(15) (2011) 3700-11.
[5] I. Wong, C.-M. Ho, Surface molecular property modifications for poly(dimethylsiloxane) (PDMS) based microfluidic devices, Microfluid Nanofluid 7(3) (2009) 291-306.
[6] Y.L. G. Bartalena, T. Zambellid and J. G. Snedeker, Biomaterial surface modifications can dominate cell–substrate mechanics: the impact of PDMS plasma treatment on a quantitative assay of cell stiffness, Soft Matter 8(3) (2012) 673-681.
[7] M.Y.a.J. Fang, Hydrophilic PEO-PDMS for microfluidic applications, Journal of Micromechanics and Microengineering 22(2) (2012).
[8] G. Lamour, A. Hamraoui, A. Buvailo, Y. Xing, S. Keuleyan, V. Prakash, A. Eftekhari-Bafrooei, E. Borguet, Contact Angle Measurements Using a Simplified Experimental Setup, Journal of Chemical Education 87(12) (2010) 1403-1407.
[9] G.K. A.F. Stalder, D. Sage, L. Barbieri, P. Hoffmann A Snake-Based Approach to Accurate Determination of Both Contact Points and Contact Angles, Colloids And Surfaces A: Physicochemical And Engineering Aspects 286(1-3) (2006) 92-103.
[10] H.T. Kim, J.K. Kim, O.C. Jeong, Hydrophilicity of Surfactant-Added Poly(dimethylsiloxane) and Its Applications, Japanese Journal of Applied Physics 50(6) (2011) 06GL04.
[11] D. Fuard, T. Tzvetkova-Chevolleau, S. Decossas, P. Tracqui, P. Schiavone, Optimization of poly-di-methyl-siloxane (PDMS) substrates for studying cellular adhesion and motility, Microelectronic Engineering 85(5-6) (2008) 1289-1293.
[12] J. Li, D. Han, Y.-P. Zhao, Kinetic behaviour of the cells touching substrate: the interfacial stiffness guides cell spreading, Sci. Rep. 4 (2014).
[13] B. Trappmann, J.E. Gautrot, J.T. Connelly, D.G.T. Strange, Y. Li, M.L. Oyen, M.A. Cohen Stuart, H. Boehm, B. Li, V. Vogel, J.P. Spatz, F.M. Watt, W.T.S. Huck, Extracellular-matrix tethering regulates stem-cell fate, Nature materials 11(7) (2012) 642-649.

[14] J.H. Wen, L.G. Vincent, A. Fuhrmann, Y.S. Choi, K.C. Hribar, H. Taylor-Weiner, S. Chen, A.J. Engler, Interplay of matrix stiffness and protein tethering in stem cell differentiation, Nature materials 13(10) (2014) 979-87.
[15] S. Kuddannaya, Y.J. Chuah, M.H. Lee, N.V. Menon, Y. Kang, Y. Zhang, Surface chemical modification of poly(dimethylsiloxane) for the enhanced adhesion and proliferation of mesenchymal stem cells, ACS Appl Mater Interfaces 5(19) (2013) 9777-84.
[16] A.L. Paguirigan, D.J. Beebe, From the cellular perspective: exploring differences in the cellular baseline in macroscale and microfluidic cultures, Integrative biology : quantitative biosciences from nano to macro 1(2) (2009) 182-95.
[17] B.M. Baker, C.S. Chen, Deconstructing the third dimension: how 3D culture microenvironments alter cellular cues, J Cell Sci 125(Pt 13) (2012) 3015-24.
[18] D.P. Dowling, I.S. Miller, M. Ardhaoui, W.M. Gallagher, Effect of surface wettability and topography on the adhesion of osteosarcoma cells on plasma-modified polystyrene, J Biomater Appl 26(3) (2011) 327-347.
[19] S.K. Moon, N.S. Yu, H.C. Mi, H.K. Soon, K.K. Sun, H.C. Young, K. Gilson, L. Il Woo, L. Hai Bang, Adhesion Behavior of Human Bone Marrow Stromal Cells
on Differentially Wettable Polymer Surfaces, Tissue Engineering 13 (2007).
[20] C.-C. Wu, C.-Y. Yuan, S.-J. Ding, Effect of polydimethylsiloxane surfaces silanized with different nitrogen-containing groups on the adhesion progress of epithelial cells, Surface and Coatings Technology 205(10) (2011) 3182-3189.
[21] R.S. Lakes, Viscoelastic measurement techniques, Review of Scientific Instruments 75(4) (2004) 797.
[22] A.H. Burstein, Basic Biomechanics of the Musculoskeletal System. 3rd ed, The Journal of Bone & Joint Surgery 83(9) (2001) 1455-1455.
[23] F. Meli, A. Küng, AFM investigation on surface damage caused by mechanical probing with small ruby spheres, Measurement Science and Technology 18(2) (2007) 496-502.
[24] X. Yao, Y. Hu, B. Cao, R. Peng, J. Ding, Effects of surface molecular chirality on adhesion and differentiation of stem cells, Biomaterials 34(36) (2013) 9001-9.

Chapter 4

4 Surface-driven collagen assembly affects early osteogenic stem cell signaling

[1,2]Tojo Razafiarison, [1,2]Unai Silvan, [1]Daniela Meier, [1,2]Jess G Snedeker

[1]Department of Orthopedics, Balgrist University Hospital, University of Zurich, Lengghalde 5, 8008 Zürich, Switzerland
[2]Laboratory for Orthopedic Biomechanics, ETH Zurich, 8008 Zürich, Switzerland

This work was published in Advanced Healthcare Materials (2016)

4.1 Abstract

The nanoscale architecture of the extracellular matrix has proven to regulate stem cell behavior through topographical and mechanical cues. While many previous studies have focused on engineered nanoscale material surface topography, we sought to specifically isolate the role of supramolecular ligand assembly on given material surface topologies as a potentially significant regulator of stem cell adhesion, cell-biomaterial interaction, and osteogenic differentiation. Because surface wettability can affect protein deposition, folding, and ligand activity, we employed a previously developed PDMS-based platform with the ability to tune wettability of elastomeric substrates with otherwise equivalent topology, ligand loading, and mechanical properties. Atomic force and scanning electron microscopy both revealed markedly different assembly of covalently bound type I collagen monomers on atomically flat hydrophobic substrates with a layer of collagen aggregates compared to a smooth collagen layer on hydrophilic substrates. Cellular and molecular investigations with human bone marrow stromal cells revealed higher osteogenic differentiation and upregulation of focal adhesion-related components on the resulting smooth collagen layer coated substrates. The initial collagen assembly driven by the PDMS surface directly affected α1β1 integrin/DDR1 signaling, activation of the ERK/MAPK pathway, and eventually markers of osteogenic stem cell differentiation. We demonstrate for the first time that surface driven ligand assembly on material surfaces, even on materials with otherwise identical starting topographies and mechanical properties, can dominate the biomaterial surface-driven cell response.

4.2 Introduction

Chemical and physical properties of the extracellular matrix (ECM) dictate tissue-specific cell behavior. Stem cells interact with their microenvironment, receiving these extracellular cues that regulate diverse behaviors such as self-maintenance, migration and differentiation. These interactions are mediated by adhesion complexes that link intracellular structures to extracellular ligands. Our current understanding of stem cell-ECM interaction is based on studies that have explicitly considered the topological, mechanical and biochemical properties of a biomaterial substrate as the main factors driving stem cell fate [1-6]. While ECM ligand alone can play a decisive contextual role at the cell-material interface directing cell behavior via various signaling pathways [7], the structure of the assembled ligand can further influence cell differentiation.

Numerous studies have demonstrated this, for instance by employing denatured collagen I [8] or conformational variants of fibronectin [9, 10]. These factors can affect the targeted recruitment of the integrin receptors that mediate cell attachment to specific ECM proteins and play a role both as mechanical linkages and signaling receptors [11]. Ligand alterations have been reported to affect the accessibility to recognition sequences for integrins, by blocking cell binding sites that are normally exposed or alternately exposing cryptic binding sites that would be otherwise be hidden [8-10, 12]. Beyond the integrins as transmembrane receptors for the extracellular matrix, the discoidin domain receptors of stem cells have been shown to recognize different organization of collagen I and potentially affect osteogenic differentiation [13].

Surface wettability can play a determinant role in the supramolecular organization and function of adsorbed protein layers [12, 14, 15]. While the atomically flat surface of polydimethylsiloxane (PDMS) is often exploited to study cell-biomaterial interactions, it is markedly more hydrophobic than the porous hydrogels used in such experiments. Thus substrates of differing nanoscale topography that are otherwise viewed as “equivalent” in terms of compliance and bioactivity, could potentially differ markedly with respect to the bioactivity of an adsorbed protein layer. A thorough review of existing literature indicates that this potentially critical confounding factor appears to be either universally unappreciated or discounted without appropriate experimental controls [16].

Collagen I is the most abundant ECM protein in human body [17]. A single molecule is 300 nm long and 1.5 nm in diameter, and readily aggregates into supramolecular structures via thermodynamically driven self-assembly [18]. This process occurs more rapidly on hydrophobic surfaces [14]. To limit potential biological effects due to variation in ligand assembly, crosslinkers have been often used to covalently bind monomeric proteins to the PDMS surfaces [6, 19]. However it remains unclear if the use of crosslinker can adequately eliminate biologically relevant effects of hydrophobicity on the dynamics of protein folding and assembly.

Despite an abundance of evidence for the potential importance of hydrophobic effects on ligand deposition and conformation, many highly cited biological studies have focused on substrate design parameters such as compliance and topology without controlling for this aspect. The few studies investigating the impact of PDMS hydrophobicity and its effects on cell behavior have reported lower cell adhesion and spreading [20, 21] and an improvement of embryonic stem cell differentiation as indicated by the formation of intermediate-size embryoid bodies [22]. In contrast, experiments performed on other (non-PDMS) biomaterial platforms have shown that differential collagen assembly can alter cell function, such as adhesion and spreading [23-25]. Also, hydrophobicity has been reported to affect fibronectin conformation, another common model protein ligand for biomaterial coatings, with correspondingly affected cell activity [12, 15]. Furthermore, despite the enormous number of studies in the literature using collagen-I functionalized PDMS as a cell culture substrate, the nature of covalently bound collagen I assembly on PDMS has not been yet reported. In addition, recent studies have reported often-contradictory cell behaviors using PDMS formulations of variable stiffness [2, 6, 19, 26-42], highlighting that such systems lack sufficient controls or are neglecting wettability as an important factor. We report here a series of experiments that characterize initial ligand assembly on a previously developed PDMS-based platform (see previous chapter) with tunable wettability to demonstrate that receptor recruitment is affected with implications for cellular mechanotransduction and downstream cell fate.

In the present work, we focus on collagen I as a model ligand, and human bone marrow stromal cells (hBMSCs) as a therapeutic cell source with self-maintenance properties and capacity for differentiation toward different tissue specific lineages. This differentiation is regulated at least in part by the properties of the ECM, with these external cues being able to control cell contractility via the rho-associated protein kinase (ROCK) pathway that modulates cell differentiation through the mitogen activated protein (MAP) kinase pathway [7, 43]. In this study, we investigated how covalently bound collagen I assembly on a PDMS surface affects stem cell adhesion, early signaling events in these pathways and osteogenic differentiation. In these experiments we stringently controlled for confounding factors such as the physical, mechanical and chemical properties at the cell-biomaterial interface (Fig. 1). We used this system to demonstrate that surface driven ligand assembly is in fact a critical factor in stem cell behavior, and we then elucidated some of the downstream effects on early cell signaling, and osteogenic cell fate.

4.3 Materials and Methods

4.3.1. Tunable hydrophobic/hydrophilic PDMS substrate preparation

As previously described in the chapter 3, 12 mm glass coverslips (Thermo Scientific Menzel, 11708701) were cleaned with milli-Q H2O and ethanol. The surfactant polydimethylsiloxane-bethylene oxide (molecular weight = 600, Chemie Brunschwig, 09780) was mixed first in different amounts from 0% to 0.4% (v/w_{total}) with the base of PDMS kit (Sylgard 184, Biesterfeld, Germany) for 5 min. The catalyst of PDMS kit was then added at the standard mixing ratio 10:1 and the slurry was mixed again thoroughly for 10 min. The homogeneously mixed slurry was degased for 30 min and spin coated on the glass coverslips with a 200 µm thickness. The substrates were cured for ≈14 h at 80°C.

For cell substrate fabrication, collagen I monomers (Sigma, C3867) were covalently bound to the surface of the elastomers using the heterobifunctional linker N-sulfosuccinimidyl-6-(4’-azido-2’-nitrophenylamino) hexanoate (sulfo-SANPAH, ProteoChem, C1111). Collagen and sulfo-SANPAH were aliquoted in single-use vials and stored respectively at 4°C and -20°C. The substrates were placed in a 24-well plate and washed with milli-Q H2O. 500 µL of a 0.2 mg/mL solution of sulfo-SANPAH in 50mM HEPES (Life Technologies, 7001629) were added to each well. The substrates were then placed in a Stratalinker 2400 ultraviolet light crosslinker (Stratagene) for 10 minutes. The sulfo-SANPAH was removed and the substrates were overlaid with fresh sulfo-SANPAH and exposed again to ultraviolet light for 10 minutes. At this point the substrates were sterilized and washed three times with PBS. The substrates were coated with 10 or 50 µg/mL collagen I diluted in PBS for 3 hours at 37°C.

4.3.2. Fluorescent immunostaining of collagen-I for ligand surface coverage

Ligand surface coverage was evaluated by fluorescent immunostaining of collagen-I. Immediately after collagen coating, the substrates were washed three times with PBS and fixed with formalin solution 10% (sigma, HT5011) for 10 min, washed with PBS three times, blocked for 1 hour with 0.5% bovine serum albumin (BSA) and overlaid with the primary polyclonal antibody anti-collagen I (abcam, 96723) diluted 1:200 in 0.1% BSA for 1 hour. The substrates were washed three times with 0.1% BSA and stained with a secondary antibody labelled with FITC (Jackson ImmunoResearch, 711-095-152) diluted 50:1 in 0.1% BSA for 45 min in a dark room. The substrates were washed three times with 0.1% BSA, once with PBS and protected from light until analysis on an iMic spinning disk confocal (FEI Photonics) microscope with a 60x objective (N.A. 1.35).

4.3.3. Scanning electron microscopy imaging of ligand assembly/conformation

Immediately after collagen coating, the substrates were washed three times with PBS and fixed with gluteraldehyde 2.5% solution (Sigma) for 30 min. The substrates were then washed three times with milli-Q H_2O and dried with ethanol concentration gradient solutions from highly purified ethanol 25% (v/v) diluted in milli-Q H_2O to ethanol 100%. The substrates were sputter coated with a 3nm-layer of gold (20%) / palladium (80%) and taken to the microscope. Images were taken with an electron beam voltage of 10kV on a SEM Zeiss Supra 50 VP.

4.3.4. Atomic force microscopy imaging of ligand topography/roughness

Immediately after collagen coating, the substrates were washed three times with PBS and taken to the microscope. Images were taken on a Nanosurf

FlexAFM system with static force mode in water. Gold-coated quartz-like qp-CONT cantilevers with ~0.14N/m force constant were used.

4.3.5. Cell culture

Human bone marrow stromal cells were purchased from the institute for Regenerative Medicine at Texas A&M University. The cells were fully characterized by the institute as multipotent mesenchymal stromal cells. After expanding and aliquotting for the present study, the cells were tested for their capacity to differentiate toward adipogenesis and osteogenesis. For all the experiments, the hBMSCs were at an early P2 passage and cultured in Lonza's TheraPEAK^{TM} MSCGM-CD^{TM} chemically defined mesenchymal stem cell medium (Lonza, 190632). Medium was exchanged every three days and maintained at 37°C with 5% CO_2.

4.3.6. Cell attachment and morphology

Cell attachment was analyzed by culturing 25,000 cells/cm^2 on functionalized substrates with 10 or 50 μg/ml of collagen I for 1 h at 37°C. Substrates were washed with PBS to remove unbound cells, fixed with formalin solution 10% (sigma, HT5011) for 10 min, washed with PBS three times, and overlaid with 4',6-diamidino-2-phenylindole (DAPI) diluted in PBS, which counterstains DNA and labels the nucleus. On each replicate, at least 22 images of non-overlapping regions containing around 150 cells were randomly taken with a 10x objective on a Nikon Eclipse Ni upright microscope. Nuclei were counted using image-J software by constrat thresholding the DAPI image to obtain a binary image, and then automatically counted by analyzing the particles.

Cell morphology was examined with immunofluorescence imaging. Substrates were prepared as described above, and cells were seeded at 5,000 cells/cm^2 for 24h at 37°C. Cells were washed with PBS, fixed with formalin 10% for 10min, washed again with PBS three times, permeabilized with Triton-X 100 (sigma) and blocked for 1 hour with 0.5% BSA. After washing substrates, the primary monoclonal antibody anti-vinculin (sigma, V9131) diluted 1:400 in the washing solution (0.05% Triton; 0.1% BSA) was overlaid for 1 hour. After washing substrates three times with the washing solution, the secondary antibody Rhodamine Red (Thermo Scientific, R-6393) diluted to 1:200, Alexa Fluor 488 phalloidin (Life Technologies, A12379) diluted to 1:500 and DAPI in washing solution were overlaid on substrates for 45 min at room temperature in a dark environment. The stain was aspirated and substrates were washed three times with PBS. Images were taken on an iMic spinning disk confocal (FEI Photonics) microscope with a 40x objective (N.A. 0.95). Cell spreading was quantified with 8-10 images of non-overlapping regions on each replicate having a total cell number of at least 600 per sample with a 10x objective. Spreading area was calculated using image-J software by contrast thresholding the FITC-phalloidin channel to obtain a binary image, and then automatically measured the area. The calculated area was normalized to the number of cells present on the image (as described above).

4.3.7. Cell differentiation quantification

Bone marrow stromal cells were seeded at 5,000 cells /cm^2 and cultured for 1.5 h before changing the medium to either fresh basal growth medium or mixed induction medium, which consisted of 0.5μM dexamethasone (sigma), 10 mM β-glycerolphosphate (sigma), 50μM L-ascorbic acid 2-phosphate (sigma), 0.5μM isobutylmethylxanthine (sigma), 50μM indomethacin (sigma), and 10 μg/ml insulin (sigma). Respective medium was exchanged every three days and maintained at 37°C with 5% CO_2.

After 7 days in culture, alkaline phosphatase (ALP) was employed as the indicators of osteoblasts. Cells were first washed with PBS, then trypsinized (without EDTA) and stored at -80°C until analysis. A fluorometric assay kit (Abcam, 83371) was used to determine the alkaline phosphatase activity according to the stated protocol in the kit, where the fluorescence intensity was measured at Ex/Em 360/440 nm using a fluorescence microplate reader. A fluorometric DNA quantitation kit (Sigma, DNAQF) was used to quantify the cell proliferation and normalize the ALP activity according to the stated protocol in the kit, where the fluorescence intensity was measured at Ex/Em 360/460 nm using a fluorescence microplate reader.

4.3.8. Phosphorylated ERK1/2 quantification

Bone marrow stromal cells were seeded at 5,000 cells/ cm^2 and cultured for 7 days in co-induction medium. Level of extracellular signal-regulated kinases (ERK1/2) phosphorylation as a regulator of the ERK/MAPK pathway was determined with a PhosphoTracer ELISA kit (abcam, ab119674) according to the stated protocol in the kit, where the fluorescence intensity was measured at Ex/Em 535/595 nm using a fluorescence microplate reader.

4.3.9. Alizarin red staining for osteogenic differentiation

Bone marrow stromal cells were seeded at 5,000 cells/cm^2 and maintained in culture for 7,14 or 21 days in basal growth medium or co-induction medium as described above. At the time point, substrates were gently washed with PBS, and cells were fixed with formalin solution 10% for 30 min. The fixative was removed and substrates were washed three times with milli-Q H_2O. Alizarin red 2% staining solution was prepared by mixing alizarin red powder (Sigma) with milli-Q H_2O. The pH was adjusted to 4.2 with 10% NH_4OH (Sigma), then the solution was filtered with a 0.2µm filter. The staining solution was overlaid on substrates for 15 minutes then, the substrates were washed three times with milli-Q H_2O. Images were acquired with an EVOS digital inverted microscope with a 4x objective.

4.3.10. Real time and quantitative PCR

Expression of osteogenic markers, integrin subunit and focal adhesion-related genes were evaluated at day 1 or 7 of cell culture by performing reverse transcriptase polymerase chain reaction (RT-PCR). Substrates were prepared and maintained in culture as described above. At the time point, substrates were washed first with PBS and the total RNA was extracted using the RNeasy micro kit (Qiagen, 74004) following manufacturer's protocol. The cDNA was obtained by using a cDNA Reverse Transcription kit (Applied Biosystems, 4368814). PCR was performed on resultant cDNA using TaqMan® Universal PCR Master Mix (Life Technologies, 4364338) with TaqMan® gene expression assays (Life Technologies; for primer references, see Table 1). Data were analyzed using the $2^{-\Delta\Delta Ct}$ method, and glyceraldehyde-3-phosphate dehydrogenase (GAPDH) was chosen as the housekeeping gene. The results were normalized by the mean values of the corresponding pristine PDMS groups.

4.3.11. Fluorescence-activated cell sorting

After 7 days in culture, the substrates were washed once with PBS and overlaid with accutase (Sigma, A6964) for a gently cell detachment. After complete detachment, the cells were stained with the corresponding primary antibody anti-integrin α1 (CD49a; BD Biosciences, 559594) diluted 1:100 in accumax buffer (Sigma) or anti-integrin α2β1 (abcam, 24697) diluted 1.50 in accumax buffer for 30 min on ice. The cells were washed twice with accumax buffer and stained with the secondary antibody PE (Imgenex, 20103) diluted 1:100 in accumax buffer for 20 min on ice in a dark room. The cells were washed again twice with accumax buffer, then kept on ice and protected from light until analysis. The samples were analysed on a BD Accuri™ C6 flow cytometer with as negative control unstained cells and cells only stained with the secondary antibody. Living cells were gated from dead cells and cell debris (number of events > 10'000) on the basis of side-scattered light (SSC) characteristics versus the forward-scattered light (FSC). The data were analyzed with the FlowJo software.

4.3.12. Statistical analysis

All experiments were performed in triplicate with five independent experiments (n=5) unless indicated. Data are represented as means and standard error (bars in the figure). When only two groups were analyzed, the results were normalized by the mean values of the corresponding hydrophobic PDMS groups. For multiple comparisons, a two-way ANOVA with Bonferroni correction was applied to reveal main effect. The unpaired two-tailed student's t-test with a confidence level of 95% was applied to see if two sets of data differ significantly. Significance was indicated for $p \leq 0.05$ (*$p \leq 0.05$, **$p \leq 0.01$, ***$p \leq 0.001$, **** $p \leq 0.0001$). All the charts and analysis were processed with Prism 6 software.

4.4 Results

4.4.1 Bioactivity characterization of the different surfaces

As previously described in chapter 3, we empirically adapted the molarity of the respective ligand solutions to achieve equivalent protein loading (Fig.4A), with 10 μg/ml (5 μg/cm^2) used on standard PDMS and 50 μg/ml (25 μg/cm^2) used on PEO-PDMS. In this manner, the amount of surface bound collagen measured in chapter 3 was optimized to minimize ligand-density dependent promotion of attachment and differentiation [5]. Immunostaining of collagen-I (supplementary Fig. S4.1) indicated that both substrates were uniformly covered by collagen at the subcellular scale.

Our analysis by atomic force microscopy and electron microscopy showed that PDMS wettability influenced the deposition and folding of collagen monomers covalently bound to the surface (Fig. 4.1A and supplementary Fig. S4.2). On hydrophobic PDMS substrates, monomers appeared folded and clumped to each other in the form of molecular aggregates exhibiting a relatively rough collagen layer (Ra= 88.8 nm). On the other hand, the resulting collagen layer on hydrophilic PDMS appeared qualitatively more homogenous and smoother (R_a=6.2 nm) with AFM imaging indicating that the collagen adopted a more spread assembly (Fig. 4.1B and supplementary Fig. S4.2). A similar observation was made with a hydrophilic plasma treated PDMS (Fig. 4.1C) having clearly flattened single monomers. Briefly, those substrates were obtained via a low-energy oxygen plasma treatment (Diener FEMTO, Nagold, Germany) for 50 seconds. While hydrophobic recovery occurred after plasma treatment [44], the measured contact angle was around 60° prior to collagen coating (data not shown).

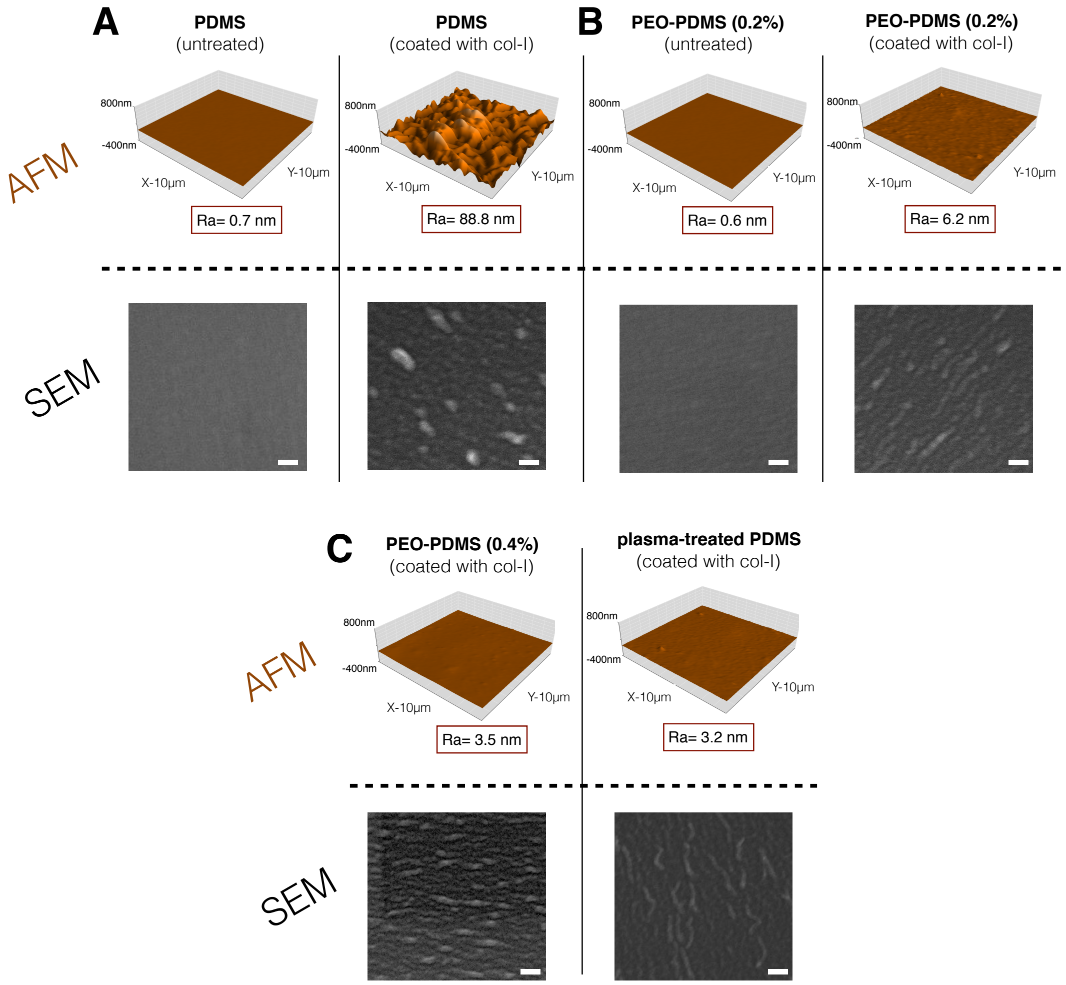
A
PDMS
(untreated)
PDMS
(coated with col-I)
B
PEO-PDMS (0.2%)
(untreated)
PEO-PDMS (0.2%)
(coated with col-I)
AFM
800nm
-400nm
X-10μm
Y-10μm
Ra= 0.7 nm
Ra= 88.8 nm
Ra= 0.6 nm
Ra= 6.2 nm
SEM
C
PEO-PDMS (0.4%)
(coated with col-I)
plasma-treated PDMS
(coated with col-I)
AFM
Ra= 3.5 nm
Ra= 3.2 nm
SEM

Figure 4.1 | Atomic Force Microscopy (AFM) and Scanning Electron Microscopy (SEM) images of various PDMS-based substrates that were untreated or coated with collagen-I monomers: (A) PDMS, (B) PEO-PDMS (0.2%), (C) PEO-PDMS (0.4%) and plasma-treated PDMS. Scale bar = 100 nm. (see supplementary S3 for additional images)

4.4.2 Cell attachment and morphology

At 1 hour after cell seeding at high density (25,000 cells/cm^2), the percentage of cell attachment as determined by DAPI staining and quantitative analysis (ImageJ) was approximately 50% of seeded cells on both the hydrophobic and hydrophilic substrates (Fig. 4.2B).

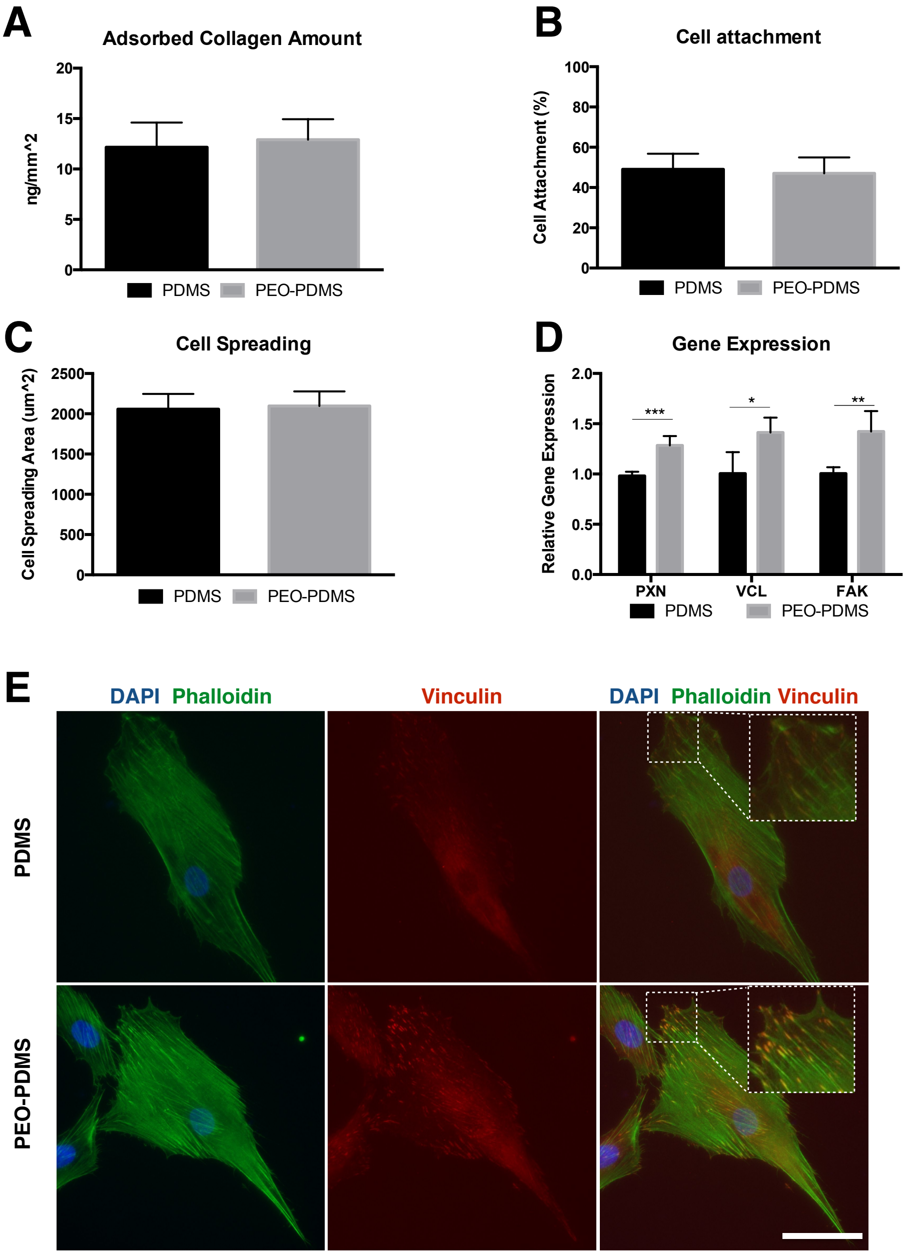

Figure 4.2 | (A) Adsorbed collagen-I amount on PDMS and PEO-PDMS (0.2%) substrates. Collagen-I monomers were coated at a concentration of 10µg/ml on pristine hydrophobic PDMS substrates and of 50µg/ml on hydrophilic PEO-PDMS substrates to obtain a similar adsorbed collagen amount on both types of substrates; mean± s.d. (B) hBMSCs attachment

on PDMS and PEO-PDMS (0.2%) substrates. PDMS and PEO-PDMS (0.2%) presented a similar cell attachment when seeded at 25’000 cells/cm^2 after 1 h culture; mean± s.d (n=3). (C) hBMSCs spreading area on PDMS and PEO-PDMS (0.2%) substrates. PDMS and PEO-PDMS (0.2%) presented a similar cell spreading area when seeded at 5’000 cells/cm^2 after 24 h culture; mean± s.d (n=4). (D) PCR analysis of hBMSCs focal adhesion related components after 1-day culture on PDMS and PEO-PDMS substrates. Paxillin (PXN) expression was higher on PEO-PDMS substrates and similar trend was observed with vinculin (VCL) and focal adhesion kinase expression (FAK); mean± s.d. ***p=0.001 (PXN); *p=0.0201 (VCL); **p=0.0077 (FAK). (E) Morphology of hBMSCs on functionalized substrates seeded at 5’000 cells/cm^2 after 24 h culture on PDMS and PEO-PDMS (0.2%) substrates. Cells were immunostained with an antibody against vinculin (red), FITC-phalloidin (green) and DAPI (blue). Scale bar = 50 µm. (see supplementary S5 for additional images)

Cell morphology was quantified on cells fixed 24 hours after cell seeding at low density (5,000 cells/cm^2) by fluorescent staining for nuclei, F-actin and vinculin. Analysis of area and aspect ratio indicated that the cells seeded on PEO-PDMS spread to a similar extent as those on standard PDMS, suggesting that the hydrophilic and hydrophobic PDMS variants were equivalently biocompatible and able to sustain cell adhesion (Fig. 4.2C). While morphology was qualitatively similar, a typically large degree of heterogeneity in cell populations was observed [45]. An apparently higher intensity of phalloidin staining on PEO-PDMS was observed (Fig. 4.2E and S4.4), consistent with higher anti-vinculin immunofluorescence intensity observed at the focal adhesions on these substrates, as well as increased expression of focal adhesion related genes after 24 h as quantified by PCR (Fig. 4.2D-E).

4.4.3 Osteogenic cell differentiation

Our main interest was to evaluate whether PDMS wettability modulates hBMSC differentiation. Previous studies [6, 19] have reported a predisposed fate toward an osteogenic lineage when stem cells were cultured on PDMS substrates having a 10:1 ratio and coated with collagen I. BMSCs were first cultured for 7 days at low density (5,000 cells/cm^2) in basal growth medium or co-induction medium. When cultured in basal growth medium, the amount of DNA present on PEO-PDMS substrates was significantly lower by 20% (p=0.0198) than the baseline amount of 5530 ng on PDMS suggesting a lower cell proliferation (Fig. 4.3A).

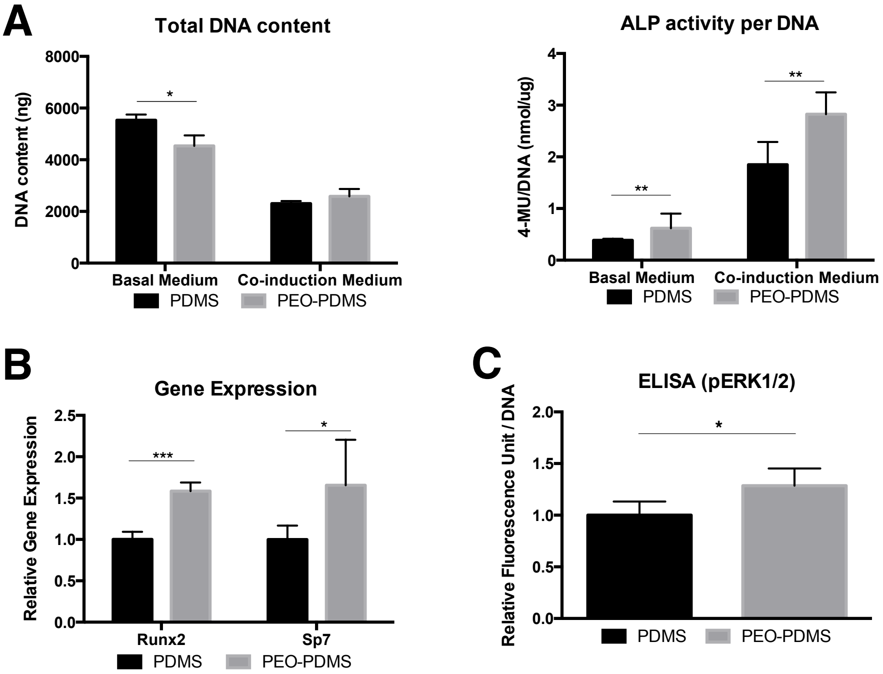

Figure 4.3 | Differentiation of hBMSCs after 7-day culture on PDMS and PEO-PDMS substrates. (A) Total DNA content of PDMS and PEO-PDMS substrates seeded at 5’000 cells/cm^2 and after 7-day culture in basal growth medium and in co-induction medium; mean± s.d (n=4-5); *p=0.0198; Total alkaline phosphatase (ALP) activity per DNA indicated a higher osteogenic differentiation on PEO-PDMS substrates when compared to PDMS substrates; mean± s.d; **p=0.0022 (basal); **p=0.0071 (co-induction). B) Molecular investigations of hBMSCs gene expression related to osteogenic differentiation after 7-day culture on PDMS and PEO-PDMS substrates in co-induction medium. Runx2 expression was higher on PEO-PDMS substrates and similar trend was observed with Sp7 expression; ****p=0.0001 (Runx2); *p=0.0237 (Sp7). (C) Semi-quantification of phosphorylated extracellular signal-regulated kinases 1 and 2 (ERK1/2) by immuno-sandwiched ELISA after 7-day culture on PDMS and PEO-PDMS substrates in co-induction medium. ERK 1/2 was more phosphorylated on PEO-PDMS substrates; mean± s.d; *p=0.0169.

When cultured in co-induction medium, no significant difference in amount of DNA was observed between the two groups of substrates. We could also observe that the DNA amounts of substrates in co-induction medium were notably 2-fold lower than the substrates cultured in basal growth medium (Fig. 4.3A). Quantification of alkaline phosphatase activity revealed 4-fold higher levels of this osteogenic marker in cultures within co-induction medium compared to basal medium, confirming capacity of the cells to differentiate (Fig. 4.3A). Most remarkably, in both cell culture media types cells on PEO-PDMS presented 50-60% higher ALP activity than the baseline activity of 1.85 4-MU/DNA on standard PDMS. This suggests that more cells were pushed to differentiate toward an osteogenic lineage within 7 days on hydrophilic substrates.

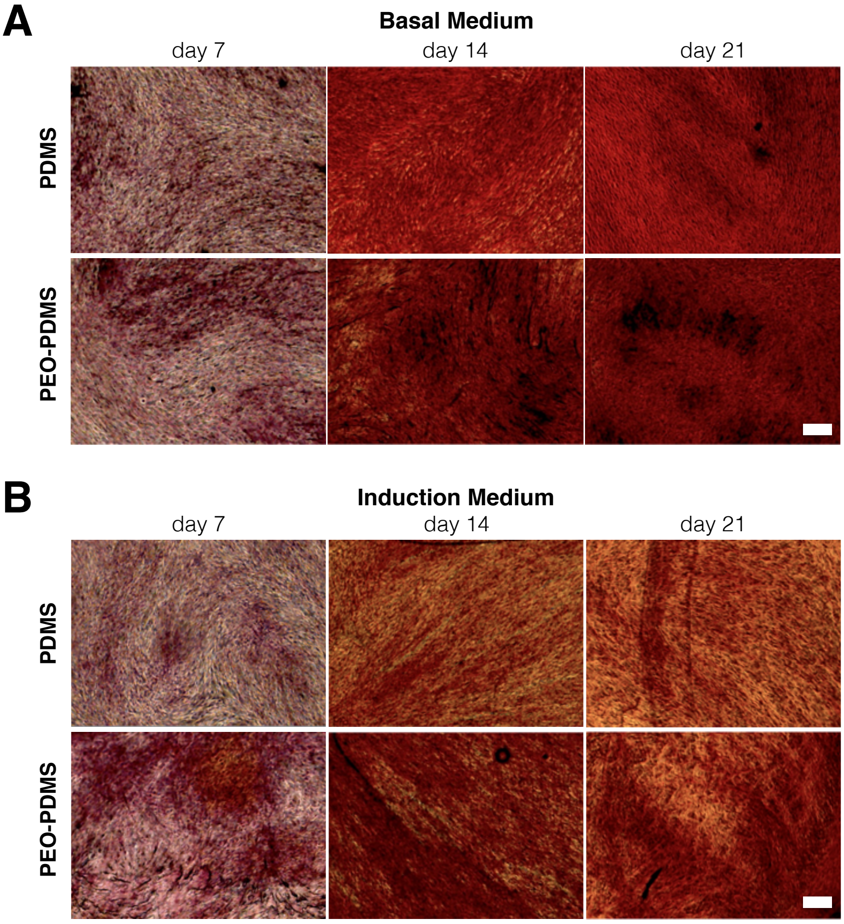

Figure 4.4 | Alizarin red staining of hBMSCs on PDMS and PEO-PDMS substrates in culture for 7, 14 and 21 days. (A) When cultured in basal growth medium, a higher calcium deposit is observed overtime on the PEO-PDMS substrates when compared to PDMS substrates; (B) A similar trend was observed when cultured in induction medium but less significant. Scale bar = 200 μm.

We performed quantitative PCR to examine changes in gene expression related to transcription factors relevant to osteogenic expression. Consistent with ALP activity, Runx2 and Sp7 expressions were higher (>50%; $p<0.0001$ (Runx2), $p=0.018$ (Sp7)) on hydrophilic substrates (Fig. 6B). ELISA analysis (Fig. 4.3C) also confirmed a higher phosphorylation by 30% of extracellular signal-regulated kinases 1 and 2 (ERK1/2) on hydrophilic substrates, which is a positive key regulator of the mitogen-activated protein kinase (MAPK) pathway involved in osteogenic differentiation [46, 47]. BMSCs were then cultured for longer time periods before staining at day 7, 14 and 21 with Alizarin Red for calcium deposits, a standard indicator of differentiated osteoblasts [48]. Consistent with ALP and gene expression, this assay of matrix production showed qualitatively a higher amount of deposited calcium over time on the hydrophilic substrates (Fig. 4.4). After 21 days, substrates cultured in basal growth medium (Fig. 4.4) presented qualitatively more calcium than substrates in co-induction medium (Fig. 4.4B).

4.4.4 Molecular investigation of focal adhesion related components, integrin and discoidin domain receptors

To elucidate signaling pathways involved in substrate driven osteogenic differentiation, we performed additional PCR to evaluate changes after 24h in gene expression related to focal adhesion related components including paxillin, vinculin and focal adhesion kinase (FAK). These important subcellular components are important for the activation of signaling cascades such as ERK pathway [49] were all upregulated on hydrophilic PEO-PDMS substrates (Fig. 4.5A). We probed also gene expression on day 1 and 7 of subunits related to two of the most well-described integrin receptors involved in collagen-I binding (α1β1 and α2β1) [11] and the discoidin domain receptors (DDR1 and DDR2) a transmembrane receptor that is also known to be activated by collagen [50]. We found that gene expression on day 1 of α1 and β1 integrin subunits were higher on PEO-PDMS but similar for α2 (Fig. 4.5A). While α1 and β1 subunits remained higher on hydrophilic substrates on day 7, α2 subunit also became upregulated on those substrates (Fig. 4.5A). Like the α1 subunit, DDR1 and DDR2 were both upregulated on day 1 and remained higher on day 7 on PEO-PDMS substrates (Fig. 4.5A). Consistent with the gene expression levels, FACS analysis on day 7 indicated the increased presence of the integrin receptors α1β1 and α2β1 on cells cultured on the more hydrophilic substrates (Fig. 4.5B).

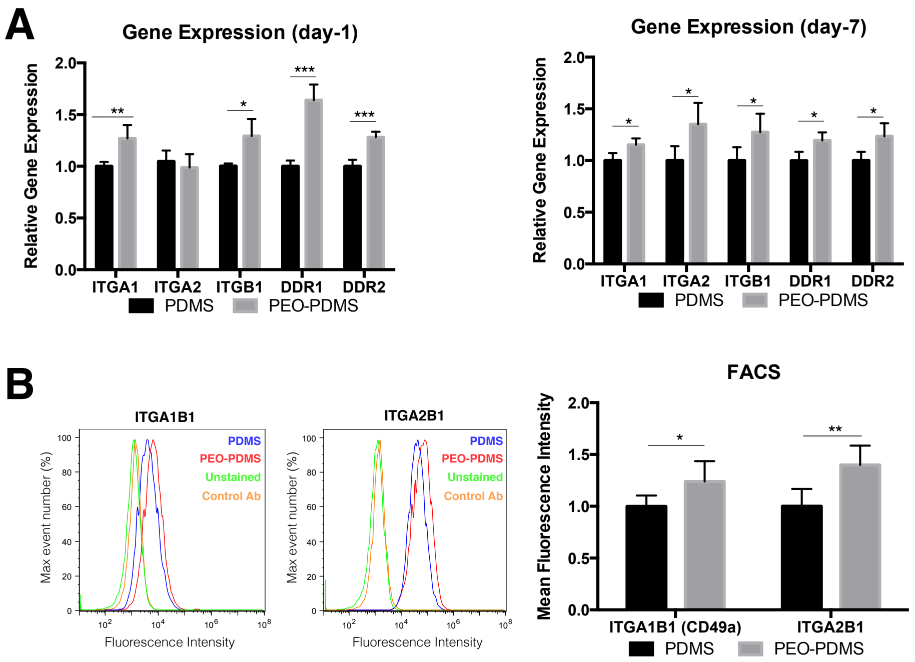

Figure 4.5 | Molecular investigations of hBMSCs gene expression after 1,7-day culture on PDMS and PEO-PDMS substrates. (A) Regarding integrin receptor subunits: on day 1, ITGA1 (integrin alpha 1) and ITGB1 (integrin beta 1) expression was higher on PEO-PDMS substrates compared to PDMS substrates but (B) similar expression for ITGA2 (integrin alpha 2) on both substrates. On day 7, ITGA1 expression still remained higher on PEO-PDMS substrates and ITGA2 expression became higher on PEO-PDMS substrates; mean± s.d.; **p=0.0073 (ITGA1$_{day1}$); *p=0.0130 (ITGB1$_{day1}$) *p= 0.0182 (ITGA1$_{day7}$); *p=0.0307 (ITGA2$_{day7}$); *p=0.0468 (ITGB1$_{day7}$). Regarding discoid domain receptors (DDR): After 1 day, DDR1 and DDR2 expression were higher on PEO-PDMS substrates and after 7 days, while DDR2 expression difference remained the same, DDR1 difference decreased but remained upregulated on PEO-PDMS. mean± s.d. ***p=0.0002 (DDR1$_{day1}$); ***p=0.0005 (DDR2$_{day1}$); *p=0.0147 (DDR1$_{day7}$); *p=0.0212 (DDR2$_{day7}$). (B) FACS analysis of integrin receptor expression levels of hBMSCs on PDMS and PEO-PDMS substrates after 7-day culture. Cells were stained with antibodies against α1β1 and α2β1 integrins (ITGA1B1; ITGA2B1). (left) Representative normalized distributions of fluorescent pulse peak areas for the antibodies ITGA1B1 and ITGA2B1. The background fluorescence is represented in green with unstained cells and in orange with cells only stained with secondary antibody. (right) ITGA1B1 receptor was more expressed on cells present on PEO-PDMS substrates compared to cells on PDMS substrates and similar trend was observed for ITGA2B1; mean± s.d. *p=0.0421 (ITGA1B1); **p=0.0074 (ITGA2B1).

4.5 Discussion

Understanding cell-material interaction is essential for the development of cell-instructive implants. Biomaterial design can exploit the mechanisms by which cells sense their environment via mechanical linkages to substrate ligands, and transduce force feedback within signaling cascades. While the mechanics and biochemistry of cellular attachment points are important, the activity state of a ligand is adsorption-dependent and can be affected by environmental properties. Although fibronectin function on hydrogels has been previously investigated [9], effects of hydrophobicity on collagen I assembly and stem cell behavior still remain unclear, especially when this model ligand has been covalently bound to PDMS. To our knowledge, the present study demonstrates for the first time that rendering PDMS hydrophilic through addition of a small amount of surfactant can alter covalently bound collagen assembly and in turn drastically affect early stem cell signaling with downstream effects on differentiation fate. This finding has potentially critical implications for numerous and heavily cited comparative studies that have employed PDMS as a cell culture model system. Beyond this major finding, another important aspect of this work was the use of a PDMS cell culture substrate that can be tuned with regard to wettability without otherwise affecting physical and mechanical properties, therefore allowing one to potentially limit confounding factors in the parametric study of cell behavior.

Collagen self-assembly relies on the interplay of collagen-collagen and collagen-substrate interactions [51], and indeed our analysis by electron microscopy showed that PDMS wettability influenced the folding of collagen monomers covalently bound to the surface. On hydrophobic PDMS substrates, monomers appeared folded and clumped to each other to form molecular aggregates. As previously described [23], once a few molecules are adsorbed to the substrate, these nucleate the accretion of molecules that are still in suspension and can predispose the formation of multi-layer aggregates rather than a monolayer in which incoming molecules occupy still available space on the biomaterial surface. On the other hand, monomers on hydrophilic PDMS seemed to have an extended conformation with ready adsorption to the exposed biomaterial surface and a reduced tendency to form aggregates, perhaps indicating a higher affinity for collagen-biomaterial interaction than for collagen-collagen interaction. However, we cannot exclude that the aggregates were already formed and present in solution prior to coating, which in such a case a hydrophobic PDMS substrate favored adsorption of these molecular aggregates [14]. Moreover, the presence of aggregates would tend to render a thicker protein layer atop the biomaterial surface, which may also play a role in cell interaction.

Surprisingly, the difference in collagen assembly did not obviously affect qualitatively assessed cell attachment and morphology. This finding contrasted with our expectation that cell binding site accessibility would be affected as previously reported [9, 23], therefore modulating the chance for cells to effectively attach. Morphological analysis after 24 hours indicated first that the cells seeded on PEO-PDMS were able to spread in a similar way as observed on standard PDMS, suggesting that the hydrophilic PDMS platform was biocompatible and able to sustain cell adhesion. While morphology appeared to be similar, it was difficult to interpret due to heterogeneity in the population [45] and due to an apparently higher intensity phalloidin fluorescence on PEO-PDMS. This observation possibly suggests increased tendency for actin polymerization into F-actin, which could affect many cellular functions including cell motility, shape and polarity [52]. It is further consistent with the observed increase in expression of focal adhesion related components after 24 h; higher F-actin polymerization would also involve increased maturation of focal adhesions through the recruitment of additional adaptor molecules such as paxillin, vinculin and FAK [53].

The present experiments was able to isolate effects of wettability from differences in mechanical properties, biochemistry, and ligand density, and demonstrated that enhanced osteogenic differentiation of hMSCs on hydrophilic substrates is mostly likely to attributable to the different collagen assembly and associated differences in surface nanotopography. Previous studies with stem cells have shown that nanotopography influences the organization of the cytoskeleton and focal adhesions [54, 55], but also differentiation fate [54]. Therefore, we suggest that hydrophilic PDMS permits a spatial organization of collagen monomers that tends to accelerate the onset of osteogenic differentiation. Another related explanation could be attributed to the variation of the ligand spacing, which is known to play a role in integrin recruitment dynamics that regulate stem cell differentiation [56]. As mentioned before, hydrophobic substrates favor to monomer aggregation and less efficient surface coverage at equivalent loading [23]. Thus at similar levels of collagen loading, PDMS and PEO-PDMS present a differential spacing of binding sites, which may affect osteogenic differentiation.

Consistent with our findings, osteogenic differentiation of hMSCs on collagen-coated substrates has been reported to involve similar molecular pathways, including focal adhesion related components (Paxillin, Vinculin and FAK) [57], osteogenic transcription factors (Runx2, Sp7) and regulators of the MAPK pathway (ERK1/2) [46]. In our study we observed clearly distinct but nonetheless small fold-changes in gene expression. We consider these small fold-changes at early time points to reflect the relatively small subpopulations of osteogenic differentiated cells within a still highly heterogeous hBMSC population [6, 45]. While we observed no difference with the subunit α2 expression on day 1, subunits α1 and β1 were both upregulated on hydrophilic PDMS. Thus, integrin α1β1 may be involved in early recognition of differential collagen assembly, as reported in an earlier study suggesting that α1β1 determines the osteoinductive effect of nanotopography on stem cells [58]. Both discoidin domain receptors DDR1 and DDR2 were upregulated on day 1 on hydrophilic PDMS, however DDR2 expression was less impacted, and similar differences in DDR receptor gene expression remained after 7 days. Based on our finding that collagen assembly on hydrophilic PDMS promotes a higher activation of DDR receptors, we suggest that differences in spatial collagen organization may regulate osteogenic differentiation via the DDR1 receptors, a hypothesis that has already been supported in studies of stem cells within 3D collagen matrices [13]. Another study has demonstrated that DDR2 downregulates FAK on self-assembling fibrillar collagen I compared to a non-fibrillar monolayer of collagen [25], which is also consistent with our results.

Regarding the cross-talk between DDR and integrin receptors, previous studies have reported that DDR1 and α1β1 receptors could converge on the same signaling pathways, including ERK1/2 activation [50, 59]; DDR1 activation occurs independently of integrins but can promote their activation [60, 61]. Based on these previous observations and our results, we conclude that both DDR1 and α1β1 may be involved in the recognition of a differential collagen assembly and lead to the recruitment of additional α2β1 integrins and activation of MAPK pathway via ERK1/2 to regulate osteogenic differentiation.

We note that most of the observed differences appear to be transient, with the integrin subunit α2 expression on PEO-PDMS reaching levels similar to standard PDMS after 7 days. This observation may reflect the fact that the original adsorbed collagen layer is eventually remodeled into a configuration that is similar on both biomaterial formulations. Additional experiments including a precise analysis of extracellular matrix production would be required to confirm this. In any case, it appears that the hydrophobic surfaces still result in osteogenesis but with a time lag in comparison to the hydrophilic variants. Detailed analyses of the kinetics of matrix remodeling, and time course of cell proliferation and subpopulation differentiation all remain grounds for future work.

Finally with regard to substrate elasticity as a key determinant of stem cell fate [1], the present work seems to indicate a critical gap between previous studies using porous hydrogels [2, 6] and amorphous, anatomically flat materials like PDMS [2, 6, 19, 26-42]. Research groups have explained unexpected lack of sensitivity of cells to PDMS substrate mechanics by highlighting the amorphous features of a PDMS surface [6], the underestimated stiffness of very soft substrates [2], or the manner by which various surface treatments affect surface mechanical properties [31]. Our study suggests that the nature of collagen assembly alone can influence the mechanical and biochemical coupling of a cell to a biomaterial surface, potentially altering the mechanosensitivity of a cell. While osteogenic differentiation rates on standard PDMS formulations have been reported to be lower than on stiff PAA [6], we demonstrate that these can be "recovered" using a hydrophilic variant of PDMS that promotes osteogenesis. The tendency for hydrophobic surfaces to induce an aggregate assembly of collagen molecules may preclude a sufficiently direct mechanical coupling that interferes with a cells ability to sense the stiffness of the substrate beneath. In this model, a hydrophobic substrate would lead to a short-term mechanical decoupling between the coated collagen layer and the bulk PDMS. Such a model could explain reported stem cell insensitivity to PDMS stiffness, whereby cells sense the elasticity of the packed collagen layer rather than the substrate. A recent study has shown that a highly dense packed collagen on hydrophobic glass can drastically impact cell spreading [23]. Further experiments are ongoing that will test this model.

4.6 Supplementary material

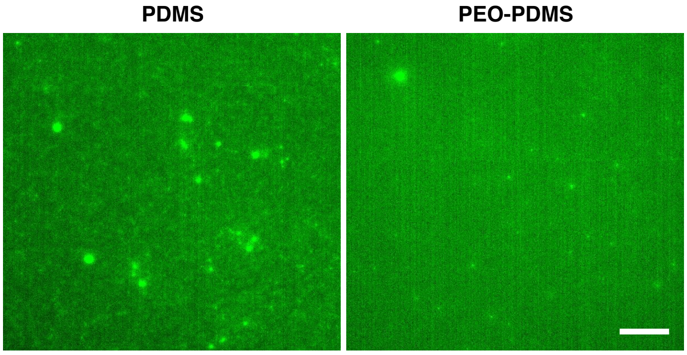

Supplementary Figure S4.1 | Immunofluorescence of collagen-I coated PDMS and PEO-PDMS (0.2%) substrates. Scale bar = 10 µm.

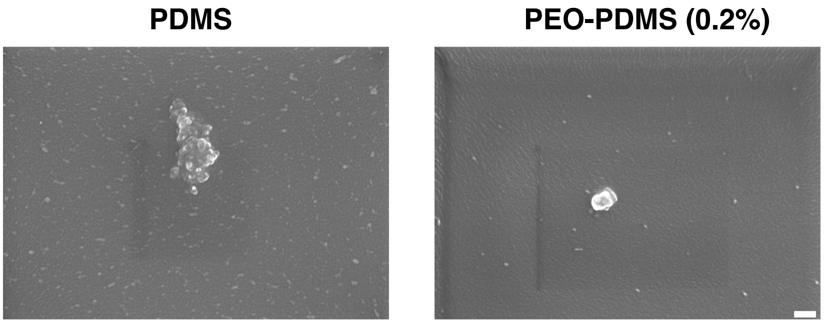

Supplementary Figure S4.2 | Scanning Electron Microscopy (SEM) images of collagen-I monomers coated on PDMS and PEO-PDMS (0.2%). Scale bar = 300 nm.

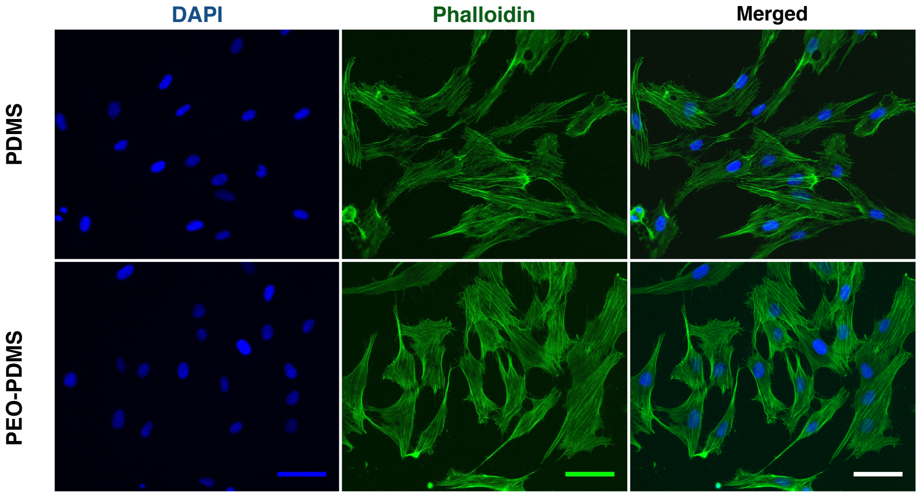

Supplementary Figure S4.3 | Morphology of hBMSCs on functionalized substrates seeded at 5’000 cells/cm^2 after 24 h culture on PDMS and PEO-PDMS (0.2%) substrates. Cells were stained with FITC-phalloidin (green) and DAPI (blue). Scale bar = 50 µm.

Type of experiment	Cell culture duration	Initial cell seeding density (cell/cm^2)
Cell attachment	1 hour	25,000
Cell morphology	1 day	5,000
Gene expression	1 day	25,000
Gene expression	7 days	5,000
Cell differentiation	7, 14 and 21 days	5,000
FACS analysis	7 days	5,000

Supplementary Table S4.1 | Summary of the different performed experiments with their cell culture duration and initial cell seeding density

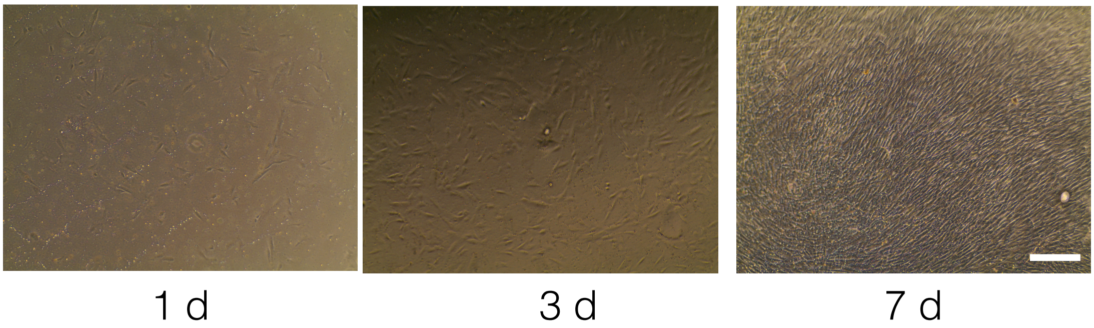

Supplementary Figure S4.4 | Morphology of hBMSCs on functionalized PDMS substrates seeded at 5’000 cells/cm^2 after 1 d, 3 d and 7 d in culture. Scale bar = 250 µm.

4.7 References

[1] A.J. Engler, S. Sen, H.L. Sweeney, D.E. Discher, Matrix Elasticity Directs Stem Cell Lineage Specification, Cell 126(4) (2006) 677-689.
[2] J.H. Wen, L.G. Vincent, A. Fuhrmann, Y.S. Choi, K.C. Hribar, H. Taylor-Weiner, S. Chen, A.J. Engler, Interplay of matrix stiffness and protein tethering in stem cell differentiation, Nature materials 13(10) (2014) 979-87.
[3] D.S. Benoit, A.R. Durney, K.S. Anseth, The effect of heparin-functionalized PEG hydrogels on three-dimensional human mesenchymal stem cell osteogenic differentiation, Biomaterials 28(1) (2007) 66-77.
[4] D.S. Benoit, M.P. Schwartz, A.R. Durney, K.S. Anseth, Small functional groups for controlled differentiation of hydrogel-encapsulated human mesenchymal stem cells, Nature materials 7(10) (2008) 816-23.
[5] X. Yao, Y. Hu, B. Cao, R. Peng, J. Ding, Effects of surface molecular chirality on adhesion and differentiation of stem cells, Biomaterials 34(36) (2013) 9001-9.
[6] B. Trappmann, J.E. Gautrot, J.T. Connelly, D.G.T. Strange, Y. Li, M.L. Oyen, M.A. Cohen Stuart, H. Boehm, B. Li, V. Vogel, J.P. Spatz, F.M. Watt, W.T.S. Huck, Extracellular-matrix tethering regulates stem-cell fate, Nature materials 11(7) (2012) 642-649.
[7] R.I. Sharma, J.G. Snedeker, Biochemical and biomechanical gradients for directed bone marrow stromal cell differentiation toward tendon and bone, Biomaterials 31(30) (2010) 7695-7704.
[8] A.V. Taubenberger, M.A. Woodruff, H. Bai, D.J. Muller, D.W. Hutmacher, The effect of unlocking RGD-motifs in collagen I on pre-osteoblast adhesion and differentiation, Biomaterials 31(10) (2010) 2827-35.
[9] R. Ayala, C. Zhang, D. Yang, Y. Hwang, A. Aung, S.S. Shroff, F.T. Arce, R. Lal, G. Arya, S. Varghese, Engineering the cell-material interface for controlling stem cell adhesion, migration, and differentiation, Biomaterials 32(15) (2011) 3700-11.
[10] B. Li, C. Moshfegh, Z. Lin, J. Albuschies, V. Vogel, Mesenchymal stem cells exploit extracellular matrix as mechanotransducer, Scientific reports 3 (2013) 2425.
[11] M. Barczyk, S. Carracedo, D. Gullberg, Integrins, Cell and tissue research 339(1) (2010) 269-80.
[12] B.G.C. Keselowsky, D.M.; Garcia, A.J, Surface chemistry modulates fibronectin conformation and directs integrin binding and specificity to control cell adhesion, Journal Biomedical Material Research A 66 (2002) 247-59.
[13] A.W. Lund, J.P. Stegemann, G.E. Plopper, Mesenchymal Stem Cells Sense Three Dimensional Type I Collagen through Discoidin Domain Receptor 1, The open stem cell journal 1 (2009) 40-53.
[14] C.C. Dupont-Gillain, I. Jacquemart, P.G. Rouxhet, Influence of the aggregation state in solution on the supramolecular organization of adsorbed type I collagen layers, Colloids and surfaces. B, Biointerfaces 43(3-4) (2005) 179-86.

[15] K.E.V. Michael, V. N.; Keselowsky, B. G.; Meredith, J. C.; Latour, R.A.; Garcia, A.J, Adsorption-Induced Conformational Changes in Fibronectin Due to Interactions with Well-Defined Surface Chemistries, Langmuir : the ACS journal of surfaces and colloids 19 (2003) 8033-8040.
[16] A.M. Schaap-Oziemlak, P.T. Kühn, T.G. van Kooten, P. van Rijn, Biomaterial–stem cell interactions and their impact on stem cell response, RSC Adv. 4(95) (2014) 53307-53320.
[17] E.M.R. Carter, C.L.; , Genetic and orthopedic aspects of collagen disorders
, Curr Opin Pediatr 21 (2009) 46-54.
[18] K. Kadler, Extracellular matrix 1: fibril-forming collagens., Protein Profile 1 (1994) 519-638.
[19] N. Evans, C. Minelli, E. Gentleman, V. LaPointe, S. Patankar, M. Kallivretaki, X. Chen, C. Roberts, M. Stevens, Substrate stiffness affects early differentiation events in embryonic stem cells, Eur Cells Mater 18 (2009) 1 - 13.
[20] G.K. Toworfe, R.J. Composto, C.S. Adams, I.M. Shapiro, P. Ducheyne, Fibronectin adsorption on surface-activated poly(dimethylsiloxane) and its effect on cellular function, Journal of biomedical materials research. Part A 71(3) (2004) 449-61.
[21] M. Wu, J. He, X. Ren, W.S. Cai, Y.C. Fang, X.Z. Feng, Development of functional biointerfaces by surface modification of polydimethylsiloxane with bioactive chlorogenic acid, Colloids and surfaces. B, Biointerfaces 116 (2014) 700-6.
[22] B. Valamehr, S.J. Jonas, J. Polleux, R. Qiao, S. Guo, E.H. Gschweng, B. Stiles, K. Kam, T.J. Luo, O.N. Witte, X. Liu, B. Dunn, H. Wu, Hydrophobic surfaces for enhanced differentiation of embryonic stem cell-derived embryoid bodies, Proceedings of the National Academy of Sciences of the United States of America 105(38) (2008) 14459-64.
[23] N.M. Coelho, C. Gonzalez-Garcia, J.A. Planell, M. Salmeron-Sanchez, G. Altankov, Different assembly of type IV collagen on hydrophilic and hydrophobic substrata alters endothelial cells interaction, European cells & materials 19 (2010) 262-72.
[24] C.P. Dupont-Gillain, E.; Denis, F.A; Rouxhet, P.G.;, Controlling the supramolecular organisation of adsorbed collagen layers, Journal of Materials Science - Materials in Medicine 15 (2004) 347-353.
[25] K. Bhadriraju, K.H. Chung, T.A. Spurlin, R.J. Haynes, J.T. Elliott, A.L. Plant, The relative roles of collagen adhesive receptor DDR2 activation and matrix stiffness on the downregulation of focal adhesion kinase in vascular smooth muscle cells, Biomaterials 30(35) (2009) 6687-94.
[26] J. Park, S. Yoo, E.-J. Lee, D. Lee, J. Kim, S.-H. Lee, Increased poly(dimethylsiloxane) stiffness improves viability and morphology of mouse fibroblast cells, BioChip J 4(3) (2010) 230-236.
[27] M. Prager-Khoutorsky, A. Lichtenstein, R. Krishnan, K. Rajendran, A. Mayo, Z. Kam, B. Geiger, A.D. Bershadsky, Fibroblast polarization is a matrix-rigidity-dependent process controlled by focal adhesion mechanosensing, Nat Cell Biol 13(12) (2011) 1457-1465.

[28] R.N. Palchesko, L. Zhang, Y. Sun, A.W. Feinberg, Development of polydimethylsiloxane substrates with tunable elastic modulus to study cell mechanobiology in muscle and nerve, PloS one 7(12) (2012) e51499.
[29] P.-Y. Wang, W.-B. Tsai, N.H. Voelcker, Screening of rat mesenchymal stem cell behaviour on polydimethylsiloxane stiffness gradients, Acta Biomaterialia 8(2) (2012) 519-530.
[30] N.R. Eroshenko, R.; Yadavailli V.; Rao. R.R, Effect of substrate stiffness on early human embryonic stem cell differentiation, Journal of Biological Engineering 7 (2013) 7.
[31] J. Li, D. Han, Y.-P. Zhao, Kinetic behaviour of the cells touching substrate: the interfacial stiffness guides cell spreading, Sci. Rep. 4 (2014).
[32] S.B. Gutekunst, C. Grabosch, A. Kovalev, S.N. Gorb, C. Selhuber-Unkel, Influence of the PDMS substrate stiffness on the adhesion of Acanthamoeba castellanii, Beilstein journal of nanotechnology 5 (2014) 1393-8.
[33] W. Zhang, D.S. Choi, Y.H. Nguyen, J. Chang, L. Qin, Studying cancer stem cell dynamics on PDMS surfaces for microfluidics device design, Scientific reports 3 (2013) 2332.
[34] S. Prauzner-Bechcicki, J. Raczkowska, E. Madej, J. Pabijan, J. Lukes, J. Sepitka, J. Rysz, K. Awsiuk, A. Bernasik, A. Budkowski, M. Lekka, PDMS substrate stiffness affects the morphology and growth profiles of cancerous prostate and melanoma cells, Journal of the mechanical behavior of biomedical materials 41 (2015) 13-22.
[35] J. Xie, Q. Zhang, T. Zhu, Y. Zhang, B. Liu, J. Xu, H. Zhao, Substrate stiffness-regulated matrix metalloproteinase output in myocardial cells and cardiac fibroblasts: implications for myocardial fibrosis, Acta Biomater 10(6) (2014) 2463-72.
[36] H. Choi, M. Kim, S.I. Ahn, E.G. Cho, T.R. Lee, J.H. Shin, Regulation of pigmentation by substrate elasticity in normal human melanocytes and melanotic MNT1 human melanoma cells, Experimental dermatology 23(3) (2014) 172-7.
[37] F. Ataollahi, S. Pramanik, A. Moradi, A. Dalilottojari, B. Pingguan-Murphy, W.A. Wan Abas, N.A. Abu Osman, Endothelial cell responses in terms of adhesion, proliferation, and morphology to stiffness of polydimethylsiloxane elastomer substrates, Journal of biomedical materials research. Part A (2014).
[38] Y. Shi, Y. Dong, Y. Duan, X. Jiang, C. Chen, L. Deng, Substrate stiffness influences TGF-beta1-induced differentiation of bronchial fibroblasts into myofibroblasts in airway remodeling, Molecular medicine reports 7(2) (2013) 419-24.
[39] W.H. Chen, S.J. Cheng, J.T. Tzen, C.M. Cheng, Y.W. Lin, Probing relevant molecules in modulating the neurite outgrowth of hippocampal neurons on substrates of different stiffness, PloS one 8(12) (2013) e83394.
[40] A. Arshi, Y. Nakashima, H. Nakano, S. Eaimkhong, D. Evseenko, J. Reed, A.Z. Stieg, J.K. Gimzewski, A. Nakano, Rigid microenvironments promote cardiac differentiation of mouse and human embryonic stem cells, Science and technology of advanced materials 14(2) (2013).

[41] J.-H. Seo, K. Sakai, N. Yui, Adsorption state of fibronectin on poly(dimethylsiloxane) surfaces with varied stiffness can dominate adhesion density of fibroblasts, Acta Biomaterialia (0) (2012).

[42] X.Q. Brown, K. Ookawa, J.Y. Wong, Evaluation of polydimethylsiloxane scaffolds with physiologically-relevant elastic moduli: interplay of substrate mechanics and surface chemistry effects on vascular smooth muscle cell response, Biomaterials 26(16) (2005) 3123-9.

[43] Y.M. Takeuchi, S.; Kikuchi, T.; Nishida, E.; Fujita, T.; Matsumoto, T.;, Differentiation and Transforming Growth Factor- b Receptor Down-regulation by Collagen- a 2 b 1 Integrin Interaction Is Mediated by Focal Adhesion Kinase and Its Downstream signals in Murine Osteoblastic cells, The Journal of biological chemistry 272(November 14) (1997) 29309-29316.

[44] D.T. Eddington, J.P. Puccinelli, D.J. Beebe, Thermal aging and reduced hydrophobic recovery of polydimethylsiloxane, Sensors and Actuators B: Chemical 114(1) (2006) 170-172.

[45] L. MacQueen, Y. Sun, C.A. Simmons, Mesenchymal stem cell mechanobiology and emerging experimental platforms, Journal of the Royal Society, Interface / the Royal Society 10(84) (2013) 20130179.

[46] K.S. Tsai, S.Y. Kao, C.Y. Wang, Y.J. Wang, J.P. Wang, S.C. Hung, Type I collagen promotes proliferation and osteogenesis of human mesenchymal stem cells via activation of ERK and Akt pathways, Journal of biomedical materials research. Part A 94(3) (2010) 673-82.

[47] C. Ge, G. Xiao, D. Jiang, R.T. Franceschi, Critical role of the extracellular signal-regulated kinase-MAPK pathway in osteoblast differentiation and skeletal development, J Cell Biol 176(5) (2007) 709-18.

[48] C.D. Hoemann, H. El-Gabalawy, M.D. McKee, In vitro osteogenesis assays: influence of the primary cell source on alkaline phosphatase activity and mineralization, Pathologie-biologie 57(4) (2009) 318-23.

[49] M.C. Subauste, O. Pertz, E.D. Adamson, C.E. Turner, S. Junger, K.M. Hahn, Vinculin modulation of paxillin-FAK interactions regulates ERK to control survival and motility, J Cell Biol 165(3) (2004) 371-81.

[50] W.G. Vogel, G.D.; Alves, F.; Pawson, T., The discoidin domain receptor tyrosine kinases are activated by collagen, Molecular Cell 1 (1997) 13-23.

[51] B. Narayanan, G.H. Gilmer, J. Tao, J.J. De Yoreo, C.V. Ciobanu, Self-assembly of collagen on flat surfaces: the interplay of collagen-collagen and collagen-substrate interactions, Langmuir : the ACS journal of surfaces and colloids 30(5) (2014) 1343-50.

[52] R. Dominguez, K.C. Holmes, Actin structure and function, Annual review of biophysics 40 (2011) 169-86.

[53] D. Harjanto, M.H. Zaman, Matrix mechanics and receptor-ligand interactions in cell adhesion, Organic & biomolecular chemistry 8(2) (2010) 299-304.

[54] E.K. Yim, S.W. Pang, K.W. Leong, Synthetic nanostructures inducing differentiation of human mesenchymal stem cells into neuronal lineage, Exp Cell Res 313(9) (2007) 1820-9.

[55] K. Kulangara, Y. Yang, J. Yang, K.W. Leong, Nanotopography as modulator of human mesenchymal stem cell function, Biomaterials 33(20) (2012) 4998-5003.

[56] J.E. Frith, R.J. Mills, J.J. Cooper-White, Lateral spacing of adhesion peptides influences human mesenchymal stem cell behaviour, J Cell Sci 125(Pt 2) (2012) 317-27.

[57] R.M. Salasznyk, R.F. Klees, W.A. Williams, A. Boskey, G.E. Plopper, Focal adhesion kinase signaling pathways regulate the osteogenic differentiation of human mesenchymal stem cells, Exp Cell Res 313(1) (2007) 22-37.

[58] A.L. Rosa, R.B. Kato, L.M. Castro Raucci, L.N. Teixeira, F.S. de Oliveira, L.S. Bellesini, P.T. de Oliveira, M.Q. Hassan, M.M. Beloti, Nanotopography drives stem cell fate toward osteoblast differentiation through alpha1beta1 integrin signaling pathway, J Cell Biochem 115(3) (2014) 540-8.

[59] P.A. Ruiz, G. Jarai, Collagen I induces discoidin domain receptor (DDR) 1 expression through DDR2 and a JAK2-ERK1/2-mediated mechanism in primary human lung fibroblasts, The Journal of biological chemistry 286(15) (2011) 12912-23.

[60] C.Z. Wang, H.W. Su, Y.C. Hsu, M.R. Shen, M.J. Tang, A discoidin domain receptor 1/SHP-2 signaling complex inhibits alpha2beta1-integrin-mediated signal transducers and activators of transcription 1/3 activation and cell migration, Molecular biology of the cell 17(6) (2006) 2839-52.

[61] H. Xu, D. Bihan, F. Chang, P.H. Huang, R.W. Farndale, B. Leitinger, Discoidin domain receptors promote alpha1beta1- and alpha2beta1-integrin mediated cell adhesion to collagen by enhancing integrin activation, PloS one 7(12) (2012) e52209.

Chapter 5

5 Biomaterials surface energy driven ligand assembly strongly regulates stem cell mechanosensitivity and fate on very soft substrates

[1,2]Tojo Razafiarison, [1,2]Claude N Holenstein, [1,2]Unai Silvan, [1,2]Milan Jovic, [1,2]Edward Vertudes, [3]Marko Loparic, [4]Maciej Kaweck, [4]Laetitia Bernard and [1,2]Jess G Snedeker

[1]Department of Orthopedics, Balgrist University Hospital, University of Zurich, Lengghalde 5, 8008 Zürich, Switzerland
[2]Laboratory for Orthopedic Biomechanics, ETH Zurich, 8008 Zürich, Switzerland
[3]Biozentrum and The Swiss Nanoscience Insitute, University of Basel, 4056 Basel, Switzerland
[4]Swiss Federal Laboratories for Materials Science and Technology (EMPA), 8600 Dübendorf, Switzerland

this work was submitted to PNAS (2017)**.**

5.1 Abstract

Although mechanisms of cell-material interaction and cellular mechanotransduction are increasingly understood, the mechanical insensitivity of mesenchymal cells to certain soft amorphous biomaterial substrates has remained largely unexplained. We reveal that surface-energy driven supramolecular ligand assembly can regulate mesenchymal stem cells (MSCs) sensing of substrate mechanical compliance and consequent cell fate. Human MSCs were cultured on collagen coated hydrophobic polydimethylsiloxane (PDMS) and hydrophilic polyethylene-oxide-PDMS (PEO-PDMS) of different stiffness. Although cell contractility was similarly diminished on soft substrates of both types, cell spreading and osteogenic differentiation occurred only on soft PDMS and not hydrophilic PEO-PDMS (elastic modulus <1kPa). Substrate surface energy yields distinct ligand topologies with accordingly distinct profiles of recruited of transmembrane cell receptors and related focal adhesion signaling. These differences did not differentially regulate Rho Associated Kinase activity, but nonetheless regulated both cell spreading and downstream differentiation.

5.2 Introduction

Studies of adherent stem cell behavior on soft biomaterials have typically employed two-dimensional platforms of synthetic polymers coated with monomeric protein ligands [1]. Such studies [2-4] have demonstrated that modulating the stiffness of porous gels can direct stem cell fate. However, experimental outcomes from studies using amorphous biomaterial substrates vary widely. Beyond the inherent biological variability in all eukaryotic cell culture systems, existing models of cell-biomaterial interaction fail to coherently explain divergence of experimental results. For instance, it is until now not understood why mesenchymal stem cells readily attach and spread on elastomeric silicone [3-5], while they tend to not spread on soft substrates such as polyacrylamide that have been coated with similar extracellular matrix ligands [3, 4, 6].

Although cell responses on synthetic hydrogels and elastomers are regularly compared, these materials present very distinct chemical and physical features [7]. Among these features, one characteristic that has been widely ignored is the inherent difference in surface energy of these material classes. In the field of biomedical implant design, surface energy has long been recognized to control protein adhesion and downstream cellular reaction [8, 9]. The property of biomaterial surface energy can be viewed as the physical work done by intermolecular forces acting to increase phase surface area. As such, surface energy depends on the charge and polarity of the outermost functional groups of the biomaterial. Surface energy can be increased by the presence of polar functional groups, with higher energy substrates having more polar groups yielding more a hydrophilic surface [10, 11]. Monomeric Type-I collagen is a widely-used model extracellular matrix ligand comprising both polar and apolar amino acid residues (Fig. 5.1). We have shown previously that biomaterial surface energy plays a dominant role in determining which groups are exposed after deposition, which influences further the supramolecular organization of adsorbed collagen layers [12]. In this earlier foundational work, we demonstrated that surface energy on stiff (2.15-2.40MPa), atomically flat substrates steers cell-material interactions and promotes osteogenic MSC differentiation by regulating the topography of the adsorbed ECM protein layer presented to the cells. To achieve these insights, we designed a PDMS-based platform in which stiffness and surface energy can be independently tailored in a straightforward manner by addition of surfactant in small quantities. The chief technical challenge was to rigorously control for, and prevent, potential confounding effects of any divergent chemical, physical and mechanical properties at the cell-material interface.

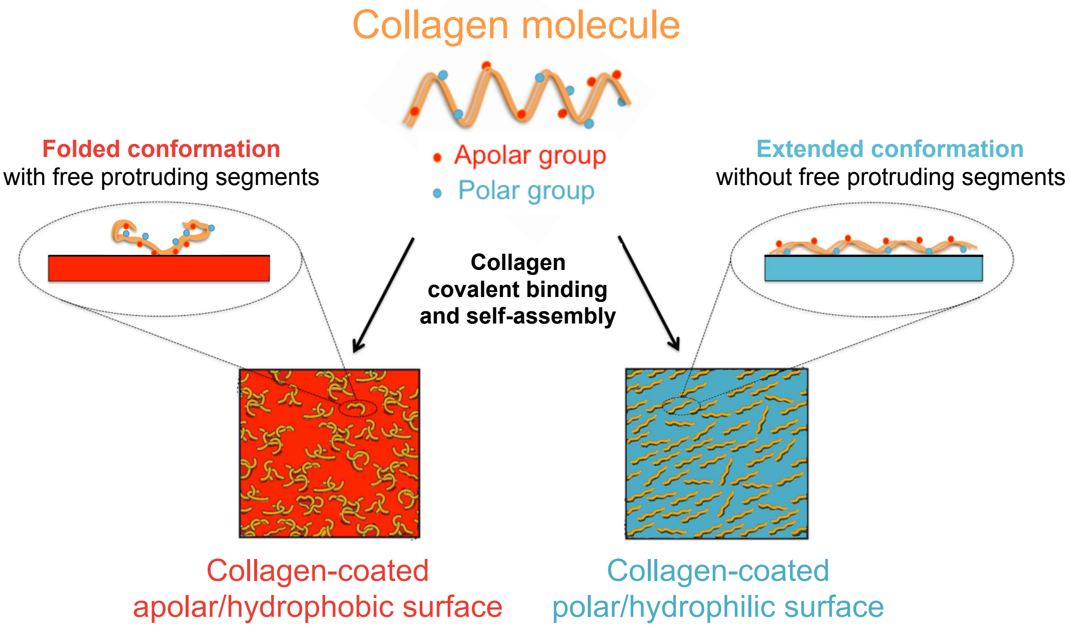
Collagen molecule
Folded conformation
with free protruding segments
Apolar group
Polar group
Extended conformation
without free protruding segments
Collagen
covalent binding
and self-assembly
Collagen-coated
apolar/hydrophobic surface
Collagen-coated
polar/hydrophilic surface

Figure 5.1 | Schematic of surface energy-driven assembly of collagen I. Collagen-I molecules containing polar and apolar amino acid residues covalently bind and self-assemble to exhibit different conformations, topologies and functionalities when coated on substrates of different surface energy.

In the current work, we adapted this tunable biomaterial system to achieve very soft substrates (elastic modulus <1kPa) to isolate and investigate the role of surface energy on human bone marrow stromal cell (hBMSC) mechanosensitivity to substrate stiffness. We again specifically focused on collagen I as a model ligand that can support osteogenic, tenogenic, or adipogenic differentiation in a substrate stiffness dependent manner [6]. Using this model we found that surface energy indeed regulates cell adhesion and differentiation on soft and hard substrates, with hydrophobic surfaces resulting in a suppression of cell mechanosensitivity to bulk material stiffness. We reveal how surface energy directs ligand topography in a manner that may alternately promote or inhibit cell mechanosensitivity and response to a soft amorphous substrate. These findings fill a critical gap in understanding that can resolve conflicting mechanistic theories on how mesenchymal stem cells sense and react to the stiffness of a soft biomaterial substrate [3, 4, 13-15]. More broadly, the present study demonstrates that biomaterial surface energy is a crucial consideration in soft biomaterial design, and one that cannot be neglected in cross-comparison of studies of stem cell-biomaterial interaction and cell fate.

5.3 Materials and Methods

5.3.1. Tunable surface energy PDMS substrate preparation

As previously described [12], 12 to 25 mm diameter glass coverslips (Thermo Scientific Menzel, 11708701) were cleaned with milli-Q H2O and ethanol. The surfactant polydimethylsiloxane-bethylene oxide (molecular weight = 600, Chemie Brunschwig, 09780) was mixed first in different amounts from 0% to 1.0% (v/w_{total}) with the base of PDMS kit (Sylgard 184, Biesterfeld, Germany) for 5 min. The catalyst of PDMS kit was then added at different mixing ratios from 10:1 to 80:1 and the slurry was mixed again thoroughly for 10 min. The homogeneously mixed slurry was degased for 30 min and spin coated on the glass coverslips with a 200 μm thickness. The substrates were cured for ≈14 h at 80°C.

For cell substrate fabrication, collagen I monomers (Sigma, C3867) were covalently bound to the surface of the elastomers using the heterobifunctional linker N-sulfosuccinimidyl-6-(4’-azido-2’-nitrophenylamino) hexanoate (sulfo-SANPAH, ProteoChem, C1111). Collagen and sulfo-SANPAH were aliquoted in single-use vials and stored respectively at 4°C and -20°C. The substrates were placed in a 24-well plate and washed with milli-Q H2O. 500 µL of a 0.2 mg/mL solution of sulfo-SANPAH in 50mM HEPES (Life Technologies, 7001629) were added to each well. The substrates were then placed in a Stratalinker 2400 ultraviolet light crosslinker (Stratagene) for 10 minutes. The sulfo-SANPAH was removed and the substrates were overlaid with fresh sulfo-SANPAH and exposed again to ultraviolet light for 10 minutes. At this point the substrates were sterilized and washed three times with PBS.

The substrates were coated with 10 or 50 µg/mL of collagen I or synthetic peptide diluted in PBS. Substrates were incubated at 37°C respectively for 3h with collagen I and for 24 h with the synthetic peptide.

In accordance with a previously described protocol [16], collagen synthetic peptide with the sequence GPC(GPP)5-GFOGER-(GPP)5GPC purchased from AAPPTec was prepared to form triple helices and remove unfolded peptides. Briefly, 1 mg GFOGER peptide was dissolved in 10mM acetic acid 2 mM TCEP then heated for 2 min to 70° C and left for 24 h at 4°C to form triple helices. The triple helical peptides (11.1 kDa) were dialyzed against 10 mM acetic acid with a 3.5–5 kDa cutoff dialysis column to remove unfolded peptides and the TCEP.

5.3.2. Ligand loading and adsorbed protein quantification

A micro-BCA protein assay kit (Thermo Scientific, 10249133) was used to determine the protein that was adsorbed on the different substrate surfaces according to the stated protocol in the kit, where the absorbance was measured at 562nm with a microplate reader. A standard curve with the collagen used for coating was plotted to determine the effective amount of collagen bound to the surface.

5.3.3. Atomic force microscopy imaging of ligand topography/roughness

After collagen coating, the samples were washed three times with PBS and stored in PBS at 4°C until imaging. The samples were imaged in PBS using a JPK NanoWizard 4 AFM (JPK, Berlin, Germany) in the HyperDrive mode using HyperDrive fluid imaging package and with SCANASYST-FLUID (Bruker) cantilever having 0.35 N m^{-1} nominal force constant. Scan rate was set in the range 1-4 Hz (faster scan rate was used for more adhesive samples). Images having a scan size of 5µm x 5µm and of 2µm x 2µm were taken on at least three different locations on the substrates of different stiffness. Images were processed with the JPK Data Processing software (6.0.63).

5.3.4. Cell culture

Human bone marrow stromal cells were purchased from the institute for Regenerative Medicine at Texas A&M University. The cells were fully characterized by the institute as multipotent mesenchymal stromal cells. After expanding and aliquotting for the present study, the cells were tested for their capacity to differentiate toward adipogenesis and osteogenesis. For all the experiments, the hBMSCs were at an early P2 passage and cultured in Lonza's TheraPEAK^{TM} MSCGM-CD^{TM} chemically defined mesenchymal stem cell medium (Lonza, 190632). Medium was exchanged every three days and maintained at 37°C with 5% CO_2.

5.3.5. Cell attachment and morphology

Cell attachment was analyzed by culturing 25,000 cells/cm^2 on functionalized substrates with 10 or 50 μg/ml of collagen I for 1 h at 37°C. Substrates were washed with PBS to remove unbound cells, fixed with formalin solution 10% (sigma, HT5011) for 10 min, washed with PBS three times, and overlaid with 4',6-diamidino-2-phenylindole (DAPI) diluted in PBS, which counterstains DNA and labels the nucleus. On each replicate, a large central region covering more than 50% of the substrate area was imaged with a 4x objective on an iMic spinning disk confocal (FEI Photonics) microscope. Nuclei were counted using image-J software by contrast thresholding the DAPI image to obtain a binary image, and then automatically counted by analyzing the particles.

Cell morphology was examined with immunofluorescence imaging. Substrates were prepared as described above, and cells were seeded at 5,000 cells/cm^2 for 24h at 37°C. Cells were washed with PBS, fixed with formalin 10% for 10min, washed again with PBS three times, permeabilized with Triton-X 100 (sigma) and blocked for 1 hour with 0.5% BSA. After washing substrates, the primary monoclonal antibody anti-vinculin (sigma, V9131) diluted 1:400 in the washing solution (0.05% Triton; 0.1% BSA) was overlaid for 1 hour. After washing substrates three times with the washing solution, the secondary antibody Rhodamine Red (Thermo Scientific, R-6393) diluted to 1:200, Alexa Fluor 488 phalloidin (Life Technologies, A12379) diluted to 1:500 and DAPI in washing solution were overlaid on substrates for 45 min at room temperature in a dark environment. The stain was aspirated and substrates were washed three times with PBS. Images were taken on an iMic spinning disk confocal (FEI Photonics) microscope with a 40x objective (N.A. 0.95). Cell spreading was quantified with 8-10 images of non-overlapping regions on each replicate having a total cell number of at least 600 per sample with a 10x objective. Spreading area was calculated using image-J software by contrast thresholding the FITC-phalloidin channel to obtain a binary image, and then automatically measured the area. The calculated area was normalized to the number of cells present on the image (as described above).

5.3.6. Cell differentiation quantification

Bone marrow stromal cells were seeded at 5,000 cells /cm^2 and cultured for 1.5 h before changing the medium to either fresh basal growth medium or mixed induction medium, which consisted of 0.5μM dexamethasone (sigma), 10 mM β-glycerolphosphate (sigma), 50μM L-ascorbic acid 2-phosphate (sigma), 0.5μM isobutylmethylxanthine (sigma), 50μM indomethacin (sigma), and 10 μg/ml insulin (sigma). Respective medium was exchanged every three days and maintained at 37°C with 5% CO_2.

After 7 days in culture, alkaline phosphatase (ALP) was employed as the indicators of osteoblasts. Cells were first washed with PBS, then trypsinized (without EDTA) and stored at -80°C until analysis. A fluorometric assay kit (Abcam, 83371) was used to determine the alkaline phosphatase activity according to the stated protocol in the kit, where the fluorescence intensity was measured at Ex/Em 360/440 nm using a fluorescence microplate reader. A fluorometric DNA quantitation kit (Sigma, DNAQF) was used to quantify the cell proliferation and normalize the ALP activity according to the stated protocol in the kit, where the fluorescence intensity was measured at Ex/Em 360/460 nm using a fluorescence microplate reader.

Bone marrow stromal cells were seeded at 5,000 cells/cm^2 and maintained in culture for 7,14 or 21 days in basal growth medium or co-induction medium as described above. At the time point, substrates were gently washed with PBS, and cells were fixed with formalin solution 10% for 30 min. The fixative was removed and substrates were washed three times with milli-Q H_2O. Alizarin red 2% staining solution was prepared by mixing alizarin red powder

(Sigma) with milli-Q H_2O. The pH was adjusted to 4.2 with 10% NH_4OH (Sigma), then the solution was filtered with a 0.2μm filter. The staining solution was overlaid on substrates for 15 minutes then, the substrates were washed three times with milli-Q H_2O. Images were acquired with an EVOS digital inverted microscope with a 4x objective. To visualize lipid formation in adipocytes, cells were fixed with 10% formalin for 30 min, rinsed with PBS. Oil red O 0.5% stock staining solution was prepared by mixing Oil Red O (Sigma) with Isopropyl Alcohol. Three parts of the Oil Red O 0.5% stock staining solution was mixed with two parts of PBS, then the solution was filtered with a 0.2 μm filter. The staining solution was overlaid on substrates for 20 min then, the substrates were washed three times with PBS.

After 14 d in culture in basal growth medium, the bone marrow stromal cells were stained for their calcium deposition as described above. The cells were also stained for alkaline phosphatase using Merck Millipore kit (SCR004) according to the manufacturer's instructions.

5.3.7. Microscopy and image analysis

Phase contrast images were acquired with an EVOS digital inverted microscope with 4x , 10x and 20x objectives. Fluorescent images were acquired with an iMic spinning disk confocal (FEI Photonics) microscope with 10x and 40x objectives. Cell attachment and spreading were processed with ImageJ as previously described [12].

5.3.8. Real time and quantitative PCR

Expression of integrin subunit, discoidin domain receptor and focal adhesion- related genes were evaluated at 24 h of cell culture by performing reverse transcriptase polymerase chain reaction (RT-PCR). Substrates were prepared and maintained in culture as described above. At the time point, substrates were washed first with PBS and the total RNA was extracted using the RNeasy micro kit (Qiagen, 74004) following manufacturer's protocol. The cDNA was obtained by using a cDNA Reverse Transcription kit (Applied Biosystems, 4368814). PCR was performed on resultant cDNA using TaqMan® Universal PCR Master Mix (Life Technologies, 4364338) with TaqMan® gene expression assays (Life Technologies; for primer references, see Table 1). Data were analyzed using the $2^{-\Delta\Delta Ct}$ method, and glyceraldehyde-3-phosphate dehydrogenase (GAPDH) was chosen as the housekeeping gene.

5.3.9. Phosphorylated ROCK quantification

Bone marrow stromal cells were seeded at 5000 cells per cm^2 and cultured for 24 h. Level of ROCK phosphorylation as a regulator of the ROCK pathway was determined with a ROCK activity assay kit (Merck Millipore, CSA001) according to the stated protocol in the kit, where the absorbance intensity was measured at 450 nm using a microplate reader.

5.3.10. Traction force microscopy

Substrates with a first layer of PDMS having a ratio 60:1 or 70:1 were prepared on 25mm diameter coverslips as described above. Adapted from a previous protocol [17], the substrates were then washed with ethanol and overlaid with 10% APTES diluted in ethanol for 45 min at 45°C. The APTES solution was removed and substrates were washed five times with ethanol, and then five times with milli-Q H_2O. 3% gluteraldehyde diluted in milli-Q H_2O was overlaid on the substrates for 1 h at room temperature. The fixative solution was removed and substrates were washed three times with milli-Q H_2O. 200nm diameter carboxylate modified polystyrene red fluorescent beads (Invitrogen) were used as surface nanoreporters and diluted 200:1 in milli-Q H_2O. The bead solution overlaid the substrates for 1 h at room temperature in the dark. The bead solution was removed and substrates were washed three times with milli-Q H_2O. The next day, substrates were blow dried and put in the oven for 30 min at 80°C. PDMS slurry was prepared as described above and spin coated on the substrates for 5 min at 10 000 rpm to obtain an upper thin layer below 2 µm. The substrates were cured in the oven overnight at 80°C and functionalized the next day as described above. Substrates were seeded at 625 cells per cm^2 and cultured for 16 h. The bone marrow stromal cells were stained with Syto 13 green fluorescent nucleic acid stain (Lubio Science) for 3-5 minutes and single cells were imaged on a spinning disk confocal microscope with a 40x objective. Cells were lysed with 10% SDS for 15 min and the previously recorded locations for every single cell were again imaged. Cell-generated traction stresses and the induced substrates deformation were measured using an previously developed high-resolution TFM approach in our group based on optical flow tracking and Fourier Transform Traction Cytometry [18] with an extension to account for the finite depth of the bead layer [19]. Further information can be found in the supplementary notes.

5.3.11. Time-of-Flight Secondary Ion Mass Spectrometry

Measurements were conducted on a ToF-SIMS.5 instrument (IONTOF, Germany). For these measurements the tuneable surface energy PDMS substrates were spin-coated on clean, polished, and plasma-treated silicon wafers of 1.3 x 1.3 mm. 25 keV Bi_3^+ primary ions were used in spectral mode for surface molecular analysis at a primary ion current of 0.65 pA. Low energy electron flooding was used for surface charge compensation. Negative secondary ions were extracted on analysis areas of 100 x 100 µm. 50 scans were acquired per spectrum to remain below the static limit. 5 randomly selected positions were investigated for each sample to ensure data reproducibility.

5.3.12. Stastistical analysis

All experiments were performed in triplicate with at least four independent experiments ($n \geq 4$) unless indicated. Data were represented as means and standard error (bars in the figure). The unpaired two-tailed student's t -test with a confidence level of 95% was used to see if two sets of data differ significantly. For multiple comparisons, one-way ANOVA with Bonferroni post hoc test was applied. Significance was indicated for $p \leq 0.05$ (* $p \leq 0.05$, ** $p \leq 0.01$, *** $p \leq 0.001$, **** $p \leq 0.0001$). All the charts and analysis were processed with Prism 6 software.

5.4 Results

5.4.1. Surface energy driven collagen assembly is consistent across different PDMS stiffness

To isolate biological effects of surface driven ligand assembly on amorphous silicone substrates, we employed our previously described PDMS-based platform for which multiple material parameters such as stiffness and surface energy can be varied independently without altering confounding surface properties. As previously explained [12], polar (hydrophilic) PDMS surfaces were obtained by adding a small amount of PDMS-b-PEO surfactant containing a neutral and polar polyether directly to the standard PDMS slurry. In the present work, we extended this platform to investigate very soft substrates (elastic modulus <1kPa) by adjusting the silicone composition.

Consistent with our previously reported observations [12], AFM analysis of the collagen coated surfaces of PDMS and PEO-PDMS of different stiffness indicated a clear difference in ligand layer topography between polar and apolar elastomer surfaces. On PDMS, all the collagen coated surfaces appeared rough with an average roughness (R_a) between 3.12 to 4.10 nm with more prominent aggregates on stiffer substrates (Fig. 5.2). On the other hand, PEO-PDMS surfaces presented a smoother ligand layer with an average roughness between 0.63 to 1.01 nm (Fig. 5.2).

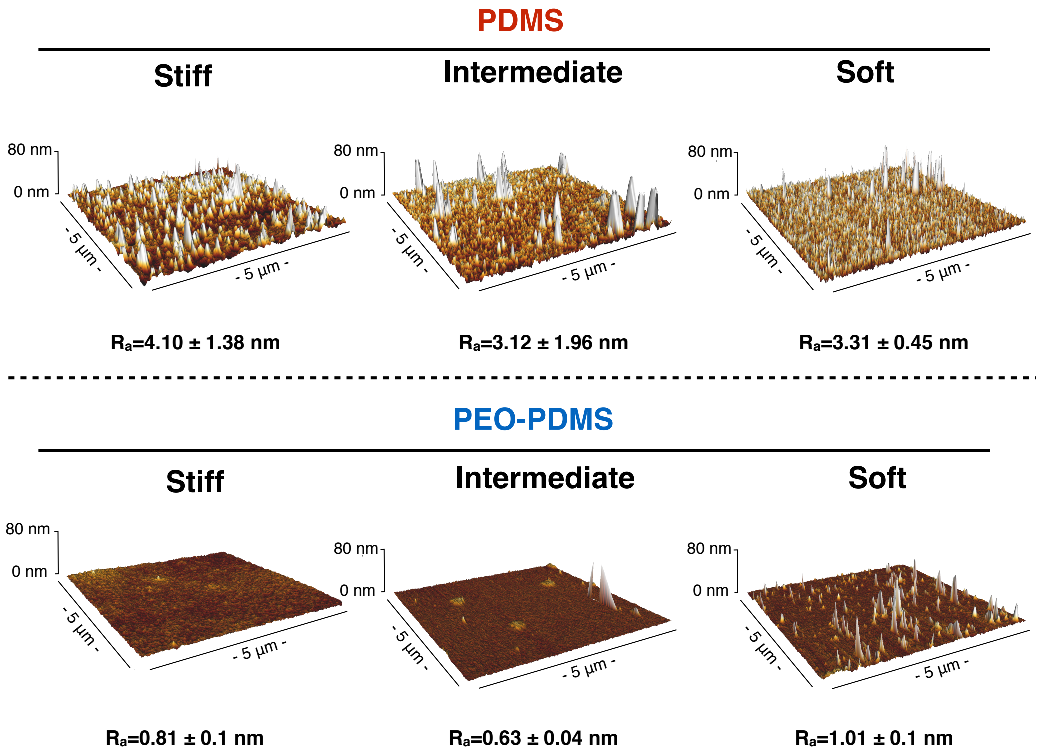
PDMS
Stiff
Intermediate
Soft
80 nm
0 nm
- 5 µm -
- 5 µm -
Ra=4.10 ± 1.38 nm
Ra=3.12 ± 1.96 nm
Ra=3.31 ± 0.45 nm
PEO-PDMS
Stiff
Intermediate
Soft
80 nm
0 nm
- 5 µm -
- 5 µm -
Ra=0.81 ± 0.1 nm
Ra=0.63 ± 0.04 nm
Ra=1.01 ± 0.1 nm

Figure 5.2 | The difference in collagen assembly on PDMS on PEO-PDMS appears to be consistent across different substrate stiffness. Representative images by atomic force microscopy of the collagen layer atop of PDMS and PEO-PDMS substrates of different stiffness (soft: 0.07-0.10 kPa; intermediate: 5-6 kPa; stiff: 2.15-2.40 MPa) with the calculated average roughness (R_a) from 3 different areas. Data are represented as mean±s.d.

Thus, as previously described for hard silicone surfaces [12], collagen conformation and supramolecular organization atop the material surfaces depends on competitive interplay of collagen-substrate and collagen-collagen interactions (Fig. 5.2). On hydrophobic PDMS, molecules are covalently bound to the surface but do not lie flat. Instead, immobilized monomers adopt a folded conformation that may interact with further collagen molecules that are still in suspension. These intermolecular collagen interactions typically result in the formation of multilayer molecular aggregates. Such aggregation suggests a higher affinity for collagen-collagen interaction than for collagen-surface interaction. On the contrary, collagen molecules seeded onto hydrophilic PEO-PDMS lie flat within a relatively smooth collagen layer. This tendency of collagen to lie in monolayer on the more polar PEO-PDMS indicates that collagen-surface affinity dominates the complex interactions involved in collagen deposition on this hydrophilic material [20, 21]. While the kinetics of collagen attachment to the two material classes is similar (Supplementary Fig. S3.1) there was approximately three-fold increased density of sulfo-SANPAH crosslinker on the hydrophobic PDMS substrates used in these experiments (Supplementary Fig. S5.1). Importantly, this suggests that moderately higher amounts of covalent surface cross-linker cannot overcome the effects of material surface energy that drive biologically relevant differences in conformation and further supramolecular assembly.

5.4.2. Surface energy regulates cell adhesion and dominates substrate stiffness

To test whether surface energy affects cell adhesion on elastomers of different stiffness, we cultured hBMSCs on PDMS and PEO-PDMS substrates and measured both cell attachment and spreading. At 1 h after cell seeding at high density (25 000 cells per cm^2), the percentage of cell attachment evaluated by fluorescent nuclear staining on a large central area of each substrate was found to be similar, with approximately 50% of seeded cells attaching to all tested substrates (Fig. 5.3b). As expected, cell morphology 24 h after cell seeding at low density (5 000 cells per cm^2) was not diminished on low stiffness PDMS with an apolar, hydrophobic surface (Fig. 5.3a-c). However, cell spreading was markedly diminished on soft hydrophilic elastomeric PEO-PDMS. The attachment footprint of cells on soft PEO-PDMS (80:1) was approximately three-fold smaller than that of cells on all other substrates (Fig. 5.3c). Similarly, Vertelov et al. recently reported reduced cell spreading on soft commercially available silicone gels (SoftSubstrates^{TM}) [15]. While phalloidin staining of cells seeded on stiff PDMS showed a more pronounced actin cytoskeleton with localized focal adhesions (anti-vinculin immunostaining) at the cell edge, cells on soft PDMS presented more dispersed cytoskeletal elements (Fig. 5.3a), consistent with previous reports [5]. These results suggest that surface energy affects cell spreading and can dominate cell response to substrate stiffness cues.

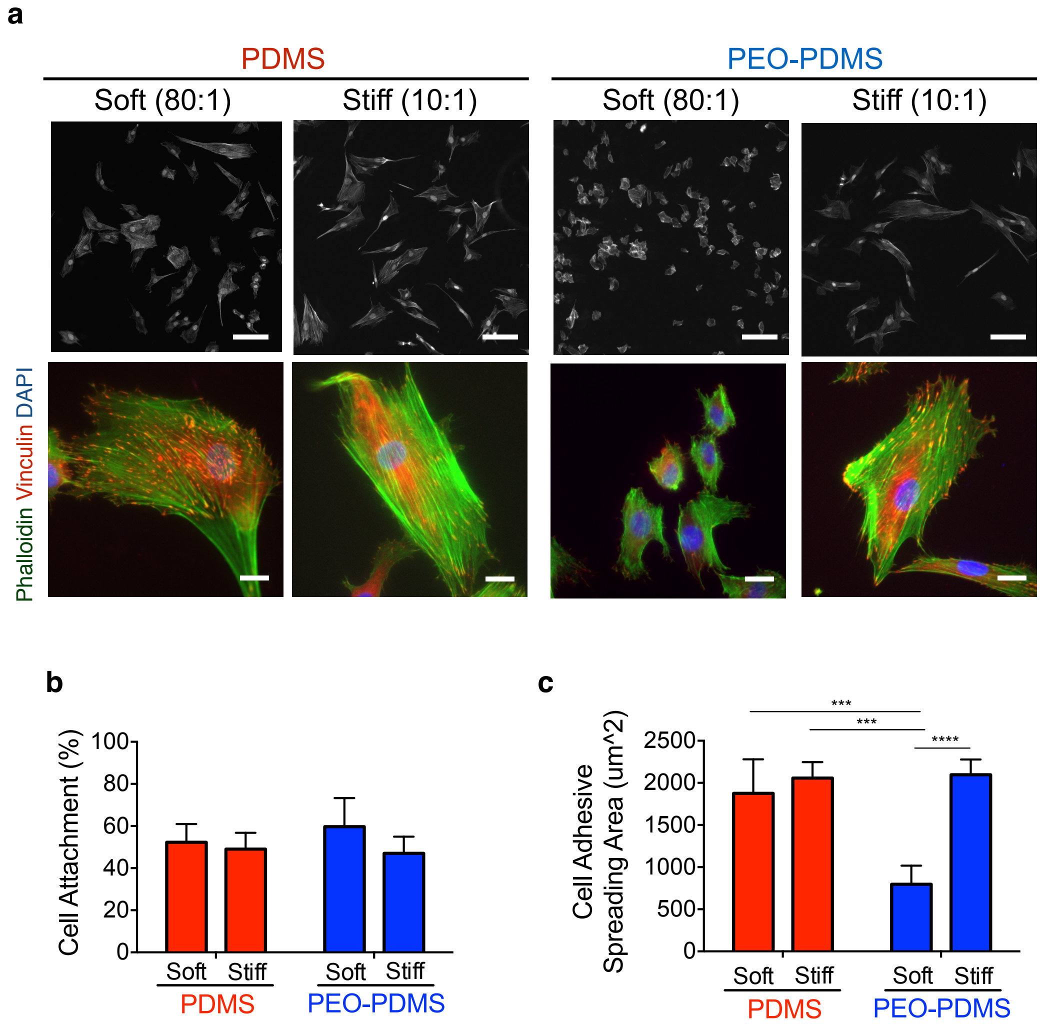

Figure 5.3| Cell spreading is affected by the surface energy on elastomer substrates of different stiffness and is not predominantly mediated by ROCK on soft apolar surface. (a) Morphology of hBMSCs on functionalized substrates seeded at 5000 cells per cm^2 after 24 h culture on PDMS and PEO-PDMS substrates of different stiffness (soft: 0.07-0.10 kPa; stiff: 2.15-2.40 MPa). Cells were immunostained with an antibody against vinculin (red), Alexa-488-phalloidin (green), and DAPI (blue). Upper row scale bar = 100 μm; lower row scale bar = 20 μm. Images of cells on stiff substrates were reported from our previous publication [12]. (b) Attachment of hBMSCs on PDMS and PEO-PDMS substrates when seeded at 25 000 cells per cm^2 after 1 h culture. (n = 3). Data on stiff substrates were reported from our previous publication [12] (c) hBMSCs spreading area on PDMS and PEO-PDMS when seeded at 5000 cells per cm2 after 24 h culture; (n = 4; number of cells ≥ 2400). Data on stiff substrates were taken from our previous publication [12]. Data are represented as mean±s.d.; Significance was indicated for $p \leq 0.05$ (*$p \leq 0.05$, **$p \leq 0.01$, ***$p \leq 0.001$, ****$p \leq 0.0001$).

5.4.3. Surface energy directs stem cell differentiation

To evaluate the role of surface energy in modulating stem cell differentiation, we first cultured hBMSCs for 7 d at low density (5000 cells per cm^2) in co-induction medium containing osteogenic and adipogenic inducers. Cells were stained with Alizarin Red for calcium deposits, a standard marker of differentiated osteoblasts. Cultures were also stained with Oil Red O for lipid droplets, an indicator of the degree of adipogenesis. In contrast to all the other substrates, soft PEO-PDMS substrates presented very low calcium deposits and a substantial amount of formed lipid droplets (Fig. 5.4a). Consistent with previous reports [3], hBMSCs cultured on both soft and stiff PDMS presented similar DNA amounts and alkaline phosphatase (ALP) activity (Fig. 5.4b-c), however the amount of DNA on soft PEO-PDMS substrates was significantly lower compared to the other substrates suggesting reduced proliferation[22] (Fig. 5.4b). Quantification of ALP activity revealed a threefold lower expression of this osteogenic marker on soft PEO-PDMS compared to the stiff material (Fig. 5.4c).

We further investigated the hBMSC differentiation in basal growth medium for 14 d at low seeding density (5000 cells per cm^2) by staining for ALP and calcium deposition. Previous studies [4, 12] have reported a tendency for differentiation toward osteogenic lineages when stem cells are cultured on PDMS substrates independently of their stiffness. Consistent with this observation, hBMSCs cultured on all tested substrates, except for soft PEO-PDMS, exhibited a positive staining for ALP and a high calcium deposit (Fig. 3d). Collectively, our data suggest that surface energy is a key factor in stem cell differentiation as driven by substrate stiffness.

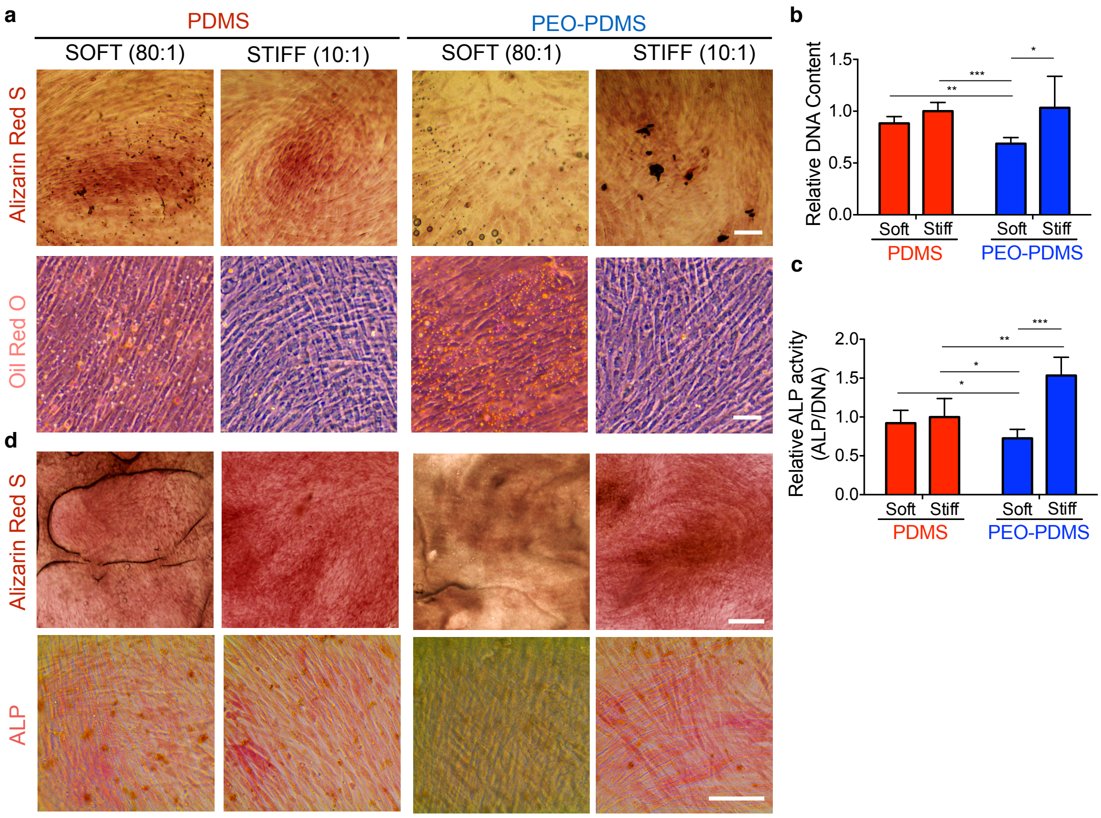

Figure 5.4 | Surface energy directs osteogenic stem cell differentiation independently of bulk substrate stiffness. hBMSCs after 7 d culture in mixed-induction medium on PDMS and PEO-PDMS substrates of different stiffness (soft: 0.07-0.10 kPa; stiff: 2.15-2.40 MPa) seeded at 5000 cells per cm^2: **(a)** staining with alizarin red for calcium deposit (scale bar = 100 μm) and with oil red o for lipid droplets (scale bar = 200 μm); **(b)** total DNA content, data on stiff substrates were adapted from our previous studies [12]. (n = 4-5); **(c)** total ALP activity per DNA normalized by the mean value of the stiff PDMS, data on stiff substrates were adapted from previous publication [12]. (n = 4-5). **(d)** Staining of hBMSCs after 14 d culture in basal growth medium on PDMS and PEO-PDMS substrates of different stiffness (soft: 0.07-0.10 kPa; stiff: 2.15-2.40 MPa) seeded at 5000 cells per cm^2 with alizarin red (scale bar = 500 μm) and for alkaline phosphatase (ALP) detection with a fast red violet solution (scale bar = 100 μm). Data are represented as mean±s.d.; Significance was indicated for $p \leq 0.05$ ($^{*}p \leq 0.05$, $^{**}p \leq 0.01$, $^{***}p \leq 0.001$, $^{****}p \leq 0.0001$).

5.4.4. Surface energy affects cell contractility

A novel traction force microscopy (TFM) approach was implemented in a manner that avoids confounding effects of bead coating chemistry and topography that accompanies standard use of this assay. Fluorescent beads were covalently attached to a substrate of appropriate stiffness before addition of a 2μm spincoat layer of bulk material (Fig. 5.5a and Supplementary Fig. S5.3). Cells were cultured for 16 h at low seeding density

(650 cells per cm^2), before measuring traction with an optimized tracking algorithm [18] (see Supplementary for further details). Mean surface traction stress exerted by the cells on PDMS of either a soft (0.2-0.3kPa) or an intermediate stiffness (5-6kPa) was significantly higher than for cells on PEO-PDMS (Fig. 5.5b-d). Substrates with an intermediate stiffness (60:1) were used in place of the stiffer substrates (10:1) in order to allow cell substrate deformations that could be sensitively resolved by light microscopy; Cells on these intermediate substrates adopted highly spread cell morphologies consistent with the stiffer substrates that they were intended to represent. Cell spreading area was equivalent on all the substrates except for cells cultured on soft PEO-PDMS (Fig. 5.5c).

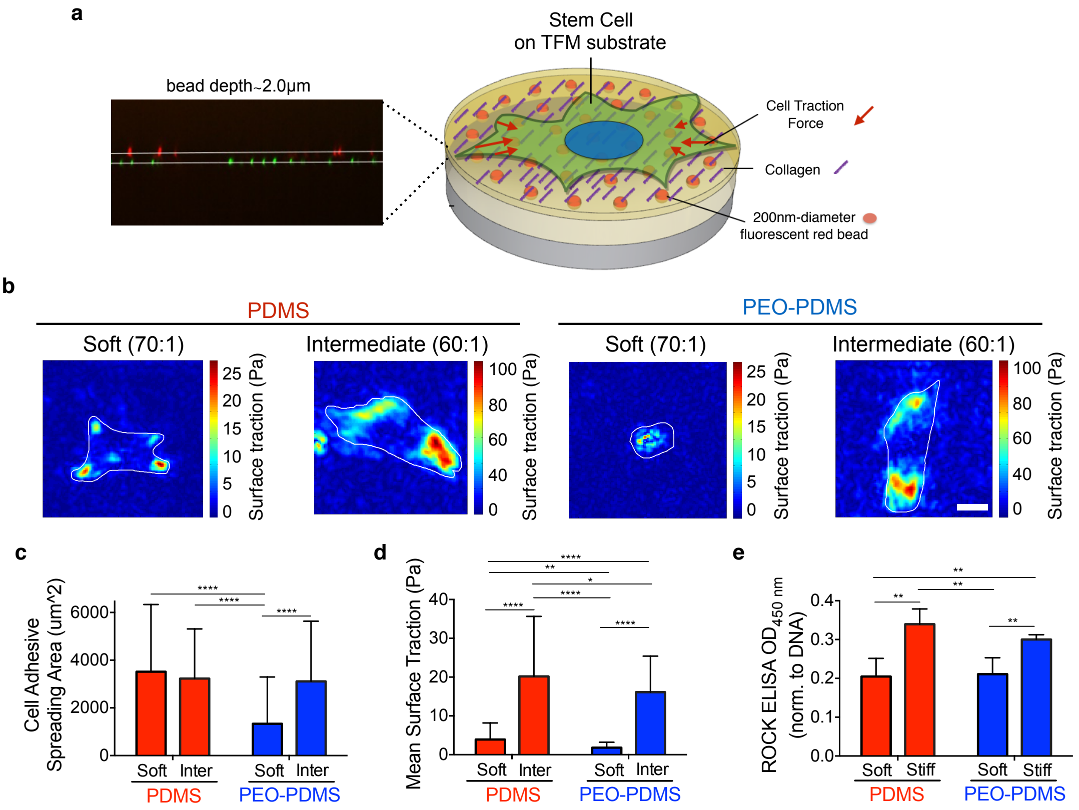

Figure 5.5 | Traction force microscopy indicates cells spread on soft PDMS without strongly contracting. (a) Schematic for PDMS-based TFM platform with embedded 200nm-diameter fluorescent trackers at a depth of 2.0 μm. (b) Snapshots of traction stress map with color values corresponding to different stress values (see corresponding axis) generated by hBMSCs on PDMS and PEO-PDMS of different stiffness (soft: 0.22-0.35 kPa; intermediate: 5-6 kPa) seeded at 625 cells per cm^2 after 16 h in culture. Scale bar = 25 μm. (c) Quantification of the corresponding cell spreading areas with the fluorescent live-cell nucleic

acid Syto-13 stain. (n = 56-90). (d) Quantification of the corresponding mean surface tractions (see supplementary for details about data processing). (n = 56-90). (e) Semi-quantification of phosphorylated Rho-associated kinase by immune-sandwiched enzyme linked-immunosorbent assay when seeded at 5000 cells per cm^2 after 24 h culture on PDMS and PEO-PDMS substrates of different stiffness (soft: 0.07-0.10 kPa; stiff: 2.15-2.40 MPa). (n = 4-5). Data are represented as mean±s.d.; Significance was indicated for $p \leq 0.05$ (*$p \leq 0.05$, **$p \leq 0.01$, ***$p \leq 0.001$, ****$p \leq 0.0001$).

Interestingly, although spreading was equivalent, mean surface traction of cells cultured on soft PDMS was five-fold lower than the cells cultured on intermediate stiffness PDMS (Fig. 5.5d).

To further assess the level of cellular contractility on the various substrates, we cultured cells for 24 h at low seeding density (2500 cells per cm^2) and determined the level of ROCK phosphorylation, a key regulator of the cytoskeleton and cellular contraction [23]. ROCK phosphorylation was found to be significantly higher on both stiff PDMS and PEO-PDMS than on soft substrates (Fig. 5.5e). We thus conclude that cell spreading appears to be at least partly decoupled from ROCK mediated cellular contractility.

5.4.5. Surface energy alters gene expression of collagen receptors and focal adhesion elements

To evaluate downstream effects of surface energy on collagen binding receptors and focal adhesion components, we analyzed gene expression by quantitative polymerase chain reaction (qPCR) after 24 h when seeded at high density (25 000 cells per cm^2). Different characteristic cell response on PDMS compared to PEO-PDMS was evident. Substantially diminished signaling related to focal adhesion maturation including diminished integrin alpha 1, integrin alpha 2, vinculin, paxillin and focal adhesion kinase expression on the softer PEO-PDMS substrates. This trend was reversed on PDMS, with signaling related to most of these elements increasing on soft PDMS substrates compared to the stiffer material (Fig. 5.6). The discoidin domain receptors including DDR1 and DDR2, which are also activated by collagen, were upregulated on both soft materials, but more significantly on pristine (apolar) PDMS (Fig. 5.6). Taken together, the results suggest that integrin and DDR pathways are differently regulated by collagen when coated on PDMS and PEO-PDMS. As previously described [12, 24], DDRs may be involved in the recognition of a differential spatial collagen organization and lead to the activation of further downstream signalling.

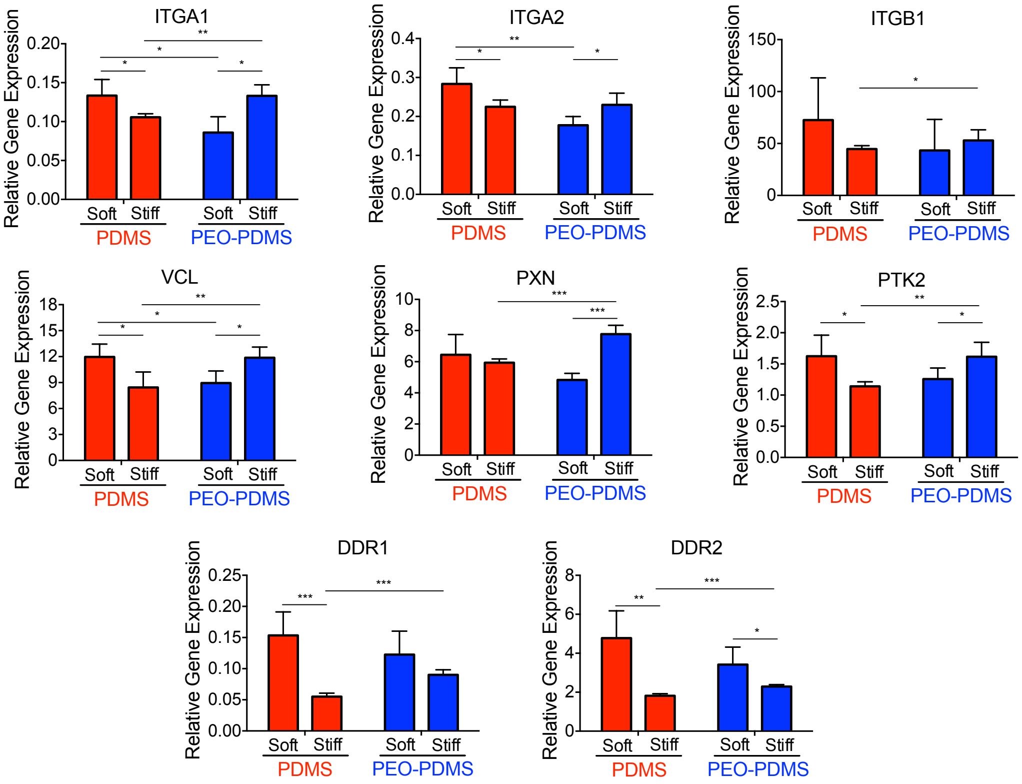

Figure 5.6 | Surface energy alters gene expression of collagen receptors and focal adhesion elements. Molecular investigations of hBMSC gene expression of collagen receptors and focal adhesion elements after 1 d culture when seeded at 25 000 cells per cm^2 on PDMS and PEO-PDMS substrates of different stiffness (soft: 0.07-0.10 kPa; stiff: 2.15-2.40 MPa): ITGA1 (integrin α1), ITGA2 (integrin α2), ITGB1 (integrin β1), VCL (vinculin), PXN (paxillin), PTK2 (protein tyrosine kinase 2 also known as focal adhesion kinase), DDR1 (discoidin domain receptor 1) and DDR2 (discoidin domain receptor 2). (n = 4-5). data on stiff substrates were adapted from our previous studies[12]. Data are represented as mean±s.d.; Significance was indicated for $p \leq 0.05$ (*$p \leq 0.05$, **$p \leq 0.01$, ***$p \leq 0.001$, ****$p \leq 0.0001$).

5.4.6. Coating with a minimal collagen synthetic peptide rescues mesenchymal stem cell sensitivity to PDMS stiffness

To test whether the observed differences in cell behavior could be attributed to surface energy driven differences in collagen self-assembly, we employed a well-described collagen-mimetic peptide containing the minimal GFOGER cell-binding sequence that binds the $\alpha_2\beta_1$ integrin receptor [25]. This model ligand does not self-assemble into larger structures, a process that in the native collagen molecule depends on specific amino acid sequences that are absent from the synthetic peptide [26]. Additionally, the GFOGER peptide has a comparatively small molecular weight of 11.1kDa compared to the full length collagen molecule with a mass of 300kDa [27]. As in all experiments, we first ensured that PDMS and PEO-PDMS presented similar amounts of ligand to the cells by adjusting the molarity of the peptide solutions adsorbed to the surface (Supplementary Fig. S5.3).

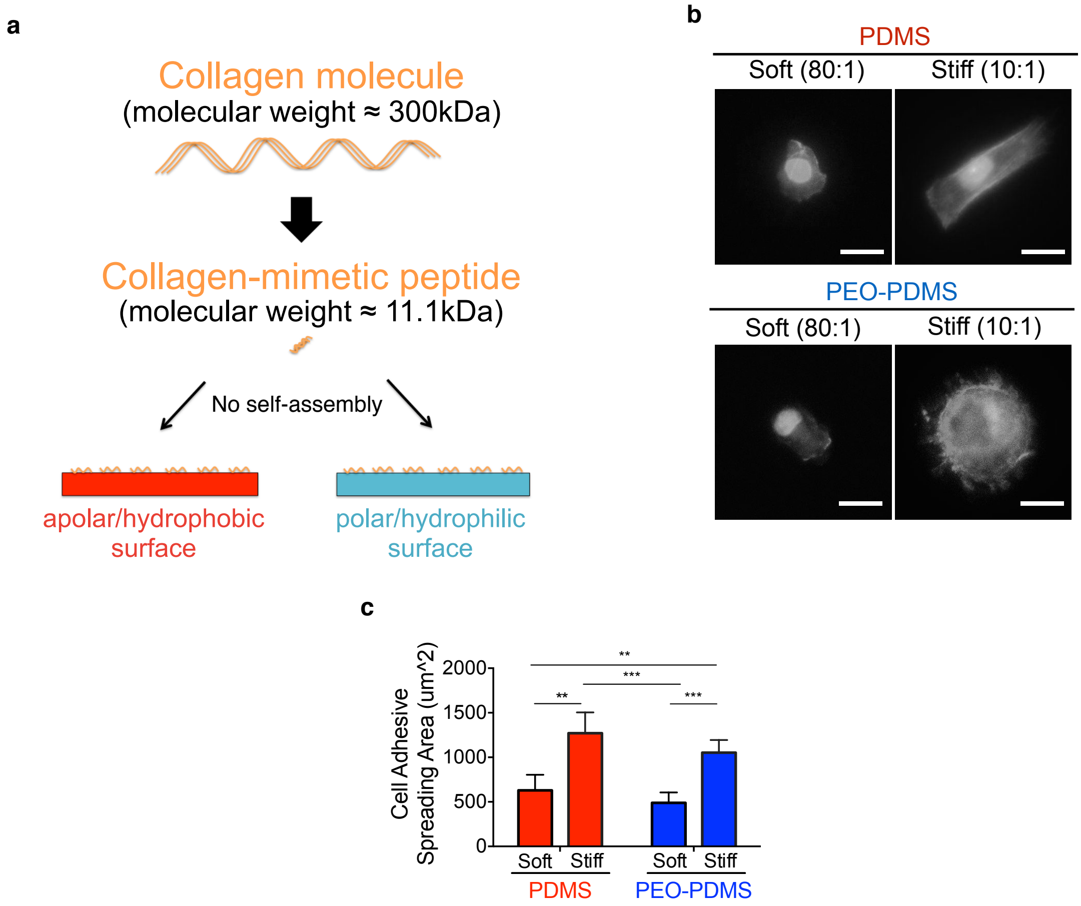

Figure 5.7 | Inactivation of collagen self-assembly promotes cell spreading according to PDMS stiffness (a) schematic for inactivation of collagen self-assembly by employing a collagen-mimetic (GFOGER) peptide. (b) Morphology of hBMSCs on PDMS and PEO-PDMS substrates of different stiffness (soft: 0.07-0.10 kPa; stiff: 2.15-2.40 MPa) when seeded at 2500 cells per cm^2 after 24 h stained with Alexa-488-phalloidin and DAPI. Scale bar = 50 µm. (c) Quantification of the cell spreading area on the corresponding substrates. (n = 4-5; number of cells ≥ 500). Data are represented as mean±s.d.; Significance was indicated for p ≤ 0.05 (*p ≤ 0.05, **p ≤ 0.01, ***p ≤ 0.001, ****p ≤ 0.0001).

In contrast to experiments using the native collagen molecule, mesenchymal stem cells plated on soft PDMS did not fully spread, adopting a small rounded shape on both soft PDMS and soft PEO-PDMS (Fig. 5.7b). In contrast, cells on both stiff PDMS and PEO-PDMS could spread (Fig. 5.7b). Cell spreading on stiff substrates was more than twofold higher than on the soft materials (Fig. 5.7). These results clearly suggest that larger aggregate structures driven by surface energy [12] override any mechanically driven mesenchymal stem cell response to soft PDMS substrates.

5.5 Discussion

Understanding cell-material interaction is essential for biomaterial design. While the mechanics and biochemistry of cellular attachment points are important, the activity state of a given ligand may be adsorption-dependent and can be affected by various physical factors [28, 29]. We have shown previously [12] that surface energy-driven ligand assembly and the resulting surface nanotopography on rigid elastomeric bulk material can strongly affect osteogenic stem cell signaling. We extended these studies to soft substrates aiming to potentially resolve the large body of conflicting evidence regarding stem cell sensitivity, or rather insensitivity, to soft PDMS [3, 4, 15]. We hypothesized a potentially critical role of surface-driven ligand topography in regulating mesenchymal cells detection of and response to mechanical cues at the cell-material interface.

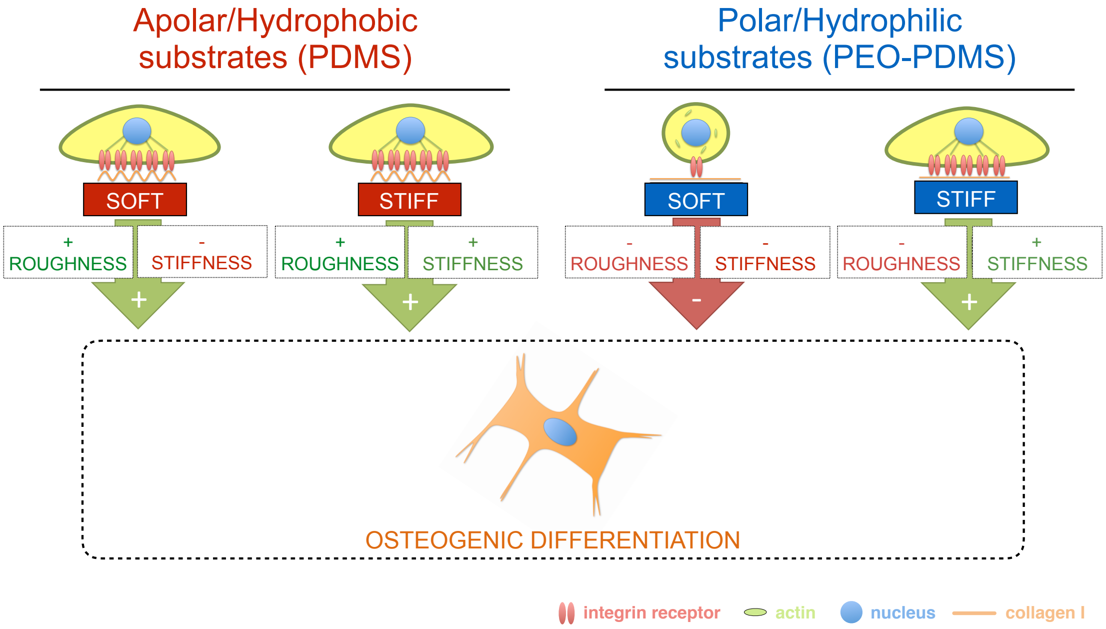
Apolar/Hydrophobic substrates (PDMS)
Polar/Hydrophilic substrates (PEO-PDMS)
SOFT
STIFF
SOFT
STIFF
+ ROUGHNESS
- STIFFNESS
+ ROUGHNESS
+ STIFFNESS
- ROUGHNESS
- STIFFNESS
- ROUGHNESS
+ STIFFNESS
+
+
-
+
OSTEOGENIC DIFFERENTIATION
integrin receptor
actin
nucleus
collagen I

Figure 5.8 | Schematic of the interplay of matrix stiffness and surface energy-driven ligand topography in osteogenic stem cell differentiation.

We developed a PDMS-based platform that can be mechanically tuned within a wide range of potential stiffness (from 70 Pa to 2.3MPa) and surface energies that enables the creation of hydrophilic and hydrophobic variants of a given material stiffness, without otherwise affecting baseline physical properties of the substrate surface – most critically, topology. This system allows one to limit variation in topology that is a key confounding factor that often plagues parametric study of cell-biomaterial interaction. We previously demonstrated through multi-scale mechanical characterization that mechanical properties of these materials were consistent across size scales (see Chapter 3).

Using this well-controlled material platform, we pinpointed surface energy as a fundamental material property that can significantly impact stem cell fate on soft biomaterials. We demonstrate that ligand topology driven by surface energy can override adherent cell response to material stiffness, even though substrate stiffness is well described as a dominant contextual cue for stem cells in culture [2, 6]. We show that collagen monomer assembly into rough nanotopography on hydrophobic surfaces [12] affects the ability of stem cells to spread and osteogenically differentiate on soft PDMS (Fig. 5.8). As previously reported [30], the presence of nanofeatures can push a cell to elongate, contract, and eventually undergo osteogenic differentiation. We further show that using non-aggregating minimal peptides on soft hydrophobic PDMS can rescue the ability of stem cells to sense and react to soft substrates, chiefly in the form of cell rounding. Although studies have investigated the effects of nanotopography on stem cell behavior on rigid substrates [31], the present study is to our knowledge the first to demonstrate a dominant effect of nanotopography on very soft substrates. This information has eluded detection until now, mostly due to the substantial technological challenges involved in fabricating soft structured substrates or characterizing very soft substrates with regard to nano-scale topology and multi-scale mechanics. On stiff substrates that are substantially easier to handle, it is well described that nanoscale disorder strongly promotes osteogenic differentiation [32]. Our data indicate that this relationship between nano-scale roughness and osteogenic signaling extends to soft substrates as well. We propose that stochastic assembly of ligand is driven by an apolar biomaterial surface in a manner that forms a sufficiently rough ligand network [12] exhibiting a lateral and vertical disorder of cell binding sites to drive bone differentiation independently of substrate rigidity. A dependency of cell behavior on material stiffness can be rescued by using a non-aggregating synthetic collagen peptide, demonstrating that in the absence of adequately rough ligand self-assembly, MSCs can detect and react to the stiffness of a soft or hard PDMS substrate with rounding or spreading, respectively. Our experiments with tight control against confounding factors add essential mechanistic support to previous studies demonstrating that stem cell sensitivity to a soft substrate can be modulated by cell-scale patterning and/or PDMS surface chemistry [15, 33].

The fact that cells with severely diminished mechanical tension and ROCK activity can nonetheless spread on very soft hydrophobic substrates, suggests that cytoskeletal tension can be a secondary factor to topology in determining cell fate. This finding echoes observations by Chaudhuri et al., in which substrate stress relaxation and decreased cytoskeletal tension were reported to enhance cell spreading on soft substrates [14]. The present study shows that spread morphology on even soft substrates functionalized with a suitable extracellular matrix ligand is sufficient to direct mesenchymal stem cells to an osteogenic fate. Conversely, previous studies have demonstrated that stiff substrates which confine cell spreading on micropatterned surfaces can promote adipogenic differentiation [34, 35]. Thus spread cell morphology, rather than the development of cytoskeletal contractility *per se*, seems to be a necessary condition to determine cell fate in the two dimensional culture conditions that form the majority basis of our understanding on stem cell mechanosensitivity. This conclusion contrasts with recent experiments with three-dimensional platforms that reported cell fate to be independent of cell morphology but rather more traction dependent [36, 37]. Still, three dimensional culture systems have their own disadvantages, including relative lack of control over hydrostatic stresses and osmotic gradients, and further work is required to determine how ROCK mediated contractility and spread cell morphology potentially interact to regulate cell signaling or act as a central checkpoint in determining cell fate.

Collectively these results are striking, with potentially critical implications for research employing Type-I collagen as a “standard” two-dimensional cell culture reagent. We demonstrate that the strong tendency of collagen to self-assemble translates to large potential for experimental variability, and/or systematically biased biological outcomes due to uncontrolled material surface. Other ECM ligands, such as fibronectin, can behave quite differently from collagen (e.g. Supplementary Fig. S5.5), and much work is yet required to characterize the combinations of biomaterials, interface chemistry, extracellular protein milieu, and cells that can yield a reliably emergent system behavior.

In conclusion, we have demonstrated that surface energy driven ligand self assembly [12] can steer a cell to very different fates on soft substrates. Controlling for surface energy enables stem cells to spread and differentiate according to PDMS stiffness. Our findings fill an important gap in our collective understanding [3, 4], explaining why stem cells spread and undergo osteogenic differentiation on soft apolar silicone when coated with collagen compared to rounding on soft polar substrates such as polyacrylamide. Although thoroughly described in the field of rigid biomaterials used in implants [8, 9], effects of surface energy on very soft substrates are difficult to control, and as such have been widely ignored in opinion leading papers on stem cell-matrix interaction [3, 4]. We suggest that surface energy is nonetheless a major biomaterial design factor that must be considered when designing cell-instructive biomaterials.

5.6 Supplementary material

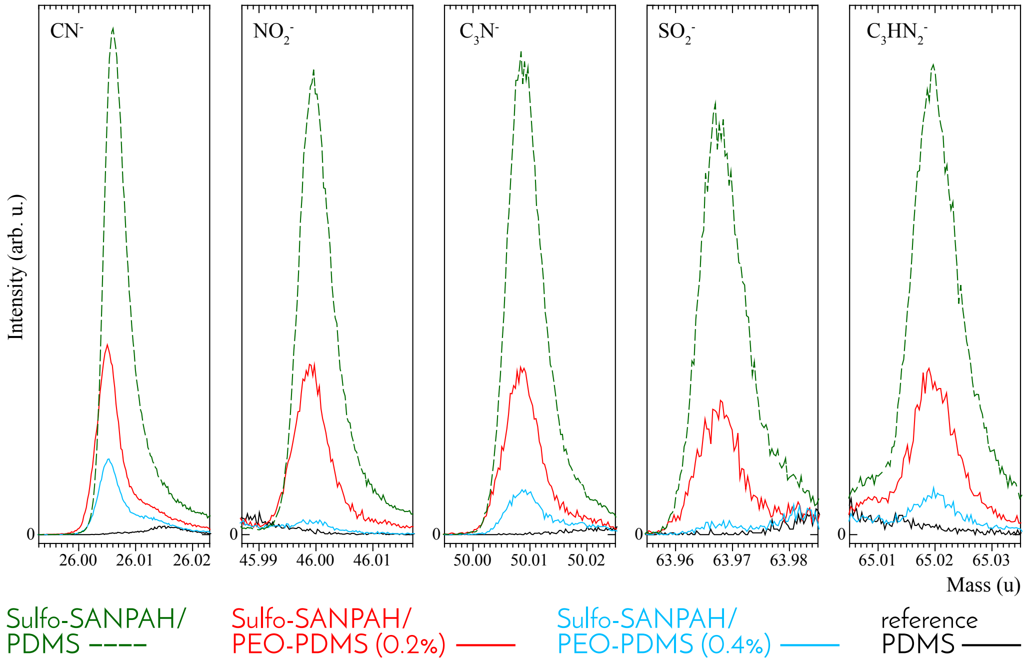

Supplementary Figure S5.1 | Spectral analysis by Time-of-Flight Secondary Ion Mass Spectrometry (TOF-SIMS) indicates a higher amount of sulfo-SANPAH bound to PDMS compared to PEO-PDMS. Zoom-ins on characteristic fragments for sulfo-SANPAH on PDMS (dashed green), PEO-PDMS (0.2%) (red) and PEO-PDMS (0.4%) (light blue) are shown and compared. The PDMS substrate (without sulfo-SANPAH, black) is also shown as reference. The spectra are normalized to the total ions counts. The semi-quantitative analysis of these characteristic peaks reveals that the sulfo-SANPAH density on the 0.2 % PEO substrate is only 33 % ± 8 % of its density on the pure PDMS substrate. On the 0.4 % PEO substrate it further decreases to 10 % ± 6 %.

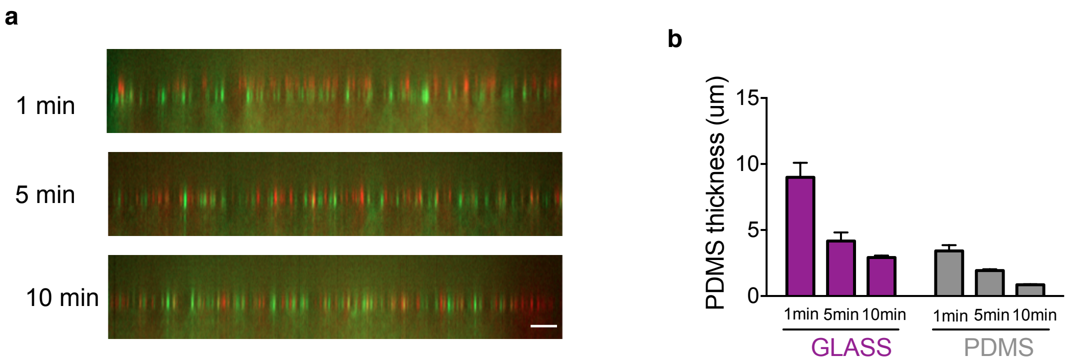

c

Spincoating time	Thickness
1 min	3.42 ± 0.60 µm
5 min	1.93 ± 0.54 µm
10 min	0.85 ± 0.36 µm

Supplementary Figure S5.2 | Depth of the beads inside the PDMS for traction force microscopy is controlled. (a) Representative images of the PDMS upper layer thickness sandwiched between two types of fluorescent beads when spin coated for 1 min, 5 min and 10 min at 10 000 rpm on PDMS base layer. (b) Quantification of the PDMS thickness when spin coated on glass and PDMS for 1 min, 5 min and 10 at 10 000 rpm. (c) Summary of the thickness values of PDMS substrates. (n = 4; number of data points per sample = 9). Data are represented as mean±s.d.

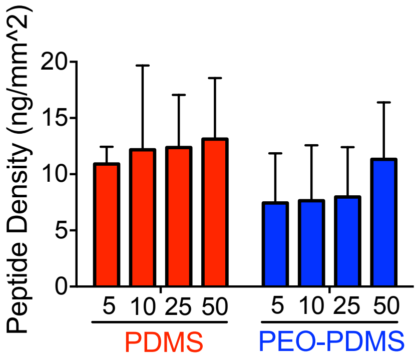

Supplementary Figure S5.3 | Ligand loading is empirically adjusted to obtain a similar ligand density on PDMS and PEO-PDMS. Adsorbed GFOGER peptide amount on PDMS and PEO-PDMS substrates when coated with different peptide solution concentration from 5 to 50 µg mL^{-1}. (n = 4-6). Data are represented as mean±s.d.

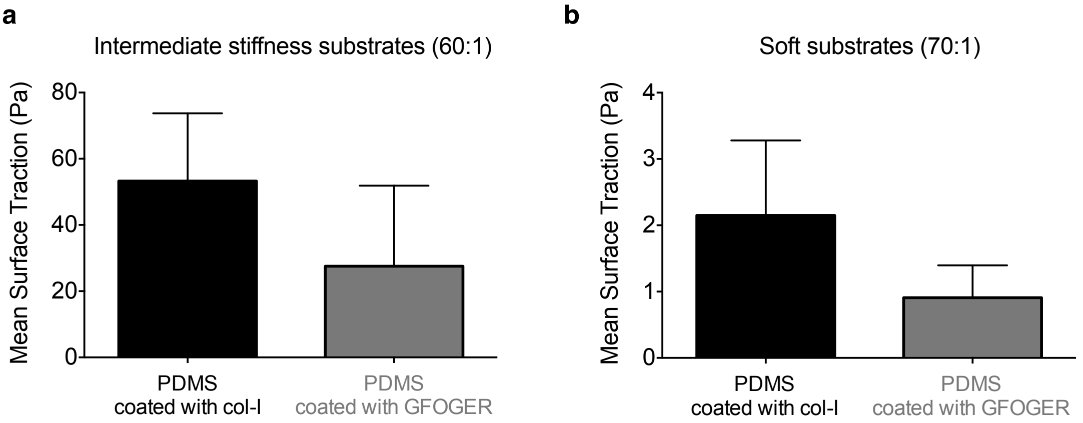

Supplementary Figure S5.4 | Traction force microscopy indicates the cell traction stress magnitude increases with substrate stiffness when coated with the minimal collagen peptide. (a) Quantification of the corresponding mean surface traction stresses generated by hBMSCs when seeded on PDMS substrates of intermediate stiffness (5-6 kPa) when coated with the minimal collagen peptide (GFOGER). PDMS coated with collagen I was used as a reference. (n = 6-23) (b) Quantification of the corresponding mean surface traction stresses generated by hBMSCs when seeded on PDMS soft substrates (0.22-0.35 kPa) when coated with the minimal collagen peptide (GFOGER). PDMS coated with collagen I was used as a reference. (n = 35-45).

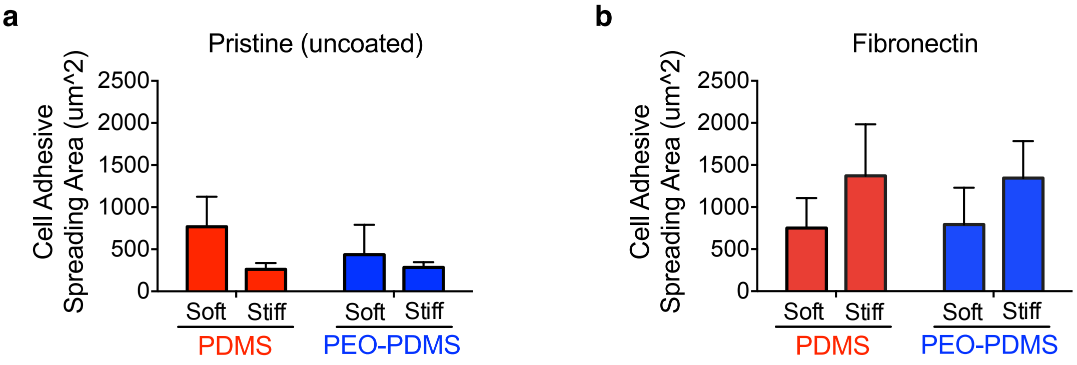

Supplementary Figure S5.5 | Cell spreading is affected differently depending on the coated ligand. (a) Spreading areas of hBMSCs on functionalized substrates after 24 h culture on PDMS and PEO-PDMS substrates of different stiffness (soft: 0.07-0.10 kPa; stiff: 2.15-2.40 MPa) when (a) without immobilized protein ligand and (b) coated with fibronectin. Cells were stained with Alexa-488-phalloidin and DAPI. (n=42-540).

Image Analysis and Traction Force Microscopy

To calculate the cell-generate traction stresses, we used a combination of methods that have been previously described [19, 38]. In a first step, z-stacks containing images of the fluorescent beads inside the gel and the cell residing on top before and after cell removal were loaded into ImageJ and split into their respective channels. Single images of the bead layer and the cell were found with the Fiji script *"Find Focused Slices"* written by Tseng et al. and exported to MATLAB (The MathWorks, Natick, MA) for further processing.

Bead images after (post) and before (pre) cell removal were aligned to compensate for experimental in-plane drift and the relative displacement between these images was calculated with the use of the *pointTracker* function within MATLAB's Computer Vision toolbox. This function is a pyramidal implementation of the Kanade-Lucas-Tomasi (KLT) optical flow feature tracker, which is a differential approach to calculate the displacement between two frames by the least squares algorithm [39-41]. The size of the search window was 16^2 pixels at each pyramid resolution (~2.5 μm at the original resolution) and the obtained displacement vectors at each feature were interpolated on a regular grid with size 8 pixels (~1.25 μm) using the *scatteredinterpolant* class in MATLAB with natural neighbor interpolation. It was shown in a previous study that the KLT tracker performs more robust than correlation-based tracking algorithms commonly used in TFM[42-44] in terms of accuracy and resolution [18].

If the displacements and corresponding strains are small enough (typically ≤ 1μm), PDMS can be considered as a isotropic homogeneous solid which elicit linear-elastic behavior[38]. We therefore employed a variation of the regularized Fourier-transform traction Cytometry [42, 44] (Reg-FTTC) with a Green's function that includes the depth of the bead plane from the surface where the tractions are applied[18]. This algorithm recovers the traction applied on the surface of the substrate given the displacements at the depth z_0 within the substrate assuming the whole substrate is sufficiently thick to approximate it by an elastic infinite half-space [45]. The regularization parameters were determined experimentally and remained constant for all measurements that were considered. After the traction stresses were calculated, we overlaid the cell image on the traction field and determined the cell projected area by manually outlining the cell boundary. Traction metrics were obtained with the average traction stress over all values within the cell area [46]. Using the relation:

$$avg(T_{xy}) = \frac{\sum_i \frac{F_i}{A_i}}{n} = \frac{\sum_i F_i}{n \cdot A} = \frac{avg(F)}{A}$$

where

$$T_{xy}(i,j) = \sqrt{T_x^2(i,j) + T_y^2(i,j)}$$

is the magnitude of the traction vector at each measurement point, average traction stress is equal to the average traction force divided by the total projected cell area.

Type of experiment	**Cell culture duration**	**Initial cell seeding density (cell/cm^2)**
Cell attachment	1 hour	25,000
Cell morphology	1 day	5,000
Gene expression	1 day	25,000
Gene expression	7 days	5,000
Cell differentiation	7, 14 and 21 days	5,000
TFM	16 hours	625

Supplementary Table S5.1 | Summary of the different performed experiments with their cell culture duration and initial cell seeding density

5.7 References

[1] L. MacQueen, Y. Sun, C.A. Simmons, Mesenchymal stem cell mechanobiology and emerging experimental platforms, Journal of the Royal Society, Interface / the Royal Society 10(84) (2013) 20130179.
[2] A.J. Engler, S. Sen, H.L. Sweeney, D.E. Discher, Matrix Elasticity Directs Stem Cell Lineage Specification, Cell 126(4) (2006) 677-689.
[3] B. Trappmann, J.E. Gautrot, J.T. Connelly, D.G.T. Strange, Y. Li, M.L. Oyen, M.A. Cohen Stuart, H. Boehm, B. Li, V. Vogel, J.P. Spatz, F.M. Watt, W.T.S. Huck, Extracellular-matrix tethering regulates stem-cell fate, Nature materials 11(7) (2012) 642-649.
[4] J.H. Wen, L.G. Vincent, A. Fuhrmann, Y.S. Choi, K.C. Hribar, H. Taylor-Weiner, S. Chen, A.J. Engler, Interplay of matrix stiffness and protein tethering in stem cell differentiation, Nature materials 13(10) (2014) 979-87.
[5] M. Prager-Khoutorsky, A. Lichtenstein, R. Krishnan, K. Rajendran, A. Mayo, Z. Kam, B. Geiger, A.D. Bershadsky, Fibroblast polarization is a matrix-rigidity-dependent process controlled by focal adhesion mechanosensing, Nat Cell Biol 13(12) (2011) 1457-1465.
[6] R.I. Sharma, J.G. Snedeker, Biochemical and biomechanical gradients for directed bone marrow stromal cell differentiation toward tendon and bone, Biomaterials 31(30) (2010) 7695-7704.
[7] A. Higuchi, Q.D. Ling, Y. Chang, S.T. Hsu, A. Umezawa, Physical cues of biomaterials guide stem cell differentiation fate, Chem Rev 113(5) (2013) 3297-328.
[8] X. Liu, J.Y. Lim, H.J. Donahue, R. Dhurjati, A.M. Mastro, E.A. Vogler, Influence of substratum surface chemistry/energy and topography on the human fetal osteoblastic cell line hFOB 1.19: Phenotypic and genotypic responses observed in vitro, Biomaterials 28(31) (2007) 4535-4550.
[9] M.D. Mager, V. LaPointe, M.M. Stevens, Exploring and exploiting chemistry at the cell surface, Nat Chem 3(8) (2011) 582-9.
[10] S.C. Ramos, A.O. Lobo, G. de Vasconcelos, E.F. Antunes, V.J. Trava-Airoldi, E.J. Corat, Influence of polar groups on the wetting properties of vertically aligned multiwalled carbon nanotube surfaces, Theoretical Chemistry Accounts 130(4) (2011) 1061-1069.
[11] P.G. de Gennes, Wetting: statics and dynamics, Reviews of Modern Physics 57(3) (1985) 827-863.
[12] T. Razafiarison, U. Silvan, D. Meier, J.G. Snedeker, Surface-Driven Collagen Self-Assembly Affects Early Osteogenic Stem Cell Signaling, Adv Healthc Mater 5(12) (2016) 1481-92.
[13] J. Li, D. Han, Y.-P. Zhao, Kinetic behaviour of the cells touching substrate: the interfacial stiffness guides cell spreading, Sci. Rep. 4 (2014).
[14] O. Chaudhuri, L. Gu, M. Darnell, D. Klumpers, S.A. Bencherif, J.C. Weaver, N. Huebsch, D.J. Mooney, Substrate stress relaxation regulates cell spreading, Nat Commun 6 (2015) 6364.
[15] G. Vertelov, E. Gutierrez, S.A. Lee, E. Ronan, A. Groisman, E. Tkachenko, Rigidity of silicone substrates controls cell spreading and stem cell differentiation, Scientific reports 6 (2016) 33411.

[16] R. Mhanna, E. Ozturk, Q. Vallmajo-Martin, C. Millan, M. Muller, M. Zenobi-Wong, GFOGER-modified MMP-sensitive polyethylene glycol hydrogels induce chondrogenic differentiation of human mesenchymal stem cells, Tissue engineering. Part A 20(7-8) (2014) 1165-74.
[17] G. Bartalena, R. Grieder, R.I. Sharma, T. Zambelli, R. Muff, J.G. Snedeker, A novel method for assessing adherent single-cell stiffness in tension: design and testing of a substrate-based live cell functional imaging device, Biomedical microdevices 13(2) (2011) 291-301.
[18] C.N. Holenstein, U. Silvan, J.G. Snedeker, High-resolution traction force microscopy on small focal adhesions - improved accuracy through optimal marker distribution and optical flow tracking, Scientific reports 7 (2017) 41633.
[19] S.V. Plotnikov, B. Sabass, U.S. Schwarz, C.M. Waterman, High-resolution traction force microscopy, Methods Cell Biol 123 (2014) 367-94.
[20] C.C. Dupont-Gillain, I. Jacquemart, P.G. Rouxhet, Influence of the aggregation state in solution on the supramolecular organization of adsorbed type I collagen layers, Colloids and surfaces. B, Biointerfaces 43(3-4) (2005) 179-86.
[21] B. Narayanan, G.H. Gilmer, J. Tao, J.J. De Yoreo, C.V. Ciobanu, Self-assembly of collagen on flat surfaces: the interplay of collagen-collagen and collagen-substrate interactions, Langmuir : the ACS journal of surfaces and colloids 30(5) (2014) 1343-50.
[22] J.D. Mih, A. Marinkovic, F. Liu, A.S. Sharif, D.J. Tschumperlin, Matrix stiffness reverses the effect of actomyosin tension on cell proliferation, J Cell Sci 125(Pt 24) (2012) 5974-83.
[23] D. Riveline, Focal contacts as mechanosensors: externally applied local mechanical force induces growth of focal contacts by an mDia1-dependent and ROCK-independent mechanism, J. Cell Biol. 153 (2001) 1175-1186.
[24] A.W. Lund, J.P. Stegemann, G.E. Plopper, Mesenchymal Stem Cells Sense Three Dimensional Type I Collagen through Discoidin Domain Receptor 1, The open stem cell journal 1 (2009) 40-53.
[25] A.M. Wojtowicz, A. Shekaran, M.E. Oest, K.M. Dupont, K.L. Templeman, D.W. Hutmacher, R.E. Guldberg, A.J. García, Coating of biomaterial scaffolds with the collagen-mimetic peptide GFOGER for bone defect repair, Biomaterials 31(9) (2010) 2574-2582.
[26] D. Prockop, A. Fertala, Inhibition of the self-assembly of collagen I into fibrils with synthetic peptides, The Journal of biological chemistry 273(25) (1998) 15598-15604.
[27] Z. Zhang, G. Li, B.L. Shi, Physicochemical Properties of Collagen, Gelatin and Collagen Hydrolysate Derived from Bovine Limed Split Wastes, Journal of the Society of Leather Technologists and Chemists 90(1) (2006) 23-28.
[28] Y. Arima, H. Iwata, Effect of wettability and surface functional groups on protein adsorption and cell adhesion using well-defined mixed self-assembled monolayers, Biomaterials 28(20) (2007) 3074-3082.
[29] A.M. Schaap-Oziemlak, P.T. Kühn, T.G. van Kooten, P. van Rijn, Biomaterial–stem cell interactions and their impact on stem cell response, RSC Adv. 4(95) (2014) 53307-53320.

[30] S. Oh, K.S. Brammer, Y.S. Li, D. Teng, A.J. Engler, S. Chien, S. Jin, Stem cell fate dictated solely by altered nanotube dimension, Proceedings of the National Academy of Sciences of the United States of America 106(7) (2009) 2130-5.
[31] M.J. Dalby, N. Gadegaard, R.O. Oreffo, Harnessing nanotopography and integrin-matrix interactions to influence stem cell fate, Nature materials 13(6) (2014) 558-69.
[32] M.J. Dalby, N. Gadegaard, R. Tare, A. Andar, M.O. Riehle, P. Herzyk, C.D. Wilkinson, R.O. Oreffo, The control of human mesenchymal cell differentiation using nanoscale symmetry and disorder, Nature materials 6(12) (2007) 997-1003.
[33] J. Fu, Y.K. Wang, M.T. Yang, R.A. Desai, X. Yu, Z. Liu, C.S. Chen, Mechanical regulation of cell function with geometrically modulated elastomeric substrates, Nature methods 7(9) (2010) 733-6.
[34] K.A. Kilian, B. Bugarija, B.T. Lahn, M. Mrksich, Geometric cues for directing the differentiation of mesenchymal stem cells, Proceedings of the National Academy of Sciences of the United States of America 107(11) (2010) 4872-7.
[35] R. McBeath, D.M. Pirone, C.M. Nelson, K. Bhadriraju, C.S. Chen, Cell Shape, Cytoskeletal Tension, and RhoA Regulate Stem Cell Lineage Commitment, Developmental Cell 6(4) (2004) 483-495.
[36] N. Huebsch, P.R. Arany, A.S. Mao, D. Shvartsman, O.A. Ali, S.A. Bencherif, J. Rivera-Feliciano, D.J. Mooney, Harnessing traction-mediated manipulation of the cell/matrix interface to control stem-cell fate, Nature materials 9(6) (2010) 518-26.
[37] S. Khetan, M. Guvendiren, W.R. Legant, D.M. Cohen, C.S. Chen, J.A. Burdick, Degradation-mediated cellular traction directs stem cell fate in covalently crosslinked three-dimensional hydrogels, Nature materials 12(5) (2013) 458-65.
[38] R.W. Style, R. Boltyanskiy, G.K. German, C. Hyland, C.W. MacMinn, A.F. Mertz, L.A. Wilen, Y. Xu, E.R. Dufresne, Traction force microscopy in physics and biology, Soft Matter 10(23) (2014) 4047-4055.
[39] B.D. Lucas, T. Kanade, An iterative image registration technique with an application to stereo vision, Proceedings of the 7th international joint conference on Artificial intelligence - Volume 2, Morgan Kaufmann Publishers Inc., Vancouver, BC, Canada, 1981, pp. 674-679.
[40] S. Jianbo, C. Tomasi, Good features to track, 1994 Proceedings of IEEE Conference on Computer Vision and Pattern Recognition, 1994, pp. 593-600.
[41] J.-Y. Bouguet, Pyramidal Implementation of the Lucas Kanade Feature Tracker Description of the algorithm, Intel Corporation Microprocessor Research Labs, 2000.
[42] B. Sabass, M.L. Gardel, C.M. Waterman, U.S. Schwarz, High resolution traction force microscopy based on experimental and computational advances, 2008.
[43] J.L. Martiel, A. Leal, L. Kurzawa, M. Balland, I. Wang, T. Vignaud, Q. Tseng, M. Thery, Measurement of cell traction forces with ImageJ, Methods Cell Biol 125 (2015) 269-87.

[44] J. Westerweel, Fundamentals of digital particle image velocimetry, Measurement Science and Technology 8(12) (1997) 1379-1392.
[45] L.D.L. Landau, J. M., Theory of Elasticity, Pergamon Press (1970).
[46] Ai K. Yip, K. Iwasaki, C. Ursekar, H. Machiyama, M. Saxena, H. Chen, I. Harada, K.-H. Chiam, Y. Sawada, Cellular Response to Substrate Rigidity Is Governed by Either Stress or Strain, Biophysical Journal 104(1) (2013) 19-29.

Chapter 6

6 Synthesis

6.1 Summary of achievement and main findings

Our understanding of cell-material interaction for the development of cell-instructive implants has drastically increased over the last decade. However, recent conflicting studies seem to indicate that the mechanism by which stem cells sense and react to the mechanical properties of their substrates is not fully understood [1, 2]. While the capacity of adult mesenchymal stem cells to spread and differentiate differentially according to substrate stiffness was commonly observed on hydrogels [3, 4], recent studies were not able to explain fully the unexpected behavior of stem cells on very soft silicone substrates that could spread and osteogenically differentiate [1, 2]. Although hydrogels and elastomers were regularly compared to decipher the cell-material interaction, they present several different features such as the physical and chemical properties. One of these features is the focus of this dissertation, which is the difference in surface energy of both materials. We decided to engineer and modulate the inherent hydrophobicity of PDMS to elucidate the unexpected ability of PDMS to promote cell spreading and osteogenic differentiation independently of its stiffness.

In chapter 3, we successfully developed a novel two-dimensional silicone-based platform for cell culture whose stiffness and surface energy could be independently modulated without altering other potential confounding factors such as mechanical properties and topography. Due to its inherent hydrophobicity, PDMS often undergoes surface treatment to render the surface more hydrophilic and more potent for protein ligand coating. However, surface treatments are either very complicated or affect the integrity of the surface mechanical properties [5]. Our first main achievement was to create a simple method to produce homogenous surface energy-tunable PDMS substrates while preserving the mechanical properties and surface topography. By simply increasing the relatively small amount of the PDMS-b-PEO surfactant directly added to the PDMS slurry as previously described [6], we observed and measured a significant reduced water contact angle from 110° (without any surfactant) to 40° (with 1% (v/w) surfactant). Based on several studies that reported an optimal cell adhesion on moderately hydrophilic substrates, we performed further characterization and biological investigation on elastomers mixed with 0.2% (v/w) surfactant resulting in a contact angle of 80° (PEO-PDMS) [7]. Since no previous studies reported the potential effects of surfactant additive on the viscoelastic properties of PDMS, we performed mechanical testing to evaluate possible differences between the pristine and 0.2% surfactant treated PDMS (PEO-PDMS). While compressive moduli were in average slightly reduced for PEO-PDMS, bulk compression testing indicated relatively similar and preserved mechanical properties. Then, we wanted to ensure that the generated substrates were homogenous in the focal adhesion dimensions. Surface micro-indentation indicated homogeneity and in contrast to previous studies [8, 9], no significant effects from the surface treatment were measured.

In chapter 4, the effects of substrate surface polarity on ligand assembly were characterized. As previously described by others [10], we observed by scanning electron microscopy (SEM) and atomic force microscopy (AFM) that substrate surface energy has a decisive role on modulating the collagen assembly and the resulting topography exposed to the cells. While the collagen layer on pristine hydrophobic PDMS appeared clumpy and rough with molecular aggregates, the collagen layer on hydrophilic PEO-PDMS substrates appeared relatively smooth with less present aggregates. Supramolecular organization on the surface was described to be driven by collagen-collagen and collagen-substrate interactions [11]. While collagen molecules are composed of amino acid residues that can present either polar or apolar groups, material surface polarity therefore dictates the nature of the collagen conformation and aggregation. Furthermore in chapter 4, the effects of surface driven ligand topography were assessed on stem cell adhesion and differentiation. The first major observation was the biocompatibility of PEO-PDMS substrates that exhibited similar cell attachment to the pristine elastomers and promoted cell spreading. Our second main observation was after culturing the cells for 2 weeks on PDMS and PEO-PDMS, indicators of osteogenic differentiation such as calcium deposit and alkaline phosphatase activity were significantly higher on the hydrophilic elastomers. Molecular investigation by qPCR and ELISA further indicated upregulation of osteogenic markers such as Runx2 and key regulators of the MAPK pathway. Analysis of the collagen-related receptors after 1 day showed significant upregulation of the integrin α1β1 and the discoidin domain receptor 1 on the hydrophilic substrates.

In chapter 5, the role of surface energy-driven ligand assembly in influencing stem cell sensitivity to a broad range of elastomer stiffness was evaluated. To enable this evaluation, various substrates of different stiffness from high ($E_{mod} > 2$ MPa) to very low young modulus ($E_{mod} < 1$ kPa) that can be either apolar (pristine hydrophobic PDMS) or polar (surfactant-treated hydrophilic PEO-PDMS) were fabricated. Our first main discovery was to observe a difference in cell morphology after culturing stem cells for 24 h at low seeding density on PDMS and PEO-PDMS. While cells could spread and present numerous F-actin stress fibers on the various PDMS substrates as previously reported [1, 2], they presented a reduced and rounded morphology on the very soft PEO-PDMS ($E_{mod} < 1$ kPa). Furthermore, cells were cultured for 1 week in mixed-induction medium containing osteogenic and adipogenic supplements on the various substrates. Consistent with the cell morphology results, we found quantitatively a reduced osteogenic differentiation and qualitatively more adipogenic cells on the soft PEO-PDMS compared to the other substrates. Collectively, ours results indicate when a substrate exposes a hydrophobicity driven-rough ligand layer, cells actually spread and differentiate towards osteogenic lineage independently of the material stiffness. The difference in collagen layer topography may activate differentially collagen receptors and further downstream signaling directing cell fate. Therefore, surface energy has a decisive effect on mesenchymal stem cell fate and can dominate bulk stiffness cue. To confirm our hypothesis, we have employed a small non-self assembling collagen-mimetic peptide and observed that stem cells can spread according to stiffness independently of surface polarity.

Furthermore in chapter 5, we developed a new traction force microscopy PDMS-based platform to quantify the force exerted by the cells on the different substrates. To limit contributions from confounding factors such as chemistry and topography resulting from the conventional surface fluorescent nanotracker coating, we embedded them within the elastomer in a controlled manner. We found that cells can spread on soft PDMS in absence of cytoskeleton tension. Molecular investigation of Rho Kinase (ROCK), which plays a key role in cellular contractility, confirmed a reduced activation on softer PDMS. This challenges the current view of mechanotransduction that cells spread by assessing the environment mechanical resistance via the cytoskeleton contraction [12].

6.2 Limitations and future research

Although we have provided a novel platform whose confounding factors were controlled, this doctoral research still presents several limitations, both technically and analytically. The first main challenging limitation is the platform itself. All our experiments were performed with cells originating from a single donor. Although our cells were characterized as multipotent mesenchymal stem cells, we cannot exclude that the observations we made were donor-specific. For instance, some preliminary experiments were performed with cells coming from a different donor and presented similar morphological observations. To further strengthen our observations, experiments including several donors would have been relevant but this would have required more resources. Similarly, we only employed collagen as a model ligand. Other common ligand proteins such as fibronectin present distinct protein structures that were also shown to have their conformation influenced by the surface chemistry [13]. Although previous studies [1, 2] have reported similar behavior on PDMS with either collagen or fibronectin, these two types of protein ligand activate different receptors and may not similarly aggregate. This creates space for further investigation with fibronectin. For instance, we observed during our preliminary experiments that cells could spread according to stiffness when coated with either fibronectin or RGD peptide on PDMS and PEO-PDMS.

For the purpose of our experiments, we have employed the amount of 0.2% surfactant to fabricate our PEO-PDMS. Although the mechanical properties remained relatively similar, we noticed that the elastic modulus of stiff PEO-PDMS having a 10:1 (base-to-catalyst) ratio was significantly lower by 20% when compared to the pristine PDMS. Incorporation of the surfactant may therefore slightly change the mechanical strength of the polymer network. In chapter 3, we have left our substrates in culture for 3 weeks, measured the compressive modulus and found a reduced difference between the substrates (10%), which may also suggest a difference in polymerization kinetics. To further investigate this aspect, additional mechanical characterization with substrates containing more surfactant would be required.

In addition to the difference in surface polarity, PDMS and PEO-PDMS exhibit another important distinction, which is the proportion of protein passive adsorption and covalent binding. In chapter 3, we have observed that in absence of crosslinker, more proteins bind to PDMS when compared to PEO-PDMS. Although others such as Prager-Khoutorsky et al. [14] have coated PDMS passively with proteins and observed a difference in cell adhesion on PDMS of different stiffness, we cannot exclude that the strength of protein binding to the surface may influence cell behavior as previously suggested by Choi et al. that a stronger coupling strength promotes cell spreading and osteogenic differentiation [15].

The main conclusion of this doctoral dissertation lies in the difference in collagen ligand assembly on hydrophobic and hydrophilic substrates.

Although we have performed various imaging of the collagen layer to confirm our observation, further characterization with higher resolution and more surface profilometry analysis would have brought more insight and strengthened our conclusion. As previously shown by Dalby et al. [16], stochastic distribution of surface nanostructures appear to be determinant in driving spontaneously osteogenic differentiation by enabling the formation of fewer but larger adhesions in osteoblastic cells [17]. Therefore, the nanoscale disorder is a key factor and may play a more dominant role than just the surface roughness. Furthermore, Huang et al. have shown previously that the disorder of RGD nanopatterns can promote cell adhesion when compared to the ordered symmetrical ligands [18]. This represents a key area for further investigation with for example different surface roughness but identical nanoscale disorder.

In our dissertation, we have focused on quantifying the level of osteogenic differentiation, which is of major interest for bone tissue regeneration. However, we have not fully characterized the diverse cell population on the various substrates after 2-week culture in basal growth medium and particularly on the soft PEO-PDMS. In contrast to the culture in mixed induction where some cells presented some visible lipid vacuoles, cells on the soft hydrophilic substrates after 2 weeks in basal medium culture did not present any particular phenotypic features, which could suggest that most of the cells remained undifferentiated. For instance, we observed that the cells had a limited spreading for the first few days and later were able to spread and cover the whole substrate, which indicates the ability of cells to remodel the surface. A further characterization of the cell population by gene deep sequencing would have better unrevealed the stem cell fate on PDMS substrates. It is also important to note here that keeping the fragile cell monolayer intact for more than 7 days was very challenging and particularly on the soft substrates, which might be explained by the lower cellular tension exerted by the cells.

Our gene expression analysis on day-1 seems to indicate a differential activation of collagen receptors and particularly the discoidin domain receptors that are still not well understood. Recent evidence has shown that DDRs and integrin receptors are activated independently but seem to cooperate and converge on a common pathway [19]. Further characterization of the various upregulated molecules by gene deep sequencing at different time points would have allowed to map the pathways involved in the recognition of different ligand assembly and driving the stem cell fate.

In chapter 5, we have developed a novel traction force microscopy platform that has the main advantage of circumventing confounding contributions from the chemically coated beads on the surface. However, our method for embedding the nanobeads within the elastomer is not an optimal and handy approach: (i) controlling for the second layer thickness requires a fully controlled and time-consuming process with critical parameters during spin coating, curing and bead coating; (ii) impact of the chemical bead coating at the two-layer interface on the substrate mechanical properties was not further evaluated; (iii) important reduction of the bead displacement signal was observed, which suggests that small displacements were probably undetectable. Furthermore, our analysis was only based on a single time point snapshot. Analysis of different time points or a continuous reading of the bead displacement as developed by others [20] would give further insight in the mechanism of stem cell contractility on various substrates.

The results from our TFM experiments indicate the ability of cells to spread in absence of cytoskeleton tension, which diverges from recent experiments in three-dimension that reported fate to be independent of cell morphology but rather more traction dependent [21, 22]. Although two-dimensional and three-dimensional platforms present distinct environmental conditions, this contradicting observation gives ground for further investigation with for example the development of an intermediate platform between two and three dimension such as a sandwiched platform to elucidate the main driving factor of stem cell differentiation between cell shape and contractility. For instance, Beningo et al. have observed a change in fibroblast cell morphology after sandwiching a flexible PAA gel with a more elongated shape and the loss of lamellipodia [23].

6.3 Conclusion

Overall, this dissertation indicates that underappreciated elements can have a major impact on the study outcome and confound similar studies. While the focus of this dissertation was on cell sensitivity to material stiffness in two dimension, studies that evaluated the effects of substrate nanotopography and particularly with titanium oxide (TiO2) nanotubes also reported some conflicting results and theories in highly cited publications. Park et al. [24] have shown by culturing MSCs on TiO2 nanotubes with different diameters ranging from 15 to 100 nm that cell adhesion and osteogenic differentiation were enhanced on smaller diameters. They concluded a 15-nm diameter presents an optimal spacing for accelerated integrin clustering and enhancing cellular activities. Furthermore, they also reported that a nanotube layer with a tube diameter larger than 50 nm drastically affects cellular activities and induces cell apoptosis. In contrast, Oh and coworkers have demonstrated by increasing the diameter from 30 to 100 nm that cells were pushed to further elongate and consequently a stronger bone differentiation was promoted [25]. This important discrepancy led to further discussion via interposed letters where von der Mark and coworkers pointed out the lack of consideration from Oh et al. of the interplay between integrin clustering and nanospacing in focal adhesion formation and cell differentiation. To answer this letter, Oh and coworkers suggested that those opposite results could be potentially explained by the difference in cell species, culture medium, surface treatment and chemistry indicating a lack of consideration over an important confounding factor [26, 27].

Similarly, the existing literature with three-dimensional platforms reports some contradicting views regarding the ability and the manner of stem cells to sense materials stiffness. Huesbch and coworkers have shown by encapsulating cells in alginate gels of different stiffness functionalized with the RGD peptide that cells underwent adipogenic differentiation in soft gels and osteogenic differentiation in stiffer gels. Furthermore, they reported that the stiffness-driven differentiation of MSCs was independent of cell morphology but cell traction dependent [22]. Conversely, Parekh et al. only observed bone differentiation of cells cultured in PEG gels also functionalized with the RGD peptide. While a stronger differentiation was observed with stiffer gels, altering the cytoskeletal integrity did not affect the modulus-driven fate [28]. To further complicate our understanding of the cell-material interactions in three dimensions, Kethan and collaborators only found preadipocytes in covalently crosslinked hyaluronic acid (HA) gels of different stiffness and could induce osteogenic differentiation when the cells were infected with an active form of ROCK. Stem cells within HA hydrogels that allow cell-mediated degradation exhibited high degrees of cell spreading and tractions, and promoted osteogenesis suggesting differentiation is independent of material stiffness but cell spreading and traction in three dimension [21]. While these three studies had for common aim to investigate the effects of 3D matrix stiffness on stem cell differentiation, they described completely different outcomes that might be explained by the difference in biomaterials that exhibit distinct physical and chemical properties. Although, some underappreciated factors may further influence the cell fate, which would require further investigation with experimental controls to decipher the cell-material interactions in three dimension.

These conflicting theories in both two and three dimension indicate that there is a need of a more unified approach with more standardized platforms and protocols to create more reliable, reproducible and comparable studies. To tackle this challenge, the more common use of high throughput analysis with large libraries of biomaterials with unbiased, random nanotopography, chemistry and stiffness would be a very efficient experimental approach. However, this kind of high-throughput material screening system would also require the development of a high throughput readout screening without affecting the course of cell behavior [29]. Because all these observations appear to be platform-dependent, our understanding of the stem cell mechanobiology still remains in its infancy. Fundamentally, future research in the field of cell mechanobiology will require novel platforms that mimic more closely the in vivo environment by further considering combinatorial interactions of factors that can either mechanical or chemical.

6.4 References

[1] J.H. Wen, L.G. Vincent, A. Fuhrmann, Y.S. Choi, K.C. Hribar, H. Taylor-Weiner, S. Chen, A.J. Engler, Interplay of matrix stiffness and protein tethering in stem cell differentiation, Nature materials 13(10) (2014) 979-87.
[2] B. Trappmann, J.E. Gautrot, J.T. Connelly, D.G.T. Strange, Y. Li, M.L. Oyen, M.A. Cohen Stuart, H. Boehm, B. Li, V. Vogel, J.P. Spatz, F.M. Watt, W.T.S. Huck, Extracellular-matrix tethering regulates stem-cell fate, Nature materials 11(7) (2012) 642-649.
[3] A.J. Engler, S. Sen, H.L. Sweeney, D.E. Discher, Matrix Elasticity Directs Stem Cell Lineage Specification, Cell 126(4) (2006) 677-689.
[4] R.I. Sharma, J.G. Snedeker, Biochemical and biomechanical gradients for directed bone marrow stromal cell differentiation toward tendon and bone, Biomaterials 31(30) (2010) 7695-7704.
[5] D. Bodas, C. Khan-Malek, Formation of more stable hydrophilic surfaces of PDMS by plasma and chemical treatments, Microelectronic Engineering 83(4-9) (2006) 1277-1279.
[6] M.Y.a.J. Fang, Hydrophilic PEO-PDMS for microfluidic applications, Journal of Micromechanics and Microengineering 22(2) (2012).
[7] S.K. Moon, N.S. Yu, H.C. Mi, H.K. Soon, K.K. Sun, H.C. Young, K. Gilson, L. Il Woo, L. Hai Bang, Adhesion Behavior of Human Bone Marrow Stromal Cells
on Differentially Wettable Polymer Surfaces, Tissue Engineering 13 (2007).
[8] Y.L. G. Bartalena, T. Zambellid and J. G. Snedeker, Biomaterial surface modifications can dominate cell–substrate mechanics: the impact of PDMS plasma treatment on a quantitative assay of cell stiffness, Soft Matter 8(3) (2012) 673-681.
[9] J. Li, D. Han, Y.-P. Zhao, Kinetic behaviour of the cells touching substrate: the interfacial stiffness guides cell spreading, Sci. Rep. 4 (2014).
[10] N.M. Coelho, C. Gonzalez-Garcia, J.A. Planell, M. Salmeron-Sanchez, G. Altankov, Different assembly of type IV collagen on hydrophilic and hydrophobic substrata alters endothelial cells interaction, European cells & materials 19 (2010) 262-72.
[11] B. Narayanan, G.H. Gilmer, J. Tao, J.J. De Yoreo, C.V. Ciobanu, Self-assembly of collagen on flat surfaces: the interplay of collagen-collagen and collagen-substrate interactions, Langmuir : the ACS journal of surfaces and colloids 30(5) (2014) 1343-50.
[12] L. MacQueen, Y. Sun, C.A. Simmons, Mesenchymal stem cell mechanobiology and emerging experimental platforms, Journal of the Royal Society, Interface / the Royal Society 10(84) (2013) 20130179.
[13] R. Ayala, C. Zhang, D. Yang, Y. Hwang, A. Aung, S.S. Shroff, F.T. Arce, R. Lal, G. Arya, S. Varghese, Engineering the cell-material interface for controlling stem cell adhesion, migration, and differentiation, Biomaterials 32(15) (2011) 3700-11.
[14] M. Prager-Khoutorsky, A. Lichtenstein, R. Krishnan, K. Rajendran, A. Mayo, Z. Kam, B. Geiger, A.D. Bershadsky, Fibroblast polarization is a

matrix-rigidity-dependent process controlled by focal adhesion mechanosensing, Nat Cell Biol 13(12) (2011) 1457-1465.
[15] C.K. Choi, Y.J. Xu, B. Wang, M. Zhu, L. Zhang, L. Bian, Substrate Coupling Strength of Integrin-Binding Ligands Modulates Adhesion, Spreading, and Differentiation of Human Mesenchymal Stem Cells, Nano Lett 15(10) (2015) 6592-600.
[16] M.J. Dalby, N. Gadegaard, R. Tare, A. Andar, M.O. Riehle, P. Herzyk, C.D. Wilkinson, R.O. Oreffo, The control of human mesenchymal cell differentiation using nanoscale symmetry and disorder, Nature materials 6(12) (2007) 997-1003.
[17] M.J. Dalby, N. Gadegaard, R.O. Oreffo, Harnessing nanotopography and integrin-matrix interactions to influence stem cell fate, Nature materials 13(6) (2014) 558-69.
[18] J. Huang, S.V. Grater, F. Corbellini, S. Rinck, E. Bock, R. Kemkemer, H. Kessler, J. Ding, J.P. Spatz, Impact of order and disorder in RGD nanopatterns on cell adhesion, Nano Lett 9(3) (2009) 1111-6.
[19] B. Leitinger, Discoidin domain receptor functions in physiological and pathological conditions, Int Rev Cell Mol Biol 310 (2014) 39-87.
[20] M. Bergert, T. Lendenmann, M. Zundel, A.E. Ehret, D. Panozzo, P. Richner, D.K. Kim, S.J. Kress, D.J. Norris, O. Sorkine-Hornung, E. Mazza, D. Poulikakos, A. Ferrari, Confocal reference free traction force microscopy, Nat Commun 7 (2016) 12814.
[21] S. Khetan, M. Guvendiren, W.R. Legant, D.M. Cohen, C.S. Chen, J.A. Burdick, Degradation-mediated cellular traction directs stem cell fate in covalently crosslinked three-dimensional hydrogels, Nature materials 12(5) (2013) 458-65.
[22] N. Huebsch, P.R. Arany, A.S. Mao, D. Shvartsman, O.A. Ali, S.A. Bencherif, J. Rivera-Feliciano, D.J. Mooney, Harnessing traction-mediated manipulation of the cell/matrix interface to control stem-cell fate, Nature materials 9(6) (2010) 518-26.
[23] K.A. Beningo, M. Dembo, Y.L. Wang, Responses of fibroblasts to anchorage of dorsal extracellular matrix receptors, Proceedings of the National Academy of Sciences of the United States of America 101(52) (2004) 18024-9.
[24] J. Park, S. Bauer, K. von der Mark, P. Schmuki, Nanosize and vitality: TiO2 nanotube diameter directs cell fate, Nano Lett 7(6) (2007) 1686-91.
[25] S. Oh, K.S. Brammer, Y.S. Li, D. Teng, A.J. Engler, S. Chien, S. Jin, Stem cell fate dictated solely by altered nanotube dimension, Proceedings of the National Academy of Sciences of the United States of America 106(7) (2009) 2130-5.
[26] K. von der Mark, S. Bauer, J. Park, P. Schmuki, Another look at "Stem cell fate dictated solely by altered nanotube dimension", Proceedings of the National Academy of Sciences of the United States of America 106(24) (2009) E60; author reply E61.
[27] S. Oh, K.S. Brammer, Y.S.J. Li, D. Teng, A.J. Engler, S. Chien, S. Jin, Reply to von der Mark et al.: Looking further into the effects of nanotube dimension on stem cell fate, Proceedings of the National Academy of Sciences 106(24) (2009) E61-E61.

[28] S. Parekh, K. Chatterjee, S. Lin-Gibson, N. Moore, M. Cicerone, M. Young, C. Simon, Modulus-driven differentiation of marrow stromal cells in 3D scaffolds that is independent of myosin-based cytoskeletal tension, Biomaterials 32 (2011) 2256 - 2264.
[29] Y. Mei, K. Saha, S.R. Bogatyrev, J. Yang, A.L. Hook, Z.I. Kalcioglu, S.-W. Cho, M. Mitalipova, N. Pyzocha, F. Rojas, K.J. Van Vliet, M.C. Davies, M.R. Alexander, R. Langer, R. Jaenisch, D.G. Anderson, Combinatorial development of biomaterials for clonal growth of human pluripotent stem cells, Nature materials 9(9) (2010) 768-778.